

# LIQUID PHASE SINTERING OF $\text{BaTiO}_3$

By

K. RAMESH CHOWDARY

ME

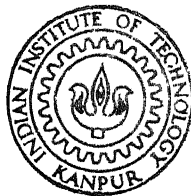
1981

M

CHO

LIS

TH  
ME/1981/M  
C4592



DEPARTMENT OF METALLURGICAL ENGINEERING  
INDIAN INSTITUTE OF TECHNOLOGY, KANPUR

AUGUST, 1981

# LIQUID PHASE SINTERING OF $\text{BaTiO}_3$

A Thesis Submitted  
in Partial Fulfilment of the Requirements  
for the Degree of  
**MASTER OF TECHNOLOGY**

By  
**K. RAMESH CHOWDARY**

to the  
**DEPARTMENT OF METALLURGICAL ENGINEERING**  
**INDIAN INSTITUTE OF TECHNOLOGY, KANPUR**  
AUGUST, 1981

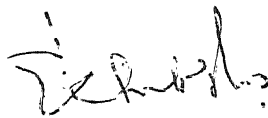
I.I.T. KANPUR  
CENTRAL LIBRARY  
Acc. No. A 70578

- 5 MAY 1982

ME - 1981 - M - CHO - LIQ

C E R T I F I C A T E

Certified that this work on ' Liquid phase sintering of  $\text{BaTiO}_3$ ' by K. Ramesh Chowdary has been carried out under my supervision and the same has not been submitted elsewhere for a degree.



E. C. Subbarao  
Professor  
Department of Metallurgical Engineering  
Indian Institute of Technology Kanpur  
K A N P U R



ACKNOWLEDGEMENTS

I am deeply indebted to Prof. E.C. Subbarao for the excellent guidance throughout the work. I immensely enjoyed the numerous lively discussions I had with him on the present work. Needless to say, this work would not have been possible without his encouragement and guidance.

I am grateful to Messrs. E.M.T. Velu, B.N. Rao, V. Bhaskar, S. Bhattacharjee, S. Pandian and S. Laha for their Co-operation and suggestions at various stages of the work.

I sincerely acknowledge the help of Mrs. Padmavati Shankar, for doing the chemical analysis, Mr. V. P. Srivastava for setting up various instruments and Mr. Mukherjee and Mr. Prasad in metallography work.

I am thankful to Messrs. Umesh Kumar, Swaminathan, Gopichand, Shaw and Arunachalam for their help during the final stages of the work. I am thankful to Mr. Vishwanath Singh, Mr. Bajpai, Mr. R.N. Misra and

Mr. Bhardwaj for their prompt and timely help in getting the thesis in the printed form.

This work was supported by the Department of Electronics, Govt. of India and their financial assistance is greatly acknowledged.

Finally I wish to thank my friends Apparao, Bose, Hemadri, Sharma, Verma, and Murty whose company was most enjoyable and helpful.

K. RAMESH CHOWDARY.

## C O N T E N T S

	Page
LIST OF TABLES	viii
LIST OF FIGURES	x
ABSTRACT	xiv
I. INTRODUCTION	1
I.1 Multilayer Capacitors	2
I.2 Internal boundary layer capacitors	2
I.3 Electrode problems	4
I.3.1 Base metal Electrodes	7
I.3.2 Liquid Phase Sintering.	7
II. STATEMENT OF THE PROBLEM	9
III. EXPERIMENTAL TECHNIQUES	14
III.1 Sample preparation	14
III.1.1 Raw Materials	14
III.1.2 Preparation of Barium Titanate	14
III.1.2.a Determination of the amount of recovery.	15
III.1.2.b Grinding	15
III.1.3 Preparation of glass	16
III.1.3.a Chemical analysis of the glass	18
III.1.4 Preparation of samples for liquid phase sintering..	19

III.1.5	Liquid Phase Sintering	19
III.2	Characterisation	23
III.2.1	Weight loss measurement. during sintering	23
III.2.2	Thermal analysis	23
III.2.3	Density Measurements	23
III.2.4	Microstructural observation	25
III.2.5	X-ray diffraction studies	25
III.2.6.a	Temp. dependence of dielectric properties	27
III.2.6.b	D.C. bias Effect on dielectric properties	29
III.2.6.c	Frequency dependence of dielectric properties.	30
IV.	RESULTS AND DISCUSSION	32
IV.1	Weight loss during sintering	32
IV.2	Thermal analysis	35
IV.3	Density	38
IV.3.1	Effect of glass additions	38
IV.3.2	Effect of sintering temperature and time	42
IV.3.3	Effect of particle size	54
IV.3.4	Effect of rate of heating	54
IV.4	Microstructural Observation	57
IV.5	X-ray diffraction studies.	63
IV.6	Densification mechanisms	74
IV.7	Dielectric measurements	86

IV.7.1	Temperature dependence of dielectric properties.	86
IV.7.1.1	Effect of glass addition	86
IV.7.1.2	Effect of sintering temperature and time.	95
IV.7.2	Voltage dependence of dielectric properties.	
IV.7.3	Frequency dependence of dielectric properties	109
V.	CONCLUSIONS AND RECOMMENDATIONS	111
VI.	APPENDIX - A - Chemical Analysis	113
VI.1.1	Determination of Bismuth	113
VI.1.2	Determination of Aluminium	114
VI.1.3	Determination of Boron	115
REFERENCES		116

LIST OF TABLES

II.1	Dielectric properties of $\text{Bi}_2\text{O}_3$ - $\text{B}_2\text{O}_3$ glasses.	- 10
II.2	Properties of Lead Germanate crystal and Bismuth Borate glass.....	- 11
III.1	Size reduction during grinding	- 17
III.2	Properties of glass used in sintering Experiments.	- 17
III.3	Different batches prepared for liquid phase sintering and their heating schedule	- 20
III.4	Instrument parameters of Derivatograph	- 25
III.5	Instrument parameters for X-ray diffraction studies.. .	- 26
IV.1	Sintered density and pct wt loss of liquid phase sintered Barium Titanate.....	- 33
IV.2	Weight loss data of liquid phase....	- 34
IV.3	Density of green and sintered pellets..	- 46
IV.4	Porosity change with temperature and time	- 48
IV.5	Effect of rate of heating on densification	- 56
IV.6	Variation of grain size and grain boundary thickness with sintering temperature and time,	- 61
IV.7	X-ray diffraction data of liquid phase sintered $\text{BaTiO}_3$ ...	- 64

contd...

IV. 8	X-ray diffraction data of the 30% glass sample....	-	66
IV. 9	X-ray diffraction data of the 74% $\text{Bi}_2\text{O}_3$ 26%/ $\text{B}_2\text{O}_3$ glass crystallized at 750°C and 525°C.	-	69
IV. 10	X-ray diffraction data of the $\text{BaTiC}_3 + 20\%$ glass mixture heated to different temperatures.	-	71
IV. 11	Comparison of observed dielectric constants and calculated values using mixed rules.	-	95
IV. 12	Variation of dielectric constants with glass addition, sintering temperature and time....	-	101

---

LIST OF FIGURES

## PAGE

I.1	Schematic representation of a multilayer capacitor...	3
I.2	Ag - Pd phase diagram	6
III.1	Temperature profile of the tube furnace used in the sintering experiments	22
III.2	Sample holder for (a) high temperature dielectric measurements (b) D.C. bias studies.	28
III.3	Circuit used for D.C. bias studies	31
IV.1	DTA and TGA plots of $\text{BaTiO}_3$ and 20% glass mixture.	36
IV.2	Density vs sintering temperature of $\text{BaTiO}_3$ with different amounts of glass addition (Sintering time 2 hours.)	39
IV.3	Density vs wt% glass addition to $\text{BaTiO}_3$ at different sintering temperatures (sintering time: 2 hours)	40
IV.4	Densification of $\text{BaTiO}_3$ as a function of sintering time with 20% glass addition.	49
IV.5	Densification of $\text{BaTiO}_3$ as a function of sintering time with 10% glass addition,	50
IV.6	Geometrical density vs. sintering time for $\text{BaTiO}_3$ with 10% glass addition at different sintering temperatures.	51



IV.7	Displacement density vs. sintering time BaTiO <sub>3</sub> with 10% glass addition at different sintering temperatures.	52
IV.8	Geometrical density vs. Sintering time for BaTiO <sub>3</sub> with 0.4 and 2% glass.	53
IV.9	Effect of particle size on densification of BaTiO <sub>3</sub> with 10% glass addition at differ- ent sintering temperatures and times.	55
IV.10-14	Microstructures of liquid phase sintered BaTiO <sub>3</sub> samples with different glass contents.	58
IV.15-18	Microstructures of liquid phase sintered BaTiO <sub>3</sub> samples with 10% glass addition sintered at 1000°C for different times.	59
IV.19-22	Microstructures of liquid phase sintered BaTiO <sub>3</sub> samples with 10% glass addition sintered at 1100°C for different times.	60
IV.23	Formation of BaBi <sub>4</sub> Ti <sub>4</sub> O <sub>15</sub> at various sintering temperatures and times.	68 a.
IV.24	Hypothetical densification curve for the three stages of liquid phase sintering.	75
IV.25	Dihedral angle formed by the liquid phase at the grain boundary.	75
IV.26	Volume shrinkage vs. sintering time for BaTiO <sub>3</sub> with 10% glass addition at different sintering temperatures.	81

IV.27	Volume shrinkage vs. sintering time for $\text{BaTiO}_3$ with 10% and 20% glass addition at 1000 and 1100°C.	83
IV.28	Temperature dependence of dielectric constant for the samples with different glass additions.	87
IV.29	Variation of dielectric constant with glass addition.	88
IV.30	Temperature dependence of the dielectric constant of the hot pressed samples heat treated at 700°, 900, 1100 and 1300°C.	93
IV.31	Relative dielectric constant vs. temperature for the samples with 20% glass addition sintered at 1000°C for different times (upto 200°C)	96
IV.32	Relative dielectric constant vs. temperature for the samples with 20% glass addition sintered at 1100°C for different times.	97
IV.33	Relative dielectric constant vs. temperature for the samples with 10% glass addition sintered at 1000°C for different times.	98
IV.34	Relative dielectric constant vs. temperature for the samples with 10% glass addition sintered at 1100°C for different times.	99

IV.35	Relative dielectric constant vs. temperature for the samples with 10% glass addition sintered at 1050°C for different times.	100
IV.36	Relative dielectric constant vs. temperature for the samples with 20% glass addition sintered at 1000°C for different times (upto 420°C).	106
IV.37	Percent change in permittivity and dissipation factor with d.c. bias	107
IV.38	Comparison of permittivity vs. d.c. bias for different BaTiO <sub>3</sub> samples.	108
IV.39	Frequency dependence of dielectric constant for liquid phase sintered BaTiO <sub>3</sub> .	110.

A B S T R A C T

Ba Ti O<sub>3</sub> ceramics are conventionally sintered at 1300 - 1400°C. Lower sintering temperatures result in energy savings as well as enable the use of cheaper electrode materials than expensive Pd and Pt electrodes in multilayer capacitors. Lead germanate glass has been used to lower the sintering temperature of Ba Ti O<sub>3</sub> ceramics. In the present work, bismuth borate glass (upto 40 wt percent) is admixed with Ba Ti O<sub>3</sub> and sintering experiments carried out at temperatures between 800 to 1200°C for a period of 10min to 3hrs. Density, microstructure, phase identification by X-ray diffraction, dielectric constant and loss have been studied as a function of glass content and sintering conditions. Reasonably dense bodies ( greater than 85% theoretical density) are obtained with 10 to 20% glass additions by sintering at 1000-1050°C, which can be used with 70 Ag-30Pd alloy electrodes. There is no shift of the x-ray diffraction lines or the Curie temperature of Ba Ti O<sub>3</sub>, indicating no solid solutions are formed with Ba Ti O<sub>3</sub> by the glass constituents. X-ray studies revealed the formation of Bi<sub>4</sub>Ti<sub>3</sub>O<sub>12</sub> and Ba Bi<sub>4</sub>Ti<sub>4</sub>O<sub>15</sub>, the latter being the prominent and its amount depending upon the amount of glass and sintering conditions. Microstructure shows the glass

present as a coating over the grains. Densification mechanisms during liquid phase sintering are discussed. Dielectric properties are measured with respect to temperature, voltage and frequency. These measurements show that the dielectric properties are not **affected** markedly with glass addition upto 20% and exhibit better temperature characteristics than pure Ba Ti O<sub>3</sub>.

## I. INTRODUCTION

Majority of the capacitors produced today are made of ceramic materials. More than 95 percent of these ceramic materials are ferroelectric in nature. Ferroelectric materials have a high dielectric constant which makes them ideal for capacitor industry.

A ceramic capacitor consists of a ceramic dielectric material sandwiched between two parallel metal plates, which serve as the electrodes. The usual electrode material is silver. Before world war II, Titanium dioxide with a dielectric constant of around 100, was the favoured dielectric material. During the world war II, it was discovered that barium titanate has a high dielectric constant (1500-2000). Thus barium titanate became the basic dielectric material for ceramic capacitors for the last 35 years. This enabled the size (volume) of the capacitor to be decreased correspondingly. The capacitance of a normal parallel plate capacitor can also be increased either by reducing the thickness or by increasing the electrode area. Due to the brittle nature of the ceramic materials the capacitors with a large area and small thickness are very fragile and cannot be used without any mechanical support. The drive towards miniaturization led to the development of i) Multilayer capacitors and ii) Internal boundary layer capacitors.

## I.1 Multilayer Capacitors:

Schematic representation of a multilayer capacitor is given in Figure I.1. These are generally rectangular in shape with parallel electrodes brought out at the narrow ends of the rectangle. A margin of bare dielectric is allowed around the metal plate to prevent edge breakdown. Such an arrangement being compact, has a high volumetric efficiency. The whole stacking consisting of alternate layers of dielectric ceramic and the electrode is sintered around  $1350^{\circ}\text{C}$ , which necessitates the use of high melting point metals like Pt and Pt as the electrodes.

Today multilayer capacitors with 100 active layers of 20 micron thickness are not uncommon. Capacitance values of the order of microfarads are easily obtained.

## I.2 Internal Boundary Layer (IBL) Capacitors:

Commercial capacitors are usually manufactured from titanate based materials of the perovskite ( $\text{ABX}_3$ ) family, which are made semiconducting (n-type) by aliovalent chemical substitution, gaseous reduction, or combination thereof. Resistivity distributions are developed within the microstructure by boundary counter diffusion, or by sintering in the presence of a liquid phase which solidifies on cooling into an insulator. Ideally, the former method is characterized by grain to grain contact, with interfacial compensation states, and the latter by grain to grain separation, with an insulating intergranular phase. Anomalously high apparent dielectric

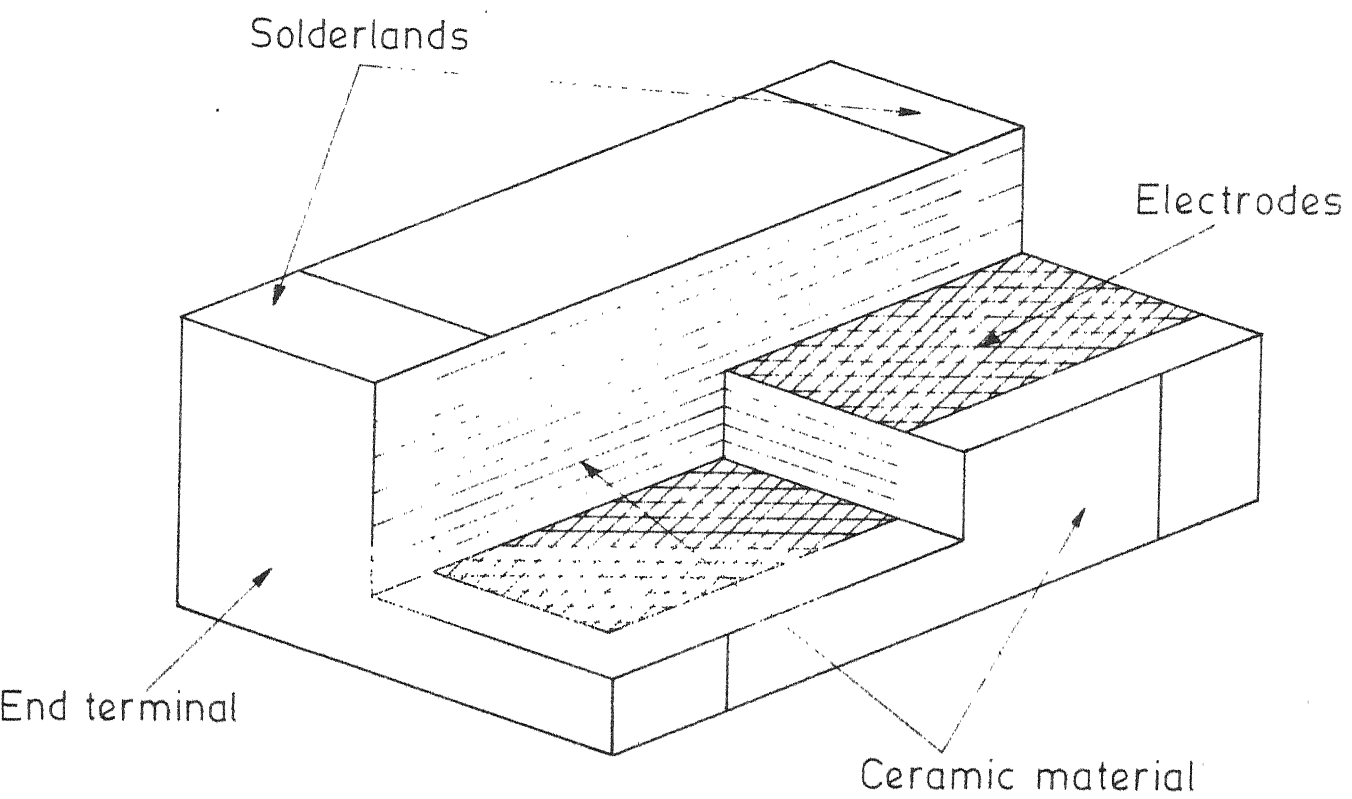


Fig I .1. Schematic representation of a multilayer capacitor .



constants (over 20,000) calculated for IBL capacitors are generally attributed to enhanced space charge polarization processes taking place between semiconducting grains and resistive boundaries.

There are certain problems to be tackled in the development of these capacitors (1).

### I.3 Electrode Problems:

All multilayer capacitors discussed previously require Pt, Au or Pd electrodes, which add substantially to their cost. Today's noble metal prices and other reasons make it imperative to search for techniques to replace them. But silver, even though a noble metal, does not belong to Au, Pt or Pd group because it is much cheaper. It is an ideal electrode material, used exclusively in discs and on the outside of the multilayer capacitors. For this reason it could and should be used to replace the other noble metals wherever possible.

The usability of a metal or an electrode material in monolithics is determined by two properties; its melting point should be higher than the sintering temperature of the ceramic and its metal/metal oxide equilibrium oxygen vapour pressure should be higher than that of the oxygen partial pressure during firing. Since the firing temperature of most ceramics is in the 1300-1400°C range, and the firing atmosphere is air, the only suitable candidates seem to be Pt (MP 1769°C) and Pd (MP 1552°C) which are indeed the two most frequently used metals. Gold (MP 1063°C) sometimes is also used, but

usually as a Pd alloy, which brings its melting point above the 1300-1400°C range. Silver has too low a melting point (961°C) and some of the transition metals (Ni, Co, Fe) which would be suitable because of their high melting temperatures are unsuitable because of their low oxygen equilibrium pressures.

So now for the replacement of Pt, Pd and Au electrodes, either we have to develop ceramics which can be fired in an atmosphere with an oxygen partial pressure lower than the equilibrium pressure of one of the transition metals at this temperature, or to lower the firing temperature of the ceramic below the melting temperature of Ag or one of the low melting Ag - Pd alloys. From the Ag-Pd phase diagram (2) given in Fig. I.2 one can see that a 70 Pd 30 Ag alloy is needed for a sintering temperature of 1300°C, whereas a 30 Pd 70 Ag alloy can be used if the sintering temperature is reduced to 1000-1050°C.

Another major advantage of lowering the sintering temperature is to bring about energy savings during sintering. For example, if the sintering temperature can be reduced to 1000°C or below we can use nichrome furnaces instead of the expensive globar furnaces or other high temperature

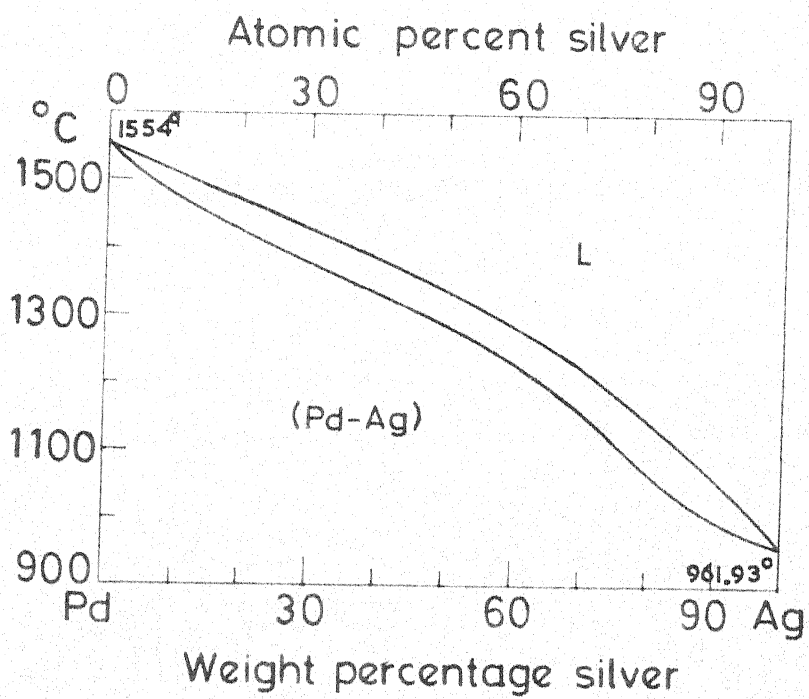


Fig. 1.2 Ag-Pd Phase diagram.

furnaces, and also the power consumption of these temperatures will be nearly one third of that needed for the conventional firing around  $1350^{\circ}\text{C}$ .

So the two possible solutions for the electrode problems are using (i) base metal electrodes or (ii) liquid phase sintering.

### I.3.1 Base metal electrodes:

A base metal, such as nickel, has a melting point higher than the sintering temperatures employed in capacitor manufacture and is much cheaper than Pd or even Ag. However, at the sintering temperatures, Ni oxidizes to NiO and in the process reduces  $\text{BaTiO}_3$  by converting a corresponding number of  $\text{Ti}^{4+}$  ions to the  $\text{Ti}^{3+}$  state. The presence of Ti in two valence states on crystallographically equivalent sites leads to large electronic conductivity and the ceramic is no longer useful as a dielectric. The reduction of  $\text{BaTiO}_3$  can be prevented by doping it with Mn (3 - 6). The disadvantage with these base metal electrodes is that they have higher resistivity values compared to noble metals, thus increasing the series resistance and in turn dissipation factor of the capacitor.

### I.3.2 Liquid phase sintering:

The use of the noble metals like Pt and Pd can also be avoided by reducing the sintering temperature of the ceramic dielectric from the usual  $1300-1400^{\circ}\text{C}$  to below the melting temperature of Ag or one of the low melting Ag-Pd alloys.

The sintering temperature is lowered by the use of a transient liquid phase. The liquid phase should possess the following characteristics (7)

- i) it should melt at or below  $800-900^{\circ}\text{C}$
- ii) it should not react with the dielectric composition
- iii) the crystalline phase, formed on cooling, should preferably have a relatively high dielectric constant, so that the dielectric constant of the composite is not too greatly reduced.
- iv) the viscosity of the liquid should be low at the sintering temperature so that the amount of liquid phase is kept to a minimum.

Lead germanate is one such additive which can meet the above requirements using this. Park (8) has developed dielectric ceramics which can sinter at  $800-900^{\circ}\text{C}$ . The fact that crystalline lead germanate ( $\text{Pb}_5\text{Ge}_3\text{O}_{11}$ ) is ferroelectric is a distinct advantage in retaining fairly high dielectric constant of the composite.

Recently Mukherjee and Ravishankar reported the liquid phase sintering of  $\text{BaTiO}_3$  using lead germanate (9). They observed that for liquid phase sintering of  $\text{BaTiO}_3$  with 0.6 to 1 mole percent glass addition a minimum of  $1150-1200^{\circ}\text{C}$  sintering temperature is needed. They also observed that above  $1200^{\circ}\text{C}$  there is no glass present and  $\text{PbO}$  and  $\text{GeO}_2$  have diffused into the  $\text{BaTiO}_3$  grains. The disadvantage with this glass addition is that during sintering lead substitutes for Ba in  $\text{BaTiO}_3$  lattice and thereby reduces the room temperature dielectric constant.

The toxic nature of lead and the high cost of germanium are other deterrent factors in the use of  $\text{Pb}_5\text{Ge}_3\text{O}_{11}$  as a sintering aid.

Using CuO additive, Hennings studied the liquid phase sintering of  $\text{BaTiO}_3$  (10). With the addition of 0.5 to 1 mole percent of CuO he was able to reduce the sintering temperature to about  $1200^\circ\text{C}$ . The problem with the CuO addition is that if it is in excess the sample becomes conductive and thus useless, and also the sintering temperature is not too greatly reduced.

## II. STATEMENT OF THE PROBLEM

Liquid phase sintering of Barium Titanate has been tried to solve the electrode problems in multilayer capacitors (8 - 10). None of these studies are completely successful in reducing the cost of these capacitors by replacing the noble metal electrodes (Pt and Pd) with Ag or low melting Ag-Pd alloys without sacrificing the dielectric properties of  $\text{BaTiO}_3$ . So an alternative additive has been sought.

In the present work, <sup>a</sup>glass from the  $\text{Bi}_2\text{O}_3 - \text{B}_2\text{O}_3$  system (11) was used as an additive. The dielectric properties of some of the glasses in this system are given in Table II.1. From there, 74 percent  $\text{Bi}_2\text{O}_3$ , 26 percent  $\text{B}_2\text{O}_3$  glass which has the highest dielectric constant and a low melting temperature ( $700-750^\circ\text{C}$ ) was chosen as the additive. Some of the properties of this glass were compared with lead germanate in Table II.2. From this one can see that the melting temperature and densities

Table II.1 : Dielectric properties of  $\text{Bi}_2\text{O}_3$  -  $\text{B}_2\text{O}_3$  glasses  
 (Dielectric constant at room temperature and  
 resistivity ( $\Omega$ -cm) at  $130^\circ\text{C}$  and  $230^\circ\text{C}$ )

Glass No.	Composition mol pct.		Dielectric constant				100 tan $\delta$		$\rho_{130}$ ( $\times 10^{14}$ ) $\Omega$ -cm	$\rho_{230}$ ( $\times 10^{11}$ ) $\Omega$ -cm
	$\text{Bi}_2\text{O}_3$	$\text{B}_2\text{O}_3$	$10^3$ c/s	$10^5$ c/s	$10^7$ c/s	$9.6 \times 10^9$ c/s	$10^3$ c/s	$9.6 \times 10^9$ c/s		
19	26	74	14.1	13.9	13.6	10.3	0.13	0.84	34	340
25	32	68	21.8	21.8	21.4	16.1	0.15	1.24	6.4	10
26	40	60	28.0	28.0	26.6	19.1	0.14	2.88	1.3	5.9
27	46	54	31.0	31.1	29.8	22.1	0.18	3.29	0.55	0.70
22	54	46	31.1	31.1	29.9	21.5	0.32	2.41	0.16	0.25
60	60	40	37.6	37.1	36.2	24.3	0.22	1.72	0.023	0.042
28	66	34	38.8	38.7	36.5	26.6	0.22	1.98	0.013	0.022
29	74	26	42.5	42.5	41.2	31.1	0.21	1.90	0.0017	0.0058

Table II.2 : Properties of Lead Germanate Crystals (13)  
and Bismuth Borate Glass.

Property	$\text{Pb}_5\text{Ge}_3\text{O}_{11}$ single crystal	74 pct $\text{Bi}_2\text{O}_3$ 26 pct $\text{B}_2\text{O}_3$ glass
Melting point ( $^{\circ}\text{C}$ )	$738^{\circ}$	$700 - 750^{\circ}$
Density (g/cc)	7.38	7.74
Linear thermal expansion coefficient	-	$115 \times 10^{-7}/^{\circ}\text{C}$
Dielectric constant at 1 KHz	$\epsilon_{11\text{RT}} - 22$ $\epsilon_{33\text{RT}} - 36$ $\epsilon_{33\text{Max}} - 2300$	$\epsilon_{\text{RT}} - 42.5$
Curie point $^{\circ}\text{C}$	$178^{\circ}$	-



of both are comparable, and the dielectric constant at room temperature for Bismuth Borate glass is higher than that of lead germanate crystal in both crystallographic directions.

The aim of the present work is to study the usability of this glass as an additive for liquid phase sintering of  $\text{BaTiO}_3$  and to sinter  $\text{BaTiO}_3$  at temperatures where we can use 70 Ag 30 Pd alloy or even lower melting alloys of this system as an electrode, without sacrificing the dielectric properties significantly.

More specifically, the aims of the present work are:

- i) to investigate the effect of glass addition on sintering temperature (upto 40 wt pct of glass was used)
- ii) to study the effect of amount of glass addition, sintering temperature and sintering time on densification
- iii) to attempt an explanation on the mechanism of sintering in the presence of liquid phase
- iv) to relate the dielectric properties to structural and microstructural changes during sintering.

The sintered pellets are investigated using

- i) weight loss measurements during sintering
- ii) DTA
- iii) chemical analysis
- iv) x-ray diffraction
- v) density
- vi) volume shrinkage
- vii) microstructure observation, and
- viii) variation of dielectric constant and dissipation factor

with

- a) temperature
- b) dc bias, and
- c) frequency

## III. EXPERIMENTAL TECHNIQUES

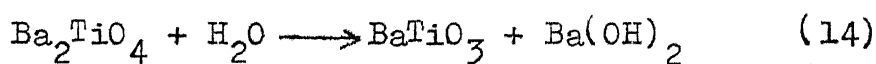
## III.1 : Sample Preparation

## III.1.1: Raw materials:

Raw materials used were (all of them are AR Grade, more than 99.5 percent purity) barium carbonate (Sarabhai Chemicals, India), boric acid (Sarabhai Chemicals, India), titanium Dioxide (Baker Analysed Reagent, USA), bismuth oxide (Mayfair and Raydon, England).

## III.1.2 : Preparation of Barium Titanate:

$BaTiO_3$  was prepared by calcining equimolar amounts of  $BaCO_3$  and  $TiO_2$  (14). These powders were mixed thoroughly in an alumina ball mill using alumina balls and acetone. The mixes were then compacted at 40,000 psi pressure using a hydraulic press to improve reaction during calcination. Calcination was done in an alumina crucible at  $1250^\circ C$  for 4 to 6 hrs. After calcination the material was crushed and ground into a fine powder. X-ray analysis of the calcined powder showed the presence of  $Ba_2TiO_4$  phase in addition to  $BaTiO_3$  (15). The calcined powder was then boiled in hot water, filtered and washed with hot water repeatedly till the filtrate shows a pH of 7. These washings were done to remove any traces of  $Ba(OH)_2$  present since  $Ba(OH)_2$  will be formed when any  $Ba_2TiO_4$  present reacts with water.



### III.1.2.a : Determination of the amount of recovery:

Gravimetric analysis was done on the calcined powder to determine the amount of recovery. A weighed amount of calcined powder was taken into a baker and boiled in distilled water, filtered and washed with distilled water repeatedly till the filtrate shows a pH of 7. The filtered solution was then evaporated and weighed to determine the amount of  $\text{Ba}_2\text{TiO}_4$  dissolved. The amount of the undissolved  $\text{BaTiO}_3$  left in the filter paper was weighed after burning the filter paper. These results are given below:

wt. of calcined powder boiled in water	= 9. 4 gm
wt. of $\text{BaTiO}_3$ recovered as undissolved material	= 8.53 7 gm
wt. loss of calcined material	= 1.1279 gm
∴ percentage weight loss	= 11. 4
or recovery	= 88.4 pct.
wt. of filtrate as $\text{BaCO}_3$ after evaporating the water	= 1.3975 gm
or wt. of BaO	= 1.0858 gm

### III.1.2.b Grinding :

Two types of grinding was used.

- 1) Dry grinding: Barium titanate powder was ground in a Fritsch pulverisette using corundum ball and mortar. The sample was ground for 6 hours and then the particle size was measured using a Fisher subsieve sizer.
- 2) Wet grinding : Here the powder was ground in two grinding media

a) Grinding in an alumina jar using alumina balls and distilled water. Samples were taken intermittently and

analyzed for particle size using Fisher subsieve sizer.

The results are given in Table III.1.

b) Grinding in an agate jar using agate balls and distilled water in a Fritsch pulverisette. Here also samples were taken intermittently and analyzed for particle size. The results are given in Table III.1

### III.1.3 : Preparation of Glass:

Two batches i) 50 gm ii) 25 gm of glass were prepared. The amount of raw materials needed to prepare 50 gm batch of glass 74 pct.  $\text{Bi}_2\text{O}_3$ , 26 pct.  $\text{B}_2\text{O}_3$  are:

$\text{Bi}_2\text{O}_3$	99 pct pure	= 47.51 gm
$\text{H}_3\text{BO}_3$	AR grade	= 4.43 gm

The raw materials were mixed thoroughly in an agate mortar using acetone. The batch was then taken into an alumina crucible for melting in a muffle furnace. The furnace was kept around  $750^\circ\text{C}$  and the melts were occasionally mixed by swirling the liquid. The 25 gm batch of molten glass was cast into discs for measuring the properties of glass. During casting the glass has crystallized many times, even though it was cast using chilled water bath. Finally the glass pieces which are clear were taken for experimentation. These results are given T.III.2 Another batch of molten glass was quenched by pouring the melt into a tray containing distilled water. The glass pieces were then collected, dried and then ground in a ball mill for 12-16 hours. The particle size of the ground powder measured by Fisher subsieve sizer was 16-18  $\mu\text{m}$ .

Table III.1 : Size reduction during grinding

Grinding in an alumina jar		Grinding in an agate jar	
Grinding time	The particle size in microns	Grinding time	The particle size in micron
Starting material	18 - 20	Starting Material	18 - 20
1 h	13 - 15	6 h	5 - 6
10 h	8 - 10	12 h	3 - 4
24 h	5 - 6	24 h	2 - 25
48 h	2 - 3		

This powder was used in the initial sintering experiments. This glass powder was further ground in a Fritsch pulverisette for 2 hours and 10 hours to get a particle size of 4 - 5  $\mu\text{m}$  and 2-3  $\mu\text{m}$  respectively.

### III.1.3.a : Chemical Analysis of the glass:

Chemical analysis of the glass was done using the procedure given in appendix A. Actual analysis was done for bismuth and alumina and boron was determined by difference. Analysis was done for the two batches of glass prepared and the results are as shown below:

	wt. pct. $\text{Bi}_2\text{O}_3$	$\text{B}_2\text{O}_3^{\text{x}}$	$\text{Al}_2\text{O}_3$
Batch 1 which was ground for 12 hrs with a particle size of 1.6-1.8 $\mu\text{m}$	94.31	5.2	0.43
Batch 2 which was cast into discs	92.35	7.44	0.21
Actual amounts taken	95.01	4.99	-

<sup>x</sup>calculated as the difference

Traces of alumina were present in both the cases and it might be due to the melting of glass in an alumina crucible.

Alumina content was more in the ground sample, probably due to grinding in an alumina jar. The difference in  $\text{Bi}_2\text{O}_3$  content from the intended value may be due to the evaporation of some  $\text{Bi}_2\text{O}_3$  during melting. The difference in  $\text{Bi}_2\text{O}_3$  amounts in the two batches may be due to the crystallization of part of the glass during casting.

### III.1.4 : Preparation of samples for liquid phase sintering:

Initial experiments were carried out over a wide range of compositions and sintering temperature. Six different 10 gm batches of  $\text{BaTiO}_3$ , each containing 0.4, 2, 10, 20, 30 and 40 wt. pct. of glass were prepared. Particle size of the powders used were, 13 - 14  $\mu\text{m}$   $\text{BaTiO}_3$  and 1.6 -18  $\mu\text{m}$  glass. The raw materials were mixed thoroughly for at least 1 hr in an agate mortar using acetone. It was then made into pellets each weighing approximately 1 gm, using a  $\frac{1}{2}$ " dia die at 40,000 psi pressure for further experimentation. Five different batches were prepared with 20, 10, 2 and 0.4 wt pct. of glass. These batches along with their heating schedules are given in Table III. 3.

Raw materials were mixed in the same way as described above. Here the powder was made into pellets in a  $\frac{3}{8}$ " dia die, each weighing approximately 0.5 gm using PVA binder. Pressing was done in a double acting automatic hydraulic press at 100000psi pressure. Green densities were measured for all these pellets from geometry and weight, before firing.

### III.1.5 : Liquid phase sintering:

Initial sintering experiments were done in a global muffle furnace to which a programmable controller

Honeywell) was attached. Six different batches each containing 0.4, 2, 10, 20, 30 and 40 wt pct. of glass were fired at five different temperatures, 800, 900, 1000, 1100 and 1200°C for 2 hours. Each time five pellets were taken in a platinum crucible and were stacked one over the other keeping some loose



Table III.3 Different batches prepared for liquid phase sintering and their heating schedule.

Batch No.	Wt% glass	Particle size( $\mu\text{m}$ ) of $\text{BaTiO}_3$	Glass	Sintering temperature $^{\circ}\text{C}$ .	Sintering times (h)
1	20	13	17	1000	1/2, 1, 3
				1100	1/6, 1/2, 1
2	10	13	17	1000	1/6, 1/2, 1, 2
				1100	1/6, 1/2, 1, 2
3	10	5	4	1000	1/6, 1/2, 1, 2
				1050	1/6, 1/2, 1, 2
				1100	1/6, 1/2, 1, 2
				1150	1/6, 1/2, 1, 2
4	2	2	2.5	1100	1/6, 1/2, 1, 2
				1150	1/6, 1/2, 1, 2
				1200	1/6, 1/2, 1, 2
5	0.4	2	2.5	1100	1/6, 1/2, 1, 2
				1150	1/6, 1/2, 1, 2
				1200	1/6, 1/2, 1, 2

BaTiO<sub>3</sub> powder in between these pellets. Sintering of the five different batches mentioned previously was done in a globar horizontal tube furnace to which a proportional controller ( L and N Electromax) was attached. The temperature profile of the furnace is shown in Fig. III.1. Each time five pellets were taken in an alumina boat and were charged from one end of the furnace and pulled through the other end by a stainless steel rod which passes through a brass flange attached to the end of the tube. Two boats were connected to each other by a nichrome wire and the first boat was hooked to the stainless steel rod such that by pulling the rod from one end, the two boats will travel along the length of the furnace. The time schedule was made in such a manner that by pulling the boat through the length of the furnace it will pass through heating, soaking and cooling zones. Since two boats were connected to each other, as one boat is in the soaking zone the other will be in the heating zone, and as the first boat moves through the cooling zone the second boat will reach the soaking zone. In each case the time taken to reach the soaking zone was kept constant as 2 hours 40 minutes and soaking time was varied from 10 minutes to 2 hours and finally the time through the cooling zone was maintained constant as 2 hours.

The sintering temperatures and times followed for the five different batches mentioned previously are given in Table III.3. On batch 3 few more sintering experiments were done with longer heating cycle. Here the time taken to reach the soaking zone was made double and triple than that of the standard one, to investigate its effect on density. In these experiments the time through cooling zone

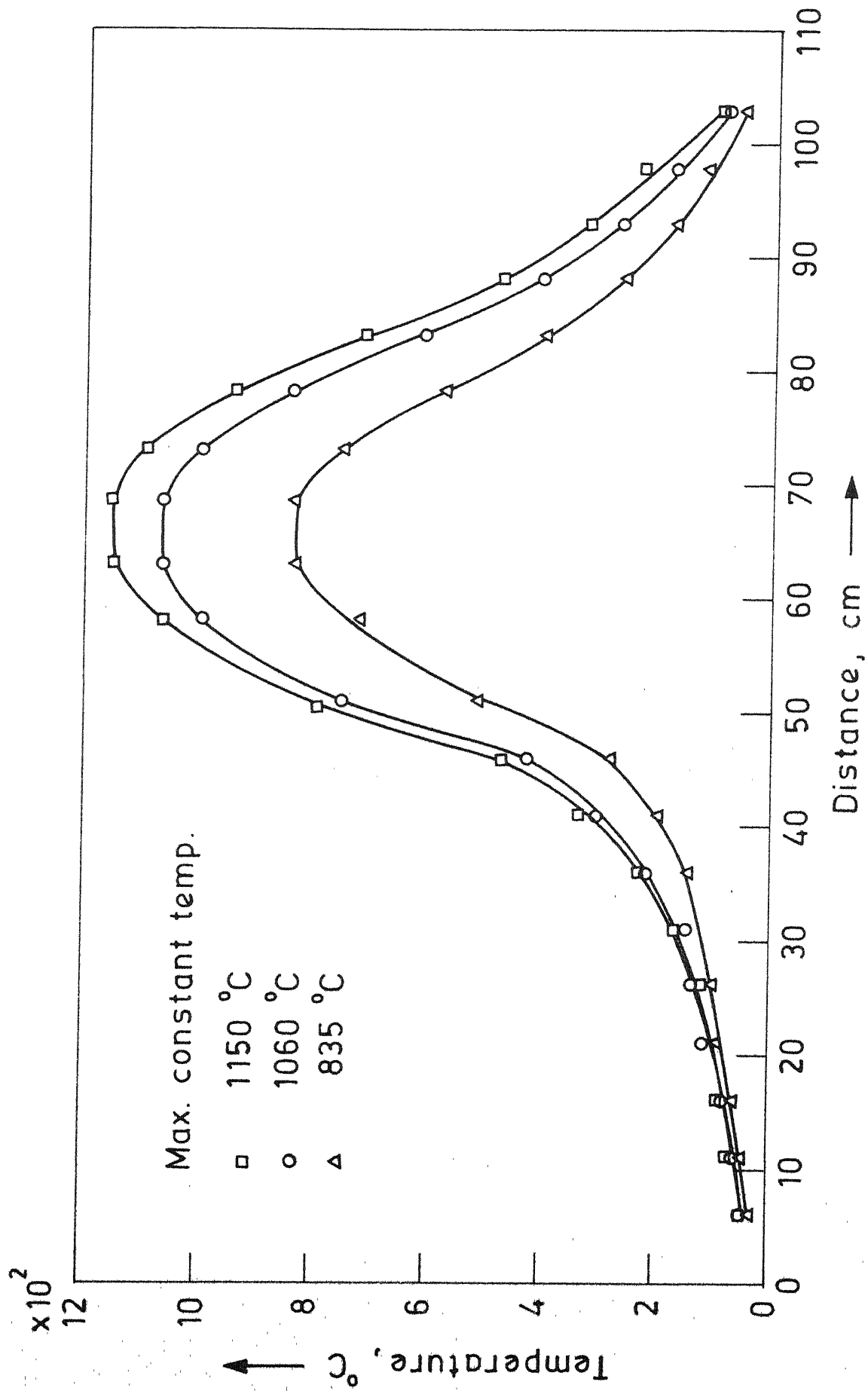


Fig. III-1 - Temperature profile of the tube furnace used in the sintering experiments.

### III.2 Characterisation:

#### III.2.1 Weight loss measurements during sintering:

Weight loss was determined for each pellet after sintering using a Mettler single pan, electric balance accuracy 0.0001 gm).

#### III.2.2 Thermal Analysis:

The simultaneous DTA, DTG and TGA studies of the mixture of  $\text{BaTiO}_3$  + 20 pct. glass sample was done on MOM Derivatograph. The instrument parameters are given in Table III.4.

#### III.2.3 Density Measurements:

Two types of densities were reported.

1) Geometrical density: Geometrical densities were measured on each sintered pellet. The pellets were weighed ( $w$ ) in a Mettler single pan, electric balance and volume ( $v$ ) of the pellet was measured using a screw guage. Density was calculated as ( $w/v$ ).

2) Bulk density: Bulk density was calculated on one pellet from each sintering experiment. Here density was measured by water displacement method. The dried pellets were weighed ( $D$ ) in a mettler single pan, electric balance. The pellets were boiled in distilled water for 5 - 6 hours and soaked for 24 hours. The water suspended wt. ( $s$ ) and water saturated wt. ( $w$ ) were determined. The bulk density was evaluated using the expression ( $\frac{D}{w-s}$ ).

Table III.4 : Instrument parameters of Derivatograph:

1. Heating rate	5°/min
2. Reference sample	Alumina
3. Sensitivity of DTA DTG	1/5 1/20
4. Maximum temperature upto which it was run	1000°C
5. Amount of the sample	2.019 gm.

### III.2.4 Microstructural observation:

For microstructural study, the samples were mounted in a thermosetting plastic so that one face of the disc was exposed. The sample was then ground on a silicon carbide powder over a glass plate using liquid paraffin. Grinding was done successively on 200, 400, 600 and 800 mesh size SiC powders. After grinding over 800 mesh powder, the sample was polished on a rotating cloth using diamond paste. Polishing was done at least for one day. After polishing the sample was etched approximately for 30 sec with a solution containing 5 pct. Hcl and 0.5 pct. HF (16). The etched sample was then observed under the NU 20 microscope using reflected light.

### III.2.5 X-ray diffraction studies:

X-ray diffraction patterns of the calcined powder and the liquid phase sintered pellets were taken with a General Electric XRD-6 and Philips Automatic x-ray diffractometer (Type PW 1730/10) fixing the instrument parameters given in Table III.5. For diffraction studies on the pellets, the samples were mounted in a perspex sample holder with two teflon screws, taking care that the sample surface was flat and in line with the sample holder. All these samples were scanned from  $2\theta = 20^\circ$  to  $60^\circ$ .

Table III.5 : Instrument parameters for x-ray diffraction studies.

Parameters	GE XRD- 6	Philips XRD Type 1730/10)
Radiation	CuK $\alpha$ with Ni filter)	CuK $\alpha$ with Ni filter)
Excitation voltage	35 KV	35 KV
X-ray current	15 mA	20 mA
Divergent slit	3°	4°
Sollar slit for incident beam	MR	MR
Sollar slit for diffracted beam	MR and HR	MR and HR
Detector slit	0.1° and 0.02°	0.20 and 1°
Scanning speed	2°/min and 0.2°/min	2°/min and 1°/min
Ghart speed	1" /min	2 cm/min
Time constant	2 - 4 sec	2 - 4 sec

### III.2.6.a Temperature Dependence of Dielectric Properties:

Dielectric properties, capacitance and dissipation factor were measured using GR - 1620 A capacitance bridge assembly. The measuring frequency was 1 KHz at 0.5V. Before measuring, the sample was made flat on both ends and its diameter and thickness were measured accurately. It was then electroded with air dry silver paint on both the flat surfaces.

A high temperature sample holder with an access to three samples used for the temperature dependence of the dielectric properties is shown in Fig. III.2. The essential parts are the two electrodes, for the sake of simplicity, with associated connections and insulations built in an all metal unit. The low potential electrode is 1/8" thick steel plate of diameter 1.6" common to all the three samples. The steel plate is held rigidly by a support rod which is welded into the base plate at one end and the other end passes through the central hole in the top brass lid and is clamped by means of araldite. The high potential leads are made up of stainless steel wires insulated from outside in a glass tube over which a grounded metal sheath is wound. This lead assembly is again insulated in a bigger glass tube. A spring loaded arrangement presses these leads on the base plate which can be raised a bit to keep the specimens in position. The lower end of the wire is made into a bead to give proper contact on the electrode while the other end soldered to a positional plug of a three position switch.



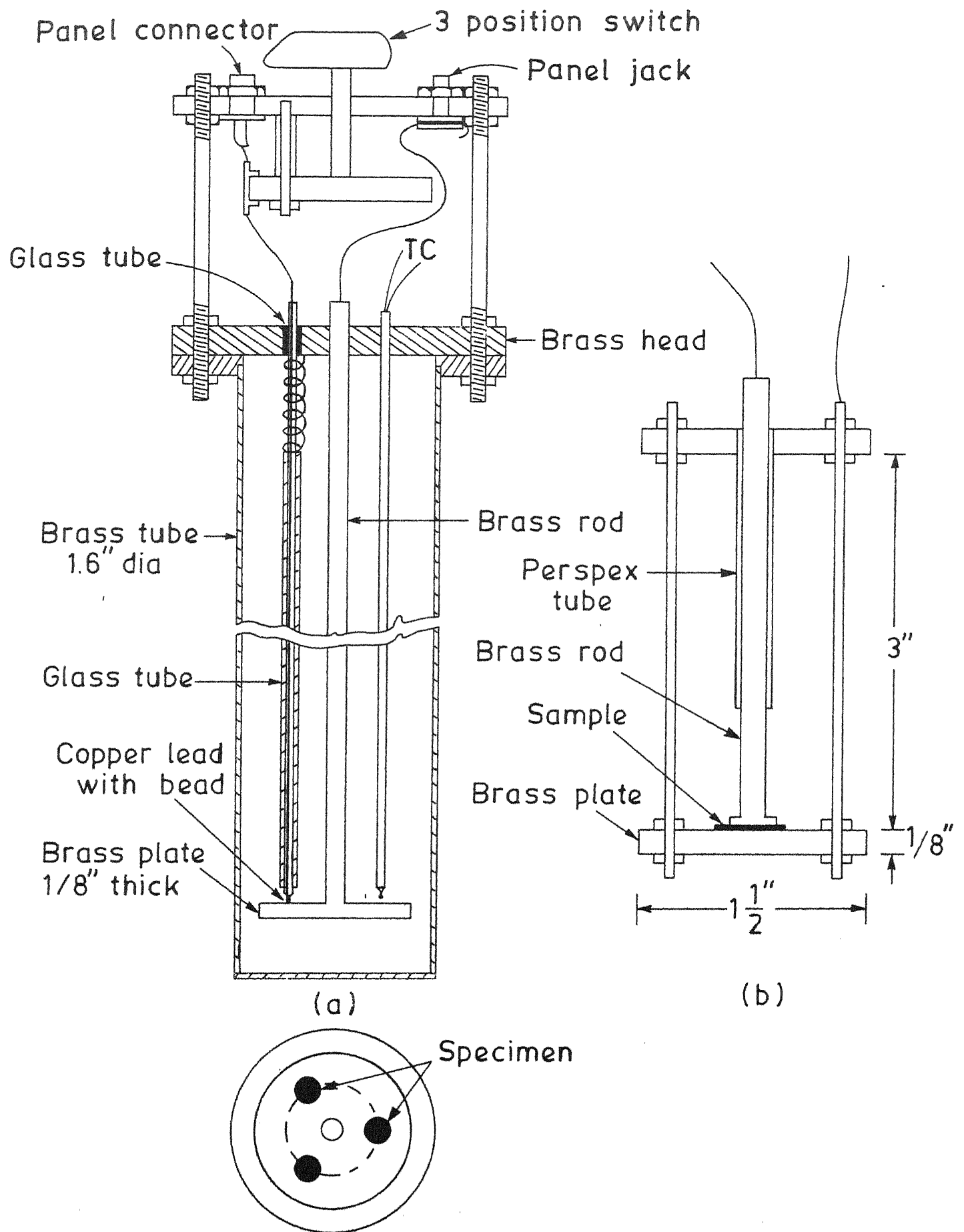


Fig. III-2 Sample holder for (a) high temperature dielectric measurements (b) DC bias studies.

The above assembly is inserted in a thin walled stainless steel tube, 2" in diameter and 18" in length. The panel carrying the connector, the jack and the switch is firmly attached to the top lid. The sample holder could be inserted into a small kanthal furnace. The heating rate ( $1^{\circ}/\text{min}$ ) was regulated manually by a variable autotransformer. The temperature was measured by a chromel-alumel thermocouple (located near the samples) with a Honeywell potentiometer. These measurements were done from room temperature to  $180^{\circ}\text{C}$  for most of the samples and upto  $410^{\circ}\text{C}$  for few samples, at an interval of  $10^{\circ}\text{C}$  from room temperature to  $10^{\circ}\text{C}$  below the Curie point and afterwards measurements were made every  $2^{\circ}$  till it crosses the Curie point.

### III.2.6.b D.C, bias effect on dielectric properties:

A different sample holder, small in size with both the high and low potential terminals free, was fabricated to study the d.c. bias effects and hysteresis loop characteristics. A sketch of the sample holder is shown in Figure III.2. The bottom electrode was a  $1/8$ " thick circular brass plate capable of transferring the majority of the heat generated within the sample to the immersant. Threaded ends of two brass rods ( $1/8$ " dia) passed through the base plate on either ends and clamped by means of a nut. The upper ends are threaded into a circular perspex disc on either ends. The upper electrode consists of an insulated brass rod threaded into the same perspex disc at the centre. The capacitor and the holder were kept immersed in dry silicone oil at room

temperature to provide protection against corona at the electrode edges and to facilitate in maintaining the sample temperature.

A high voltage d.c. supply 0.10 KV, PS 900, (Electronic Upkaran Vikas Co. Kanpur) were used to study the d.c. bias behaviour. The capacitance bridge was protected from the d.c. bias by a 100 M $\Omega$  resistor and 1  $\mu$ F blocking capacitor in series in a circuit similar to employed by Biggers et al (17) (Figure III.3). The value of the resistance was chosen to be two to three orders of magnitude higher than the reactance of the sample at 1 KHz. The capacitance value of the blocking capacitor was again chosen to be two to three orders of magnitude higher than the capacitance of the specimen.

The capacitance and dissipation factor ( $\tan \delta$ ) were measured at room temperature upto a bias field of 110-120 volts/mil. The behaviour was studied during both increasing and decreasing bias field. These measurements were made from 0 to 2400 V at an interval of 200 V.

#### III.2.6.c Frequency dependence of dielectric properties:

Type GR 1620 A capacitance bridge assembly to which a 1210 CRC oscillator unit was attached, was used to measure the frequency dependence of dielectric properties. The capacitance and dissipation factor were measured from 100 C to 100 KC frequency at 0.45 V, using the same sample holder described in section III.2.6.a.

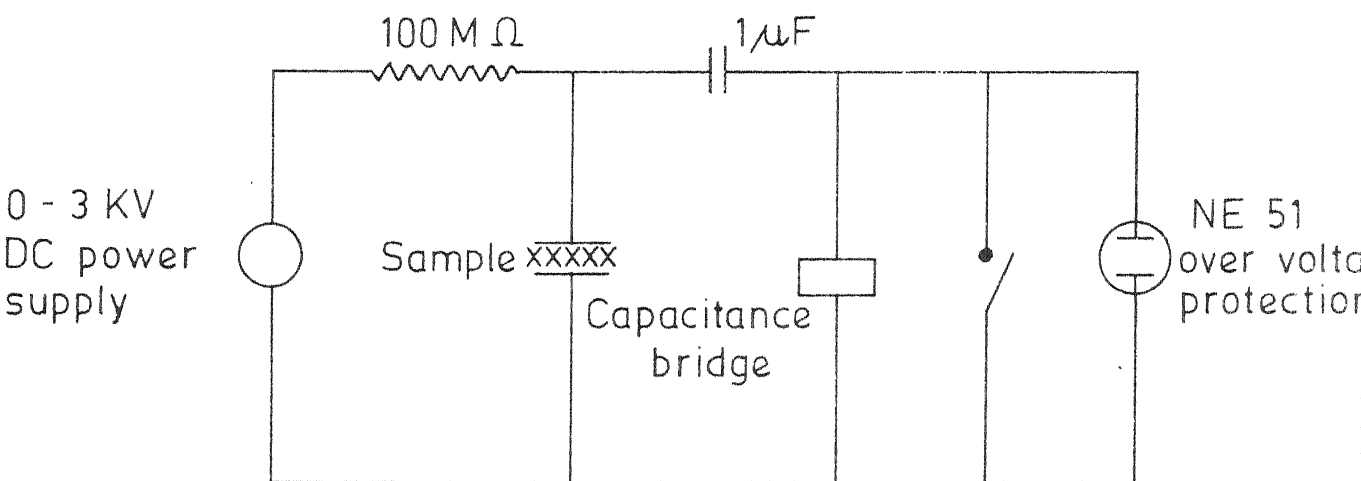


Fig. III-3- Circuit used for DC bias studies .

#### IV. RESULTS AND DISCUSSION

##### IV.1. Weight loss during sintering:

Weight loss measurements were made on all the sintered pellets. These results are shown in Tables IV.1 and IV.2.

Table IV.1 gives the weight loss measurements during the critical sintering experiments. It shows that the weight loss was almost constant at  $\leq 1$  pct. till  $1100^{\circ}\text{C}$ . This loss increases substantially from 1 to  $\geq 2$  pct. at higher temperatures and larger glass additions. For example, this change becomes prominent with 20 pct. glass addition at  $1200^{\circ}\text{C}$  with 30 pct. glass addition at  $1100^{\circ}\text{C}$  and with 40 pct. glass addition at  $1000^{\circ}\text{C}$ . Considering the whole weight loss was only due to the evaporation of the glass, a 20 pct. glass sample sintered at  $1200^{\circ}\text{C}$  with a weight loss of 2.3 pct. indicates that over 10 pct. of the glass added is evaporating after sintering. It indicates that most of the glass is still remaining in the sintered body.

Thermal analysis of the sample with 20 pct. glass addition (Fig. IV.1) heated upto  $1000^{\circ}\text{C}$  showed a total weight loss of 1.1 pct., which is comparable with the values given in Table IV.1.

Since the weight loss was not significant at temperatures below  $1100^{\circ}\text{C}$  for the next set of sintering experiments there data were given (Table IV.2) only for those samples which are sintered above  $1100^{\circ}\text{C}$ . These results also shows that the weight loss increases with increasing sintering

Table IV.1 : Sintered density (g/cc) and pct. wt. loss of liquid phase sintered BaTiO<sub>3</sub>

S.No.	Wt.pct. glass additive	Green density g/cc	Sintering Temperature														
			800°C			900°C			1000°C			1100°C			1200°C		
			Density	pct. wt. loss	pct. wt. loss	Density	pct. wt. loss	pct. wt. loss	Density	pct. wt. loss	pct. wt. loss	Density	pct. wt. loss	pct. wt. loss			
1	0.4	3.85	3.81	1.2	3.85	1.13	3.89	1.09	3.95	1.4	4.33	1.15					
2	2.0	3.83	3.84	0.79	3.86	1.02	3.93	1.15	4.16	1.09	4.62	1.13					
3	10.0	3.88	3.88	1.03	4.04	0.90	4.59	0.77	5.16 (86pct td)	1.06	5.49 (91.2 pct td)	-					
4	20.0	4.16	4.15	1.1	4.21	1.04	5.22 (86.8 pct. td.)	0.91	5.94 (98.7 pct. td.)	1.15	4.62	2.33					
5	30.0	4.41	4.49	1.05	4.52	0.9	5.24 (87.1 pct. td.)	0.98	5.70 (94.7 pct. td.)	1.57	4.74	2.03					
6	40.0	4.35	4.59	1.53	4.85	1.15	4.65	1.82	-	-	-	-					

Table IV.2 : Weight loss data of liquid phase sintered  $\text{BaTiO}_3$ 

pot. glass addition	pct. wt. loss for sintering time, hr.			
	1/6	1/2	1	2
Sintering Temperature 1150°C				
10	1.87	2.33	2.46	2.27
2	0.73	1.02	2.39	2.4
0.4	0.65	0.97	1.78	1.85
Sintering Temperature 1200°C				
2	2.43	2.50	2.20	2.35
0.4	1.78	1.77	1.69	1.64

temperature and also with increasing glass addition.

#### IV.2 Thermal Analysis:

Results of the simultaneous DTA, DTG and TGA studies of the mixture of  $\text{BaTiO}_3$  and 20 pct. glass powders sample are shown in Figure IV.1. The total weight of the sample was 2.019 gm.

The DTA curve shows two transformations, one at  $350^\circ\text{C}$  and another at  $830^\circ\text{C}$ . The transformation at  $350^\circ\text{C}$  may be due to the crystallization point of the glass. This glass has a melting point around  $700\text{--}750^\circ\text{C}$  (Table II.2), which is not clearly resolved in the DTA plot. The second transformation at  $830^\circ\text{C}$  appears to be due to the reaction of the glass with  $\text{BaTiO}_3$ , as discussed below.

TGA plot shows that there is a gradual weight loss ( $\sim 0.85$  pct.) till  $350^\circ\text{C}$ , which may be due to the evaporation of the moisture and binder. The weight change was constant till  $750^\circ\text{C}$ . This weight loss ( $\sim 0.85$  pct.) may be compared with the loss ( $\sim 1$  pct.) observed in the sintering experiments upto  $1000^\circ\text{C}$ . Around  $900^\circ\text{C}$  there is a sudden additional weight loss ( $\sim 0.45$  pct.).

To confirm these results two experiments were carried out. In one experiment X-ray diffraction studies were carried out with samples of  $\text{BaTiO}_3$  and 20 pct. glass mixture which were heated to 725, 800, 900, 1000 and  $1100^\circ\text{C}$  for 15 min. For  $725^\circ\text{C}$  samples alone, 15min. and



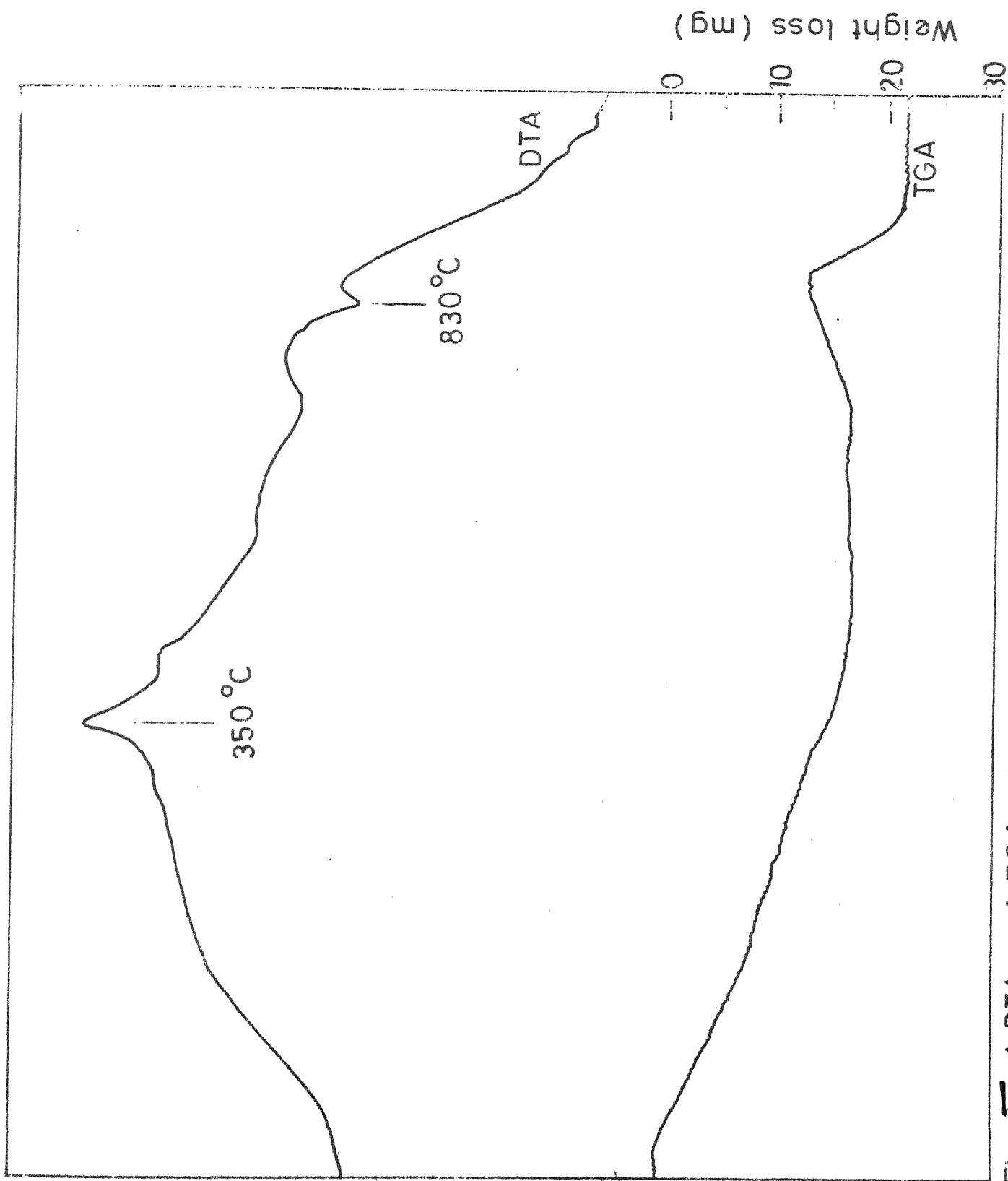


Fig. IV-1 DTA and TGA plots of  $\text{BaTiO}_3$  and 20% glass mixture.

2h heating time were provided. These results are discussed in detail in section IV.5. The diffraction pattern of the sample heated upto  $725^{\circ}\text{C}$  for 15min showed the presence of crystallized glass in the form of  $12\text{Bi}_2\text{O}_3 \cdot \text{B}_2\text{O}_3$  along with  $\text{BaTiO}_3$ . Where as at 2h the glass started reacting with  $\text{BaTiO}_3$  and the diffraction pattern showed the presence of  $\text{BaBi}_4\text{Ti}_4\text{O}_{15}$  and crystallized glass along with  $\text{BaTiO}_3$ . The sample heated upto  $800^{\circ}\text{C}$  showed the presence of  $\text{BaBi}_4\text{Ti}_4\text{O}_{15}$  phase along with  $\text{BaTiO}_3$ , but no crystallized glass phase was observed. It indicates that the glass is reacting with  $\text{BaTiO}_3$  forming  $\text{BaBi}_4\text{Ti}_4\text{O}_{15}$  around  $800^{\circ}\text{C}$ . The diffraction patterns at  $900^{\circ}\text{C}$ ,  $1000$  and  $1100^{\circ}\text{C}$  show that the formation of  $\text{BaBi}_4\text{Ti}_4\text{O}_{15}$  reaches a maximum at  $900^{\circ}\text{C}$  and its amount decreases with increasing temperature.

In another experiment a  $\text{Bi}_2\text{O}_3 \cdot \text{B}_2\text{O}_3$  (74:26) glass piece was heated in the furnace at  $525^{\circ}\text{C}$  for 8h. After cooling the sample was crystallized in  $12\text{Bi}_2\text{O}_3 \cdot \text{B}_2\text{O}_3$  and  $2 \text{Bi}_2\text{O}_3 \cdot \text{B}_2\text{O}_3$  form ( discussed in section IV.5). So from this experiment it can be concluded that the peak at  $350^{\circ}\text{C}$  in DTA plot may be due to the crystallization of glass.

From the DTA, TGA and X-ray diffraction studies it can therefore be concluded that the glass reacts with  $\text{BaTiO}_3$  forming  $\text{Ba Bi}_4\text{Ti}_4\text{O}_{15}$  at about  $725^{\circ}\text{C}$  and its amount reaches a maximum at  $900^{\circ}\text{C}$  and  $\text{BaBi}_4\text{Ti}_4\text{O}_{15}$  appears to be decomposing with increasing temperature beyond  $900^{\circ}\text{C}$ .

#### IV. 3 Density:

Sintered samples were investigated using density measurements to study the effect of various parameters on sintering.

##### IV.3.1 Effect of Glass Addition:

Effect of glass addition on density was studied using density measurements on samples with 0.4, 2, 10, 20, 30 and 40 Wt. pct glass, sintered at 800, 900, 1000, 1100 and 1200°C for 2h. Particle size of sintered powders were 13  $\mu\text{m}$  Ba Ti O<sub>3</sub> and 17  $\mu\text{m}$  glass. These results are given in Table IV.1 and shown in Figs. IV.2 and 3. All the densities measured in this case were geometrical densities except in those cases where it was not possible due to the sticking of the pellets to each other. Fig. IV.2 shows density vs glass addition for the samples sintered at different temperatures. Fig. IV.3 shows density vs sintering temperatures for the samples with different glass addition. From these figures, it can be seen that to get densities greater than 85% theoretical density of Ba Ti O<sub>3</sub> ( 6.02 g/cc) at 1000°C, a minimum of 20% glass is necessary and on the other hand with 10% glass addition, a minimum sintering temperature of 1100°C is necessary. The maximum density obtained was 5.22 g/cc (87% td) for the samples with 20% glass addition sintered at 1000°C for the particular sintering parameters employed. It can be observed

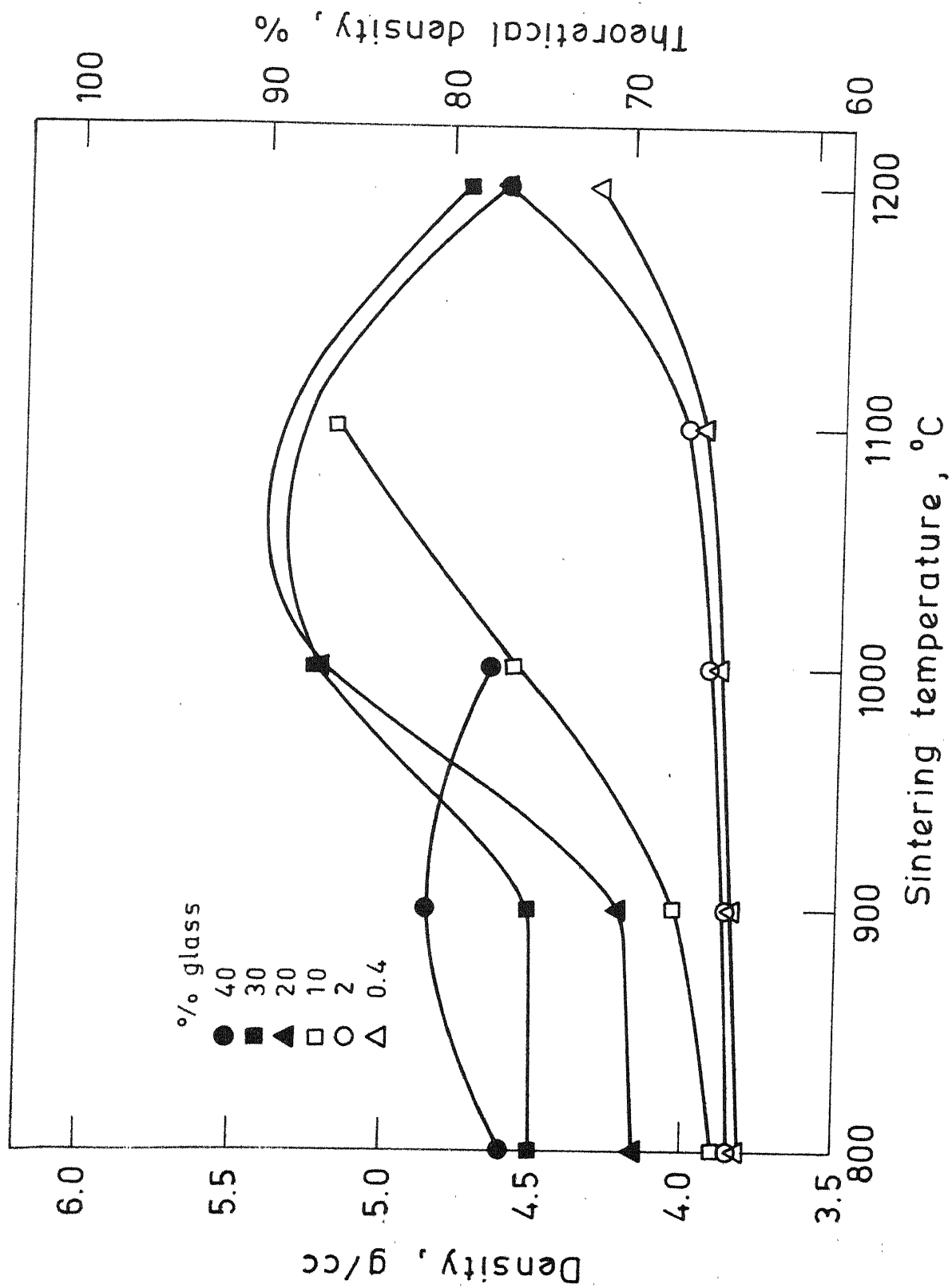


Fig. IV-2 Density vs sintering temperature of  $\text{BaTiO}_3$  with different amounts of glass addition (sintering time : 2 hours)

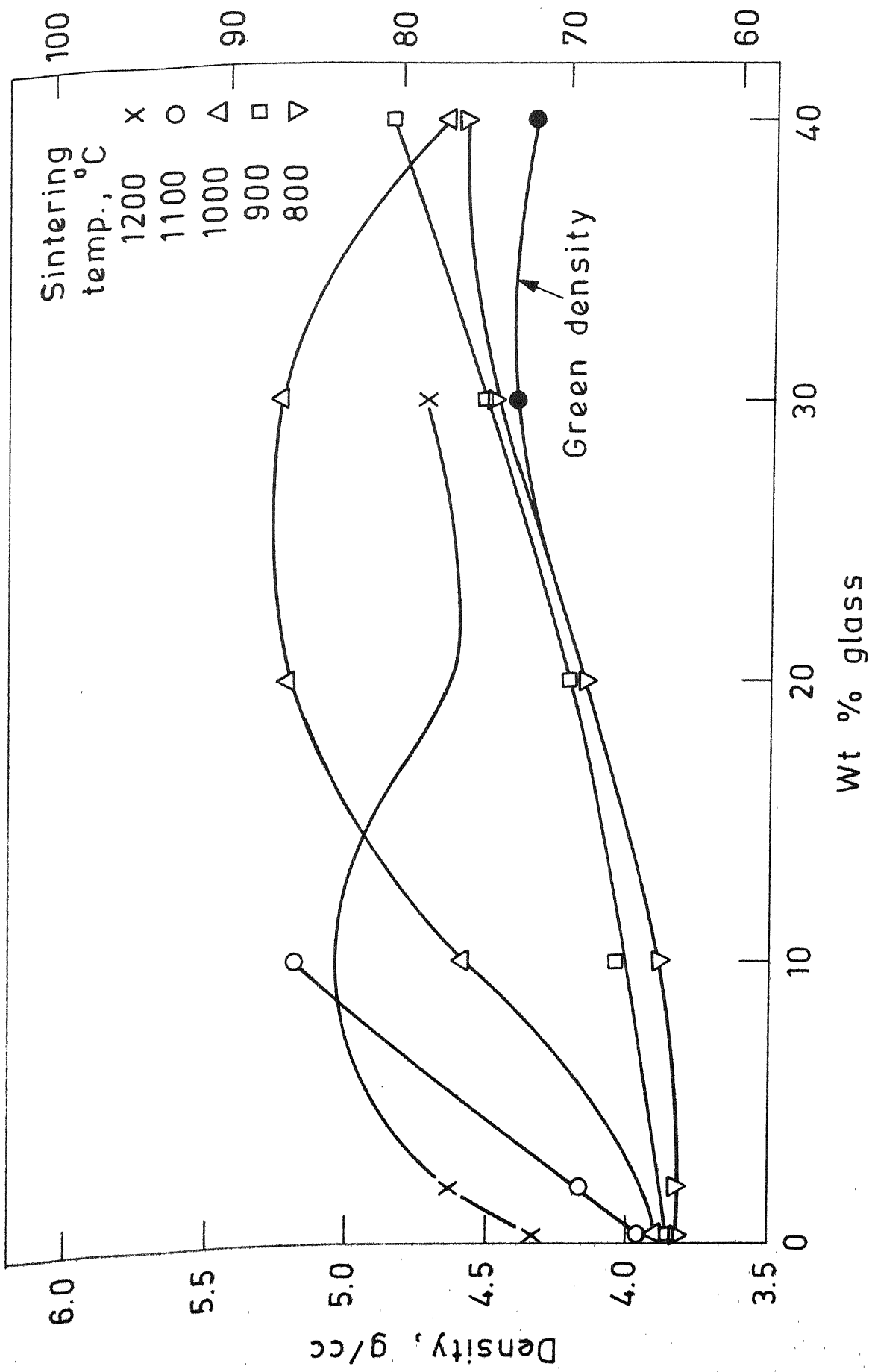


Fig. IV-3 Density vs wt % glass addition to  $\text{BaTiO}_3$  at different sintering temperatures (sintering time : 2 hours).

from these figures, that for the samples with 20% and higher glass additions, the densities were decreasing at higher sintering temperatures (above  $1100^{\circ}\text{C}$ ). Visual examination of these samples with 20% and 30% glass sintered at  $1100^{\circ}\text{C}$  and above showed that a layer of glass was collected on the bottom surface and the pellet was distorted in shape. This clearly shows that at  $1100^{\circ}\text{C}$  the viscosity of the glass is too low and it is flowing out of the pellet. From the weight loss data shown in Table IV.1 it can be observed that for 20 and 30% samples the weight loss was less than 1% till  $1000^{\circ}\text{C}$ , but afterwards it is increasing significantly from 1 to 2% at  $1200^{\circ}\text{C}$  for 20% sample and at  $1100^{\circ}\text{C}$  for 30% sample. It indicates that the glass is evaporating at these temperatures. This evaporation and oozing out of the glass must be the reasons for decrease in densities of these samples at higher sintering temperatures. It can also be observed from this figure that with 0.4 and 2% glass additions a sintering temperature of more than  $1200^{\circ}\text{C}$  is necessary to get reasonable densities.

So from these density results it can be concluded that for liquid phase sintering of  $\text{Ba Ti O}_3$  at  $1000\text{--}1100^{\circ}\text{C}$  a minimum of 10 to 20% glass addition is necessary, and also it is not possible to decrease the sintering temperature by increasing the amount of glass above 20% using the same sintering

parameters employed here.

#### IV.3.2 Effect of sintering temperature and time:

To study the densification process more closely sintering experiments were done on 20%, 10%, 2% and 0.4% glass samples with respect to temperature and time. Sintering temperatures, times and particle sizes of these different batches are given in Table IV.3 along with the green densities (average of 5 pellets) <sup>geometrical densities (avg of 5 pellets)</sup> and the displacement densities (based on one sample). The reason for considering both the densities is, that in the case of geometrical density it includes both open and closed porosity (total porosity), where as in the case of displacement densities it will include only the closed porosity. Table IV.4. gives these porosity data for the samples with 10% glass sintered at different temperatures and times. Percent theoretical density calculated by taking 6.02 g/cc as the theoretical density of  $\text{Ba Ti O}_3$ , without considering the glass addition is shown with-in brackets next to each density value. These density results are plotted in Figs. IV. 4-8. Fig. IV.4 show the geometrical and the displacement densities for the samples with 20% glass addition, sintered at 1000°C for 1/2, 1 and 3h. and at 1100°C for 1/6, 1/2 and 1h. This figure shows the displacement densities are more than geometrical

densities for all these samples as expected. It may be due to the evaporation of some of the glass from the surface at these temperatures causing more open porosity. It can also be observed from this figure that at  $1000^{\circ}\text{C}$  the density is increasing sharply between  $1/2$  and  $1\text{h.}$  and afterwards it is gradual till  $3\text{h.}$  where-as at  $1100^{\circ}\text{C}$  most of the densification is taking place with-in the first  $10\text{ min.}$  and afterwards there is very little increase in density with sintering time. This may be because of the viscosity of the glass being lower at  $1100^{\circ}\text{C}$  than  $1000^{\circ}\text{C}$ , facilitating easy densification with in a short time at  $1100^{\circ}\text{C}$ . The reason for the decrease in the displacement densities at  $1100^{\circ}\text{C}$  with increase in sintering time may be due to the oozing out of the glass from the pellet, which was observed by visual examination of the pellet. Fig. IV.5 shows the geometrical and the displacement densities for the samples with  $10\%$  glass addition sintered at  $1000$  and  $1100^{\circ}\text{C}$  for  $1/6$ ,  $1/2$ ,  $1$  and  $2\text{h.}$  Here the particle sizes of  $\text{Ba Ti O}_3$  and glass used are  $13\mu$  and  $17\mu$  respectively. It can be observed from these figures that at  $1000^{\circ}\text{C}$  the densities are increasing gradually with increasing sintering time till  $2\text{h.}$  where-as at  $1100^{\circ}\text{C}$  most of the densification is taking place with-in the first  $10\text{ min}$  and there is gradual increase in density between  $10\text{ min}$  and  $1/2\text{h.}$  and afterwards there is very little increase in density till  $2\text{h.}$  Here also it can be observed that the displacement densities



are more than geometrical densities for all the samples. Table IV.4. shows that as the sintering temperature increases from 1000-1100°C the open porosity is increasing while the closed porosity decreases. It clearly indicates that the glass is evaporating at 1100°C, causing more open porosity. Figs. IV. 6 and 7 shows the geometrical and the displacement densities for the samples with 10% glass, sintered at 1000, 1050, 1100 and 1150°C for 1/6, 1/2, 1 and 2h. Here the initial particle sizes of Ba Ti O<sub>3</sub> and glass are 5  $\mu$ m and 4  $\mu$ m respectively. These figures also show same trend as in Fig. IV.5. At 1000°C the densities are increasing gradually with increasing sintering time till 2h. At 1050 and 1100°C densities are increasing sharply upto. 1h and afterwards there is very little increase till 2h. Where-as in the case of 1150°C it can be observed that most of the densification is taking place with-in the first 10 min. and afterwards there is very little increase in density. Fig. IV.6 shows that the geometrical densities are better for the samples sintered at 1050°C than those samples sintered at 1000, 1100 and 1150°C, but Fig. IV.7 shows that the displacement densities are increasing with increasing sintering temperature. This implies that while the closed porosity decreases with increasing temperature, the open porosity reaches a minimum at 1050°C and increases at 1100

and 1150°C presumably due to the oozing out or evaporation of glass.

Fig. IV. 8. shows the geometrical densities for the samples with 2% and 0.4% glass addition, sintered at 1100, 1150 and 1200°C for 1/6, 1/2, 1 and 2h. This figure shows that the densities are increasing gradually for all the samples with increasing sintering temperature and time. It can also be observed from this figure that the densities are slightly better for 0.4 % samples than for 2% samples. This may be due to the greater evaporation of the glass from the 2% glass sample at these high temperatures. Weight loss data given in Table IV.2. also shows the weight loss for 2% samples was more than for the 0.4% samples. From these density results it can be concluded that with 20% glass addition a sintering temperature of 1100°C may be high because of the problem of glass flowing out <sup>and</sup> ~~at~~ 1000°C seems to be too low, so that the ideal temperature for these samples may be in between these two. In the case of 10% glass, samples sintered at 1050°C are showing better densities, and also a sintering time of 1h is sufficient at this temperature. With 0.4 and 2% glass addition, to get reasonable densities ( $\sim 85\%$  td) higher sintering temperatures e.g. 1200°C are necessary.

Table IV.3 Density of Green and Sintered Pellets.

Batch No.	Sample	Sintering temp. °C	Sintering time	Green density g/cc	Sintered Geometrical	Density (g/cc) Displacement
1.	BaTiO <sub>3</sub> with 20% glass using 13/um BaTiO <sub>3</sub> and 17/um glass	1000	1/2h	4.35 (72.3)	4.66 (77.4)	5.03 (83.6)
			1 h	4.33 (71.9)	5.02 (83.4)	5.18 (86.0)
			3 h	4.36 (72.4)	5.16 (85.7)	5.20 (86.4)
		1100	10min	4.33 (71.9)	5.10 (84.7)	5.41 (89.9)
			1/2 h	4.35 (72.3)	5.15 (85.5)	5.34 (88.7)
			1 h	4.35 (72.3)	5.18 (86.0)	5.25 (87.2)
2.	BaTiO <sub>3</sub> with 10% glass using 13/um BaTiO <sub>3</sub> and 17/um glass	1000	10min	4.20 (69.8)	4.78 (79.4)	4.84 (80.4)
			1/2 h	4.21 (69.9)	4.87 (80.9)	4.94 (82.1)
			1 h	4.25 (70.6)	5.03 (83.6)	5.08 (84.4)
			2 h	4.22 (70.1)	5.26 (87.4)	5.39 (89.5)
		1100	10min	4.28 (71.1)	5.06 (84.1)	5.25 (87.2)
			1/2 h	4.28 (71.1)	5.24 (87.0)	5.54 (92.0)
			1 h	4.23 (70.3)	5.25 (87.2)	5.56 (92.4)
			2 h	4.24 (70.4)	5.27 (87.5)	5.58 (92.7)
3.	BaTiO <sub>3</sub> with 10% glass using 5/um BaTiO <sub>3</sub> and 4/um glass	1000	10min	4.42 (73.4)	4.68 (77.7)	4.41 (73.8)
			1/2 h	4.41 (73.3)	4.79 (79.6)	4.75 (78.9)
			1 h	4.43 (73.6)	4.86 (80.7)	4.81 (79.9)
			2 h	4.42 (73.4)	5.01 (83.2)	5.28 (87.7)
		1050	10min	4.43 (73.6)	5.20 (86.4)	5.40 (89.7)
			1/2 h	4.43 (73.6)	5.32 (88.4)	5.48 (91.0)
			1 h	4.39 (72.9)	5.40 (89.7)	5.50 (91.4)
			2 h	4.39 (72.9)	5.37 (89.2)	5.54 (92.0)
		1100	10min	4.45 (73.9)	5.10 (84.7)	5.43 (90.2)
			1/2 h	4.44 (73.8)	5.25 (87.2)	5.61 (93.2)
			1 h	4.42 (73.4)	5.30 (88.0)	5.78 (96.0)
			2 h	4.42 (73.4)	5.27 (87.5)	5.79 (96.2)
		1150	10min	4.39 (72.9)	5.27 (87.5)	5.49 (91.2)
			1/2 h	4.40 (73.1)	5.35 (88.9)	5.63 (93.5)
			1 h	4.39 (72.9)	5.30 (88.0)	5.78 (96.0)
			2 h	4.41 (73.3)	5.31 (88.2)	5.91 (98.2)

contd.....

Batch No.	Sample	Sinter- ing temp. °C	Sinter- ing time	Green density g/cc	Sintered Geometrical Density (g/cc)	Density (g/cc) Displace- ment.
4.	BaTiO <sub>3</sub> with 2% glass using 2 $\mu$ m BaTiO <sub>3</sub> and 2.5 $\mu$ m glass	1100	10min	3.95 (65.6)	4.55	(75.6)
			1/2 h	3.96 (65.8)	4.56	(75.7)
			1 h	3.93 (65.3)	4.66	(77.4)
			2 h	3.94 (65.4)	4.70	(78.1)
		1150	10min	3.84 (63.8)	4.7	(78.1)
			1/2 h	3.98 (66.1)	4.81	(79.9)
			1 h	3.98 (66.1)	4.91	(81.6)
			2 h	4.05 (67.3)	5.08	(84.4)
		1200	10min	3.98 (66.1)	5.01	(83.2)
			1/2 h	4.00 (66.5)	5.04	(83.7)
			1 h	4.02 (66.8)	5.10	(84.7)
			2 h	4.02 (66.8)	5.20	(86.4)
5.	BaTiO <sub>3</sub> with 0.4% glass using 2 $\mu$ m BaTiO <sub>3</sub> and 2.5 $\mu$ m glass	1100	10min	4.07 (67.6)	4.55	(75.6)
			1/2 h	3.97 (65.9)	4.65	(77.2)
			1 h	3.99 (66.3)	4.52	(75.1)
			2 h	4.18 (69.4)	4.88	(81.1)
		1150	10min	4.13 (68.6)	5.03	(83.6)
			1/2h	4.12 (68.4)	5.08	(84.4)
			1 h	4.13 (68.6)	5.10	(84.7)
			2 h	4.11 (68.3)	5.22	(86.7)
		1200	10min	3.94 (65.4)	4.93	(81.9)
			1/2 h	3.98 (66.1)	5.05	(83.9)
			1 h	4.17 (69.3)	5.27	(87.5)
			2 h	4.19 (69.6)	5.45	(90.5)

IV. 4 Porosity change with sintering temperature and time.

Sample	Sintering temperature °C	Sintering Time (h)	Total porosity %	Closed porosity %	open porosity %
BaTiO <sub>3</sub> with 10% glass using 13 $\mu$ m BaTiO <sub>3</sub> and 17 $\mu$ m glass	1000	1/6	20.6	19.6	0.99
		1/2	19.1	17.9	1.16
		1	16.4	15.6	0.83
		2	12.6	10.5	2.1
	1100	1/6	15.9	12.3	3.16
		1/2	12.9	7.9	5.0
		1	12.8	7.6	5.15
		2	12.5	7.3	5.15
	BaTiO <sub>3</sub> with 10% glass using 5 $\mu$ m BaTiO <sub>3</sub> 4 $\mu$ m glass	1/6	22.2	26.2	-
		1/2	20.4	21.1	-
		1	19.3	20.1	-
		2	16.8	12.2	4.5
	1050	1/6	13.6	10.3	3.32
		1/2	11.6	8.9	2.32
		1	10.3	8.6	1.66
		2	10.8	8.0	2.82
	1100	1/6	15.3	9.8	5.48
		1/2	12.8	6.8	6.31
		1	12.0	4.0	7.97
		2	12.5	3.8	8.6
	1150	1/6	12.5	8.8	3.65
		1/2	11.1	6.5	4.65
		1	11.9	4.0	7.77
		2	11.7	1.8	1.97

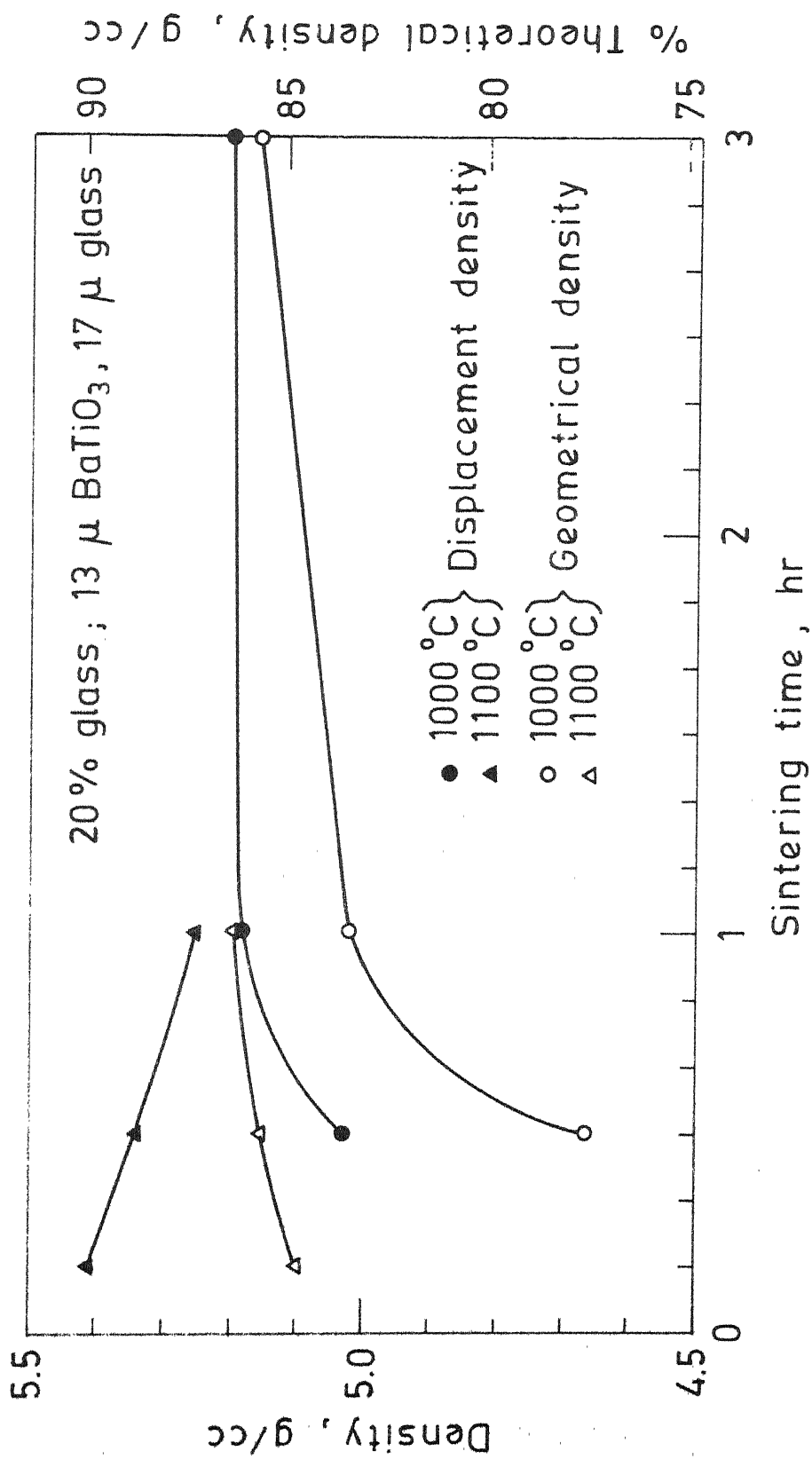
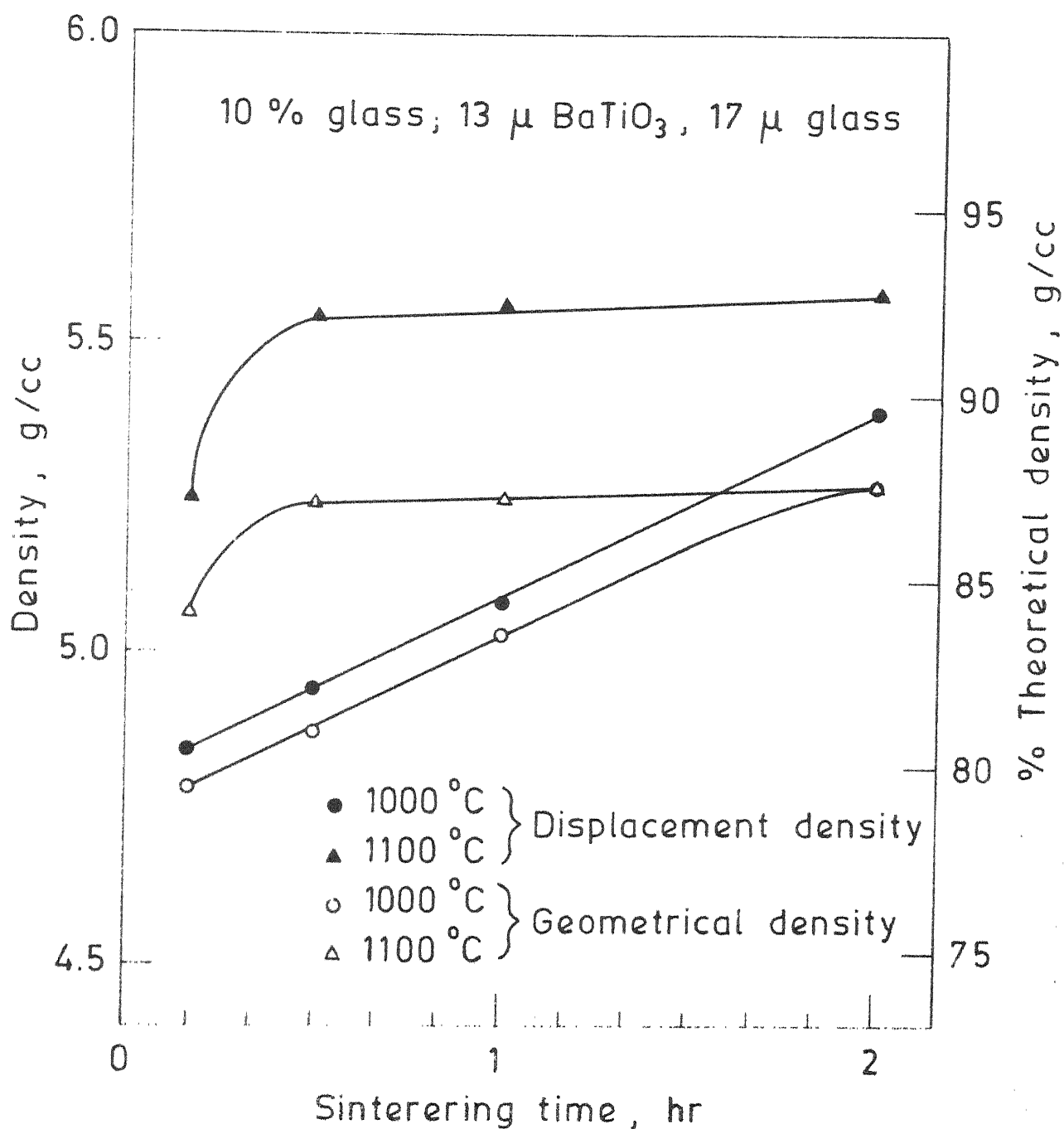
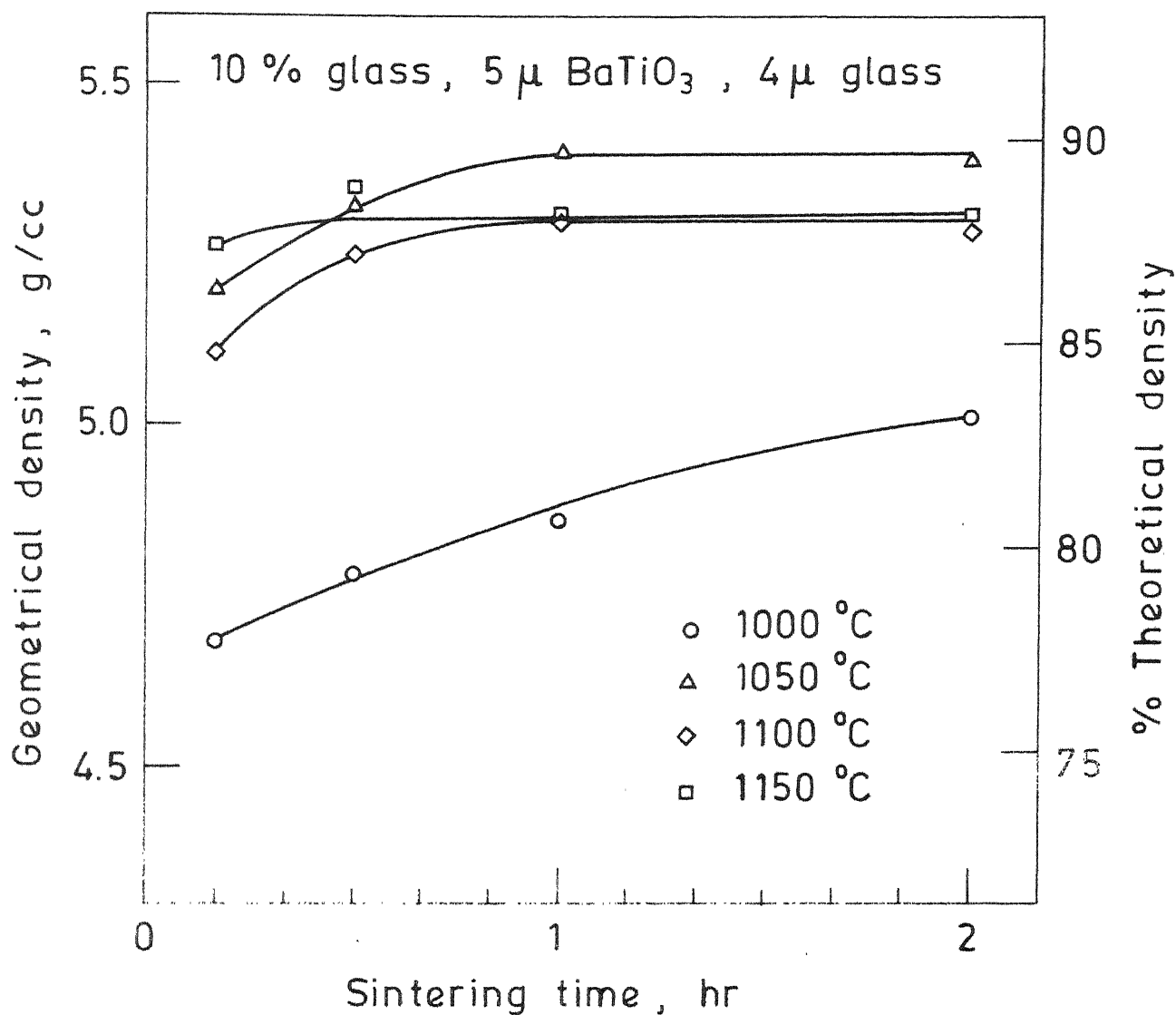


Fig. IV-4- Densification of BaTiO<sub>3</sub> as a function of sintering time with 20 % glass addition.



g. IV-5 - Densification of BaTiO<sub>3</sub> as a function of sintering time with 10 % glass addition.



g. IV 6 - Geometrical density vs sintering time for BaTiO<sub>3</sub> with 10 % glass addition at different sintering temperatures.



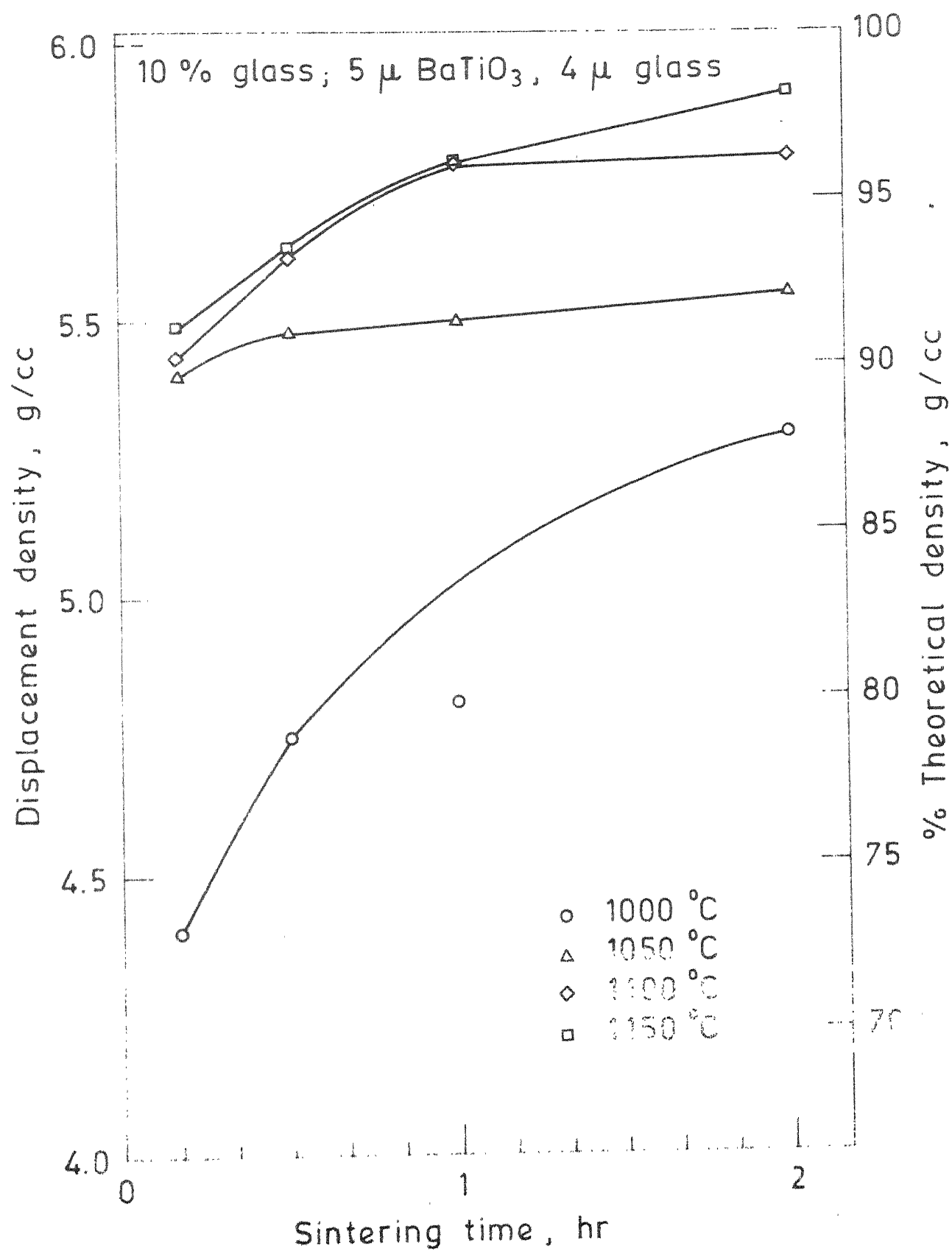


Fig. IV-7 - Displacement density vs sintering time for BaTiO<sub>3</sub> with 10 % glass addition at different sintering temperatures.

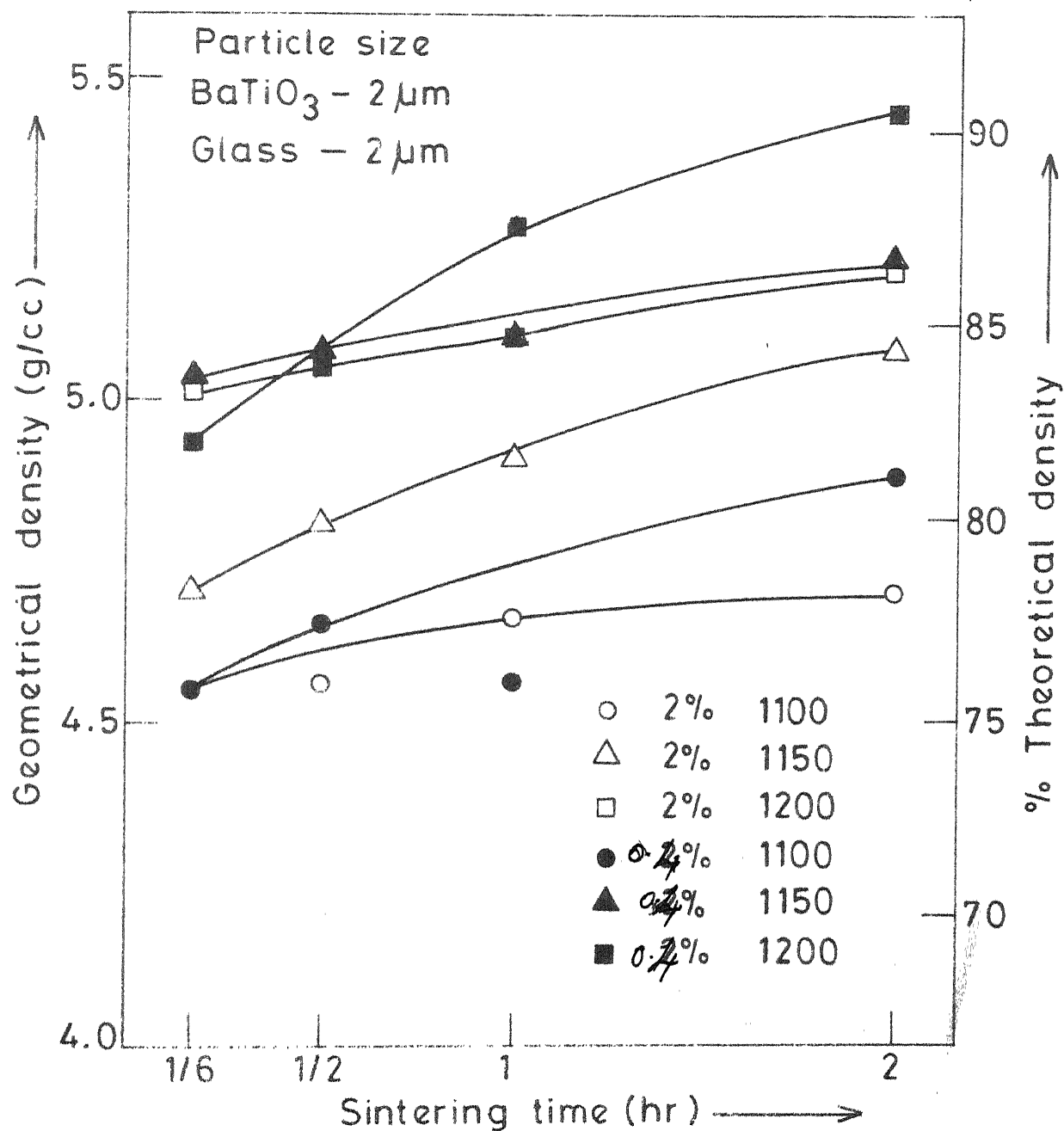


Fig. IV-8 Geometrical density vs. sintering time for BaTiO<sub>3</sub> with 0.4 and 2% glass addition at different temperatures.

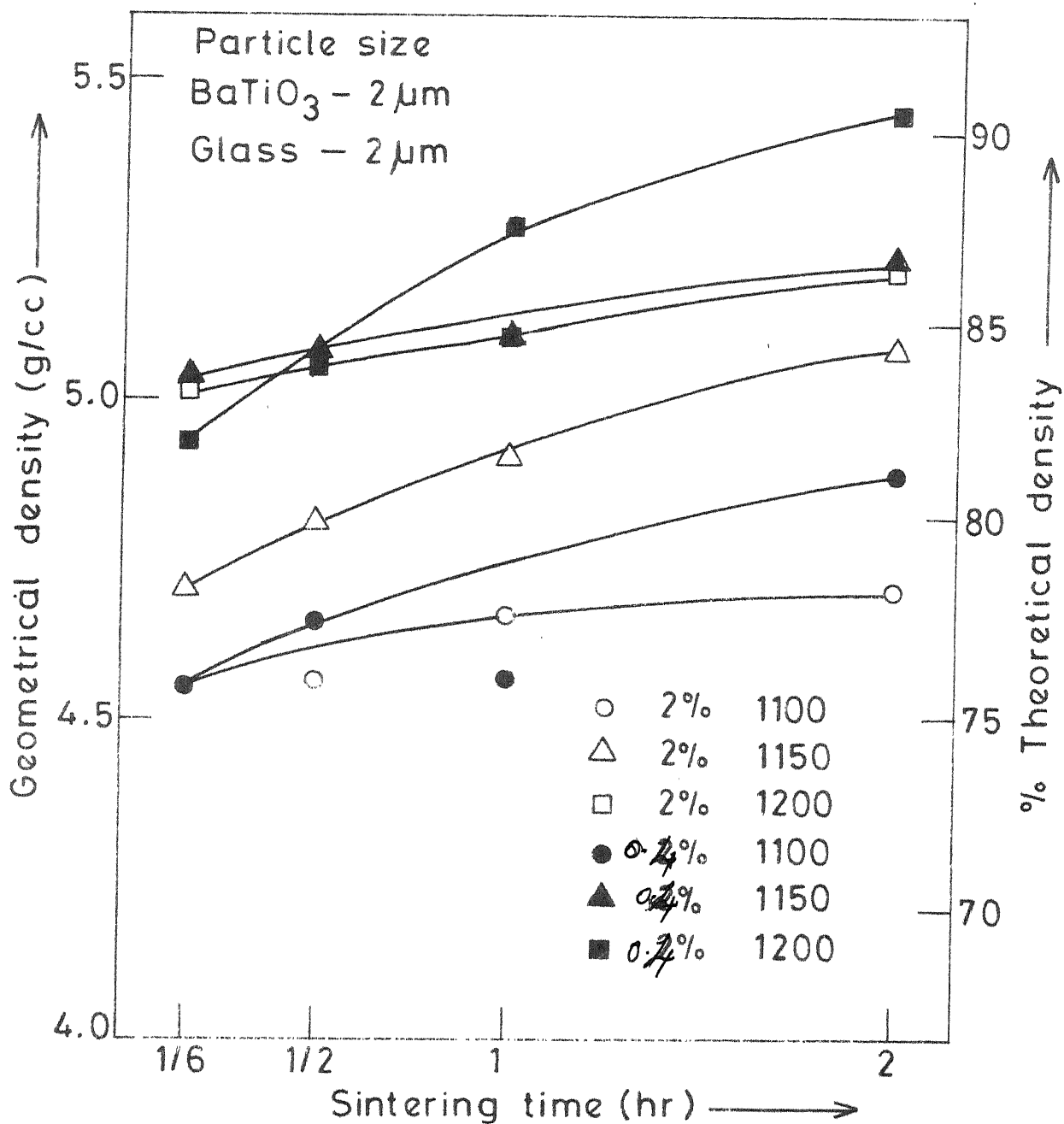


Fig. IV-8 Geometrical density vs. sintering time for BaTiO<sub>3</sub> with 0.4 and 2% glass addition at different temperatures.

#### IV. 3.3 Effect of particle size:

Effect of particle size on densification was studied on 10% glass samples sintered at 1000 and 1100°C for 1/6, 1/2, 1 and 2h. For this purpose two batches with different particle sizes of Ba Ti O<sub>3</sub> and glass ( 13/μm Ba Ti O<sub>3</sub> + 17 /μm glass and 5 /μm Ba Ti O<sub>3</sub> + 4 /μm glass) were used . Fig. IV. 9 shows the geometrical densities of these samples as a function of sintering temperature and time. It can be observed from this figure that there is no marked difference in densification in the particle size ranges used particularly at 1100°C. Still lower particle size may have some effect.

#### IV. 3.4 Effect of rate of heating:

Effect of rate of heating on densification was studied on samples with 10% glass additions sintered at 1000, 1050 and 1100°C for 10 min and 2h with three different heating rates namely 2h 40min, 5h 20min, and 8h. Particle size of the powders used in this study were 5/μm Ba Ti O<sub>3</sub> and 4/μm glass. These results are given in Table IV.5. These results show that for 8h heating schedule the densities are slightly better than at 2h 40min. But the increase in densities was not too large and there may not be much advantage in employing 8h heating schedule which is three times that of the usual 2h 40min. heating schedule used in all sintering experiments.

TABLE IV.5

Effect of rate of heating on densification

% glass	Sintering temperature (°C)	Sintering Time (h)	Heating rate (time taken to reach soaking zone)	Density (Geometrical) g/cc
10%	1000	1/6	2h 40 min.	4.68
			5h 20min.	4.64
			8h	4.75
	1000	2	2h 40min.	5.01
			5h 20min.	5.02
			8h.	5.26
	1050	1/6	2h 40min	5.20
			5h 20min.	5.18
			8h.	5.20
	1050	2	2h 40min.	5.37
			5h 20min.	5.39
			8h.	5.50
	1100	1/6	2h 40min.	5.10
			5h 20min.	5.36
			8h.	5.38
	1100	2	2h 40min.	5.27
			5h 20min.	5.43
			8h.	5.43

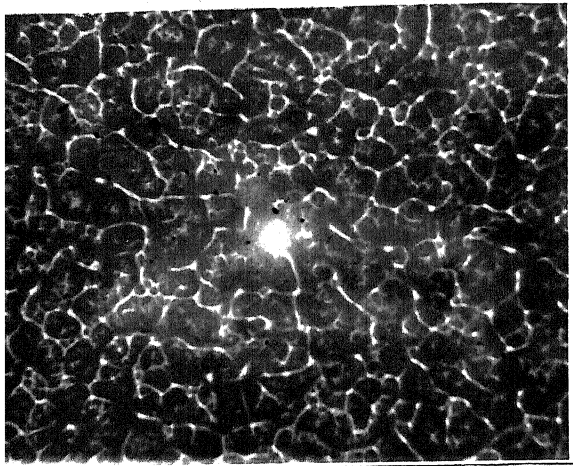
#### IV. 4. Microstructural Observation:

Samples were prepared for microstructural observation to study i) the effect of glass addition and ii) the effect of sintering temperature and time on microstructure, so as to understand the reaction Kinetics during liquid phase sintering of  $\text{Ba Ti O}_3$  with bismuth borate glass.

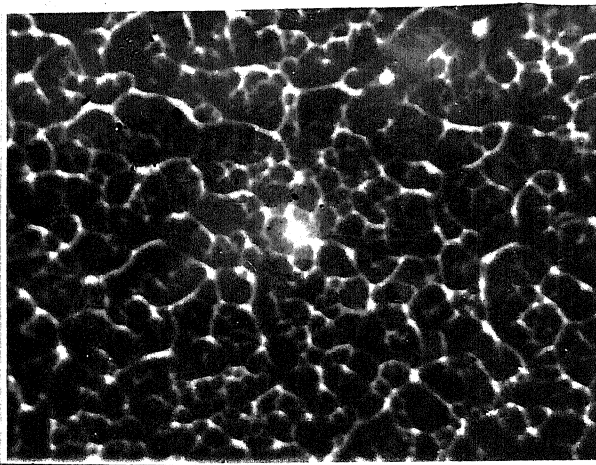
Microstructures of the sintered samples containing 0.4, 2, 10, 20 and 30 wt pct glass are shown in Figs. IV 10-14. Sintering temperature was  $1200^\circ\text{C}$  for 0.4 and 2% samples and  $1100^\circ\text{C}$  for 10, 20 and 30% samples. Sintering time was constant at 2 h for all these samples.

These figures show that a glassy phase is distributed uniformly around the grains as a coating over the grains. It can be observed that the amount of this glassy phase is increasing with increasing glass content for a fixed sintering temperature and time as expected.

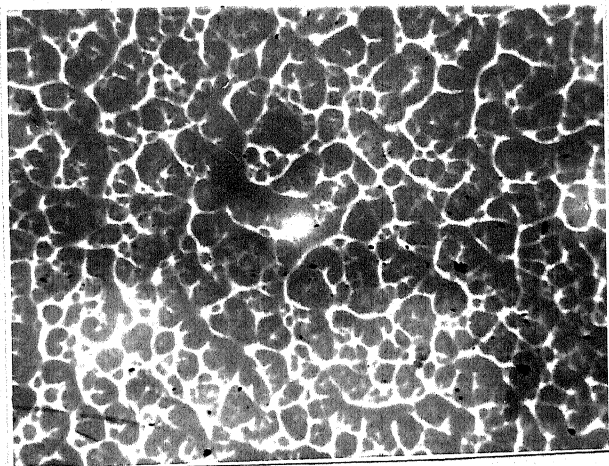
Effect of sintering temperature and time on microstructure was studied on the samples with 10% glass sintered at  $1000$  and  $1100^\circ\text{C}$  for  $1/6$ ,  $1/2$ , 1 and 2 h. The average particle size of  $\text{Ba Ti O}_3$  and glass used for making these samples were 13 and 17  $\mu\text{m}$  respectively. Figs. IV 15-18 show the microstructures of the samples sintered at  $1000^\circ\text{C}$  for 10 min. to 2 h, while Figs. IV.19-22 show the microstructures of the samples sintered at  $1100^\circ\text{C}$  for 10 min to 2 h. Average grain size and boundary layer thickness were measured quantitatively under a microscope at 250 magnification for all these samples. Measurement .....



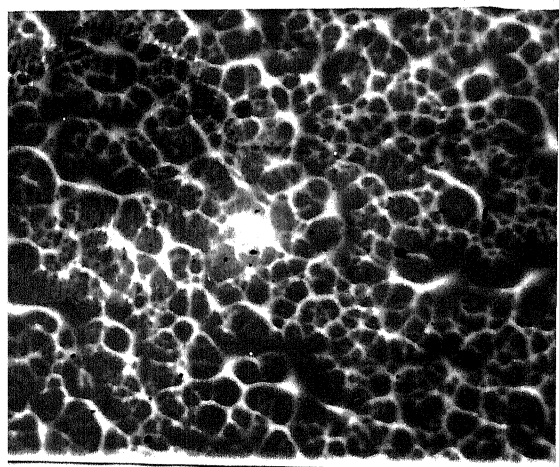
IV.10 0.4%/1200°C/3h



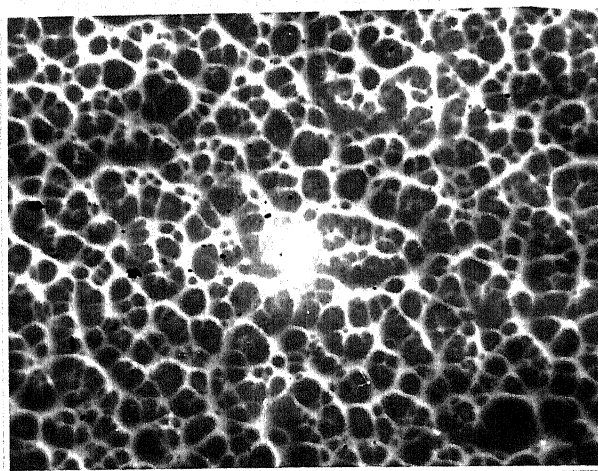
IV.11 2%/1200°C/2h.



IV.12 10%/1100°C/2h.

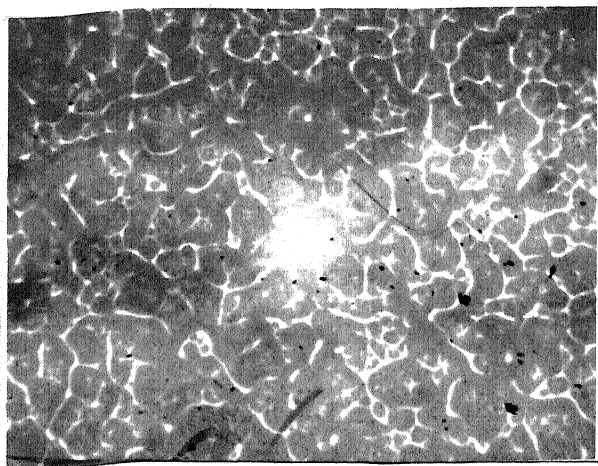


IV.13 20%/1100°C/2h

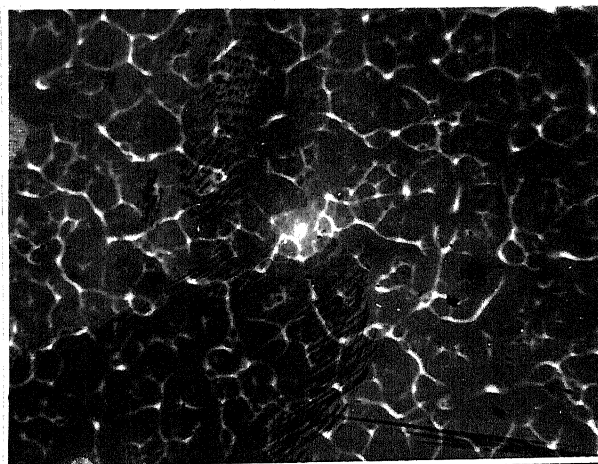


IV.14 30%/1100/2h

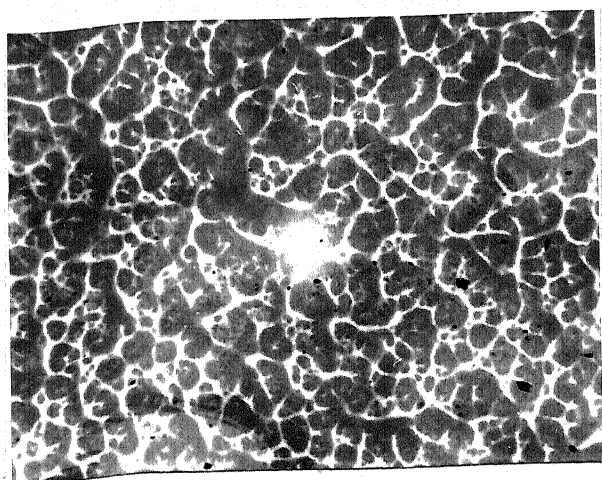
Figs. IV.10-14 Microstructures of liquid phase sintered  $\text{BaTiO}_3$  samples with different glass contents.



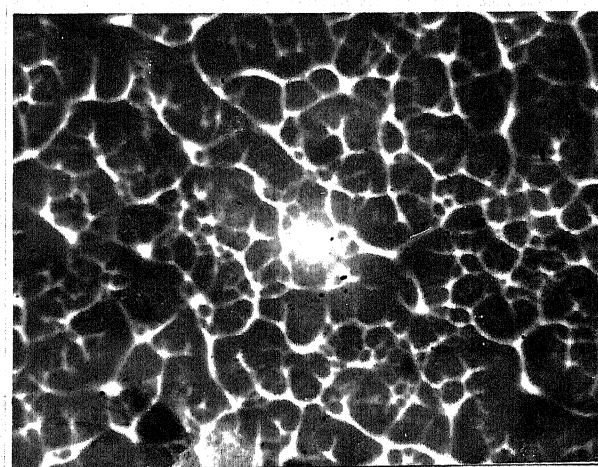
IV.15 10%/1000°C / 10 min.



IV.16: 10%/1000°C/ 1/2h.



IV.17 : 10%/1000°C/ 1h.

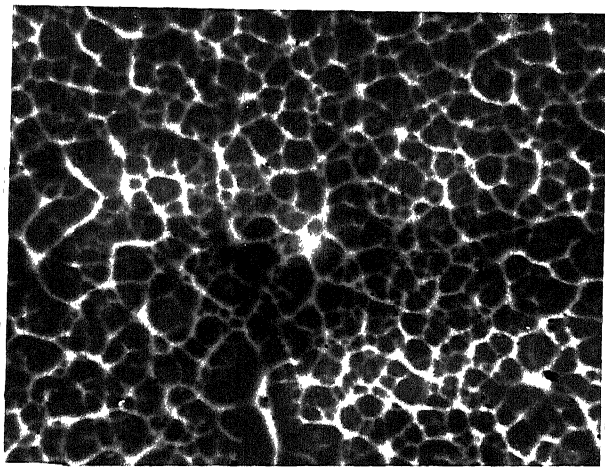


IV. 18 : 10%/1000°C/ 2h.

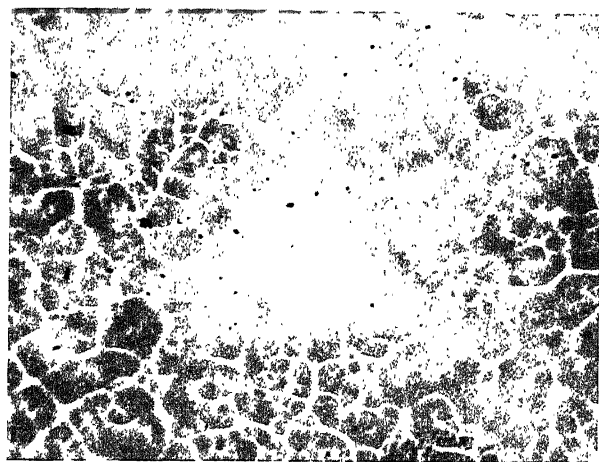
Figs. 15-18: Microstructures of liquid phase sintered  $\text{BaTiO}_3$  samples with 10% glass addition sintered at 1000°C for different times.

(x150)

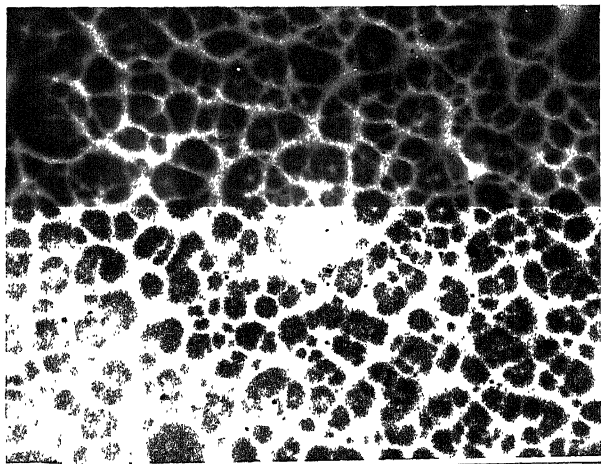




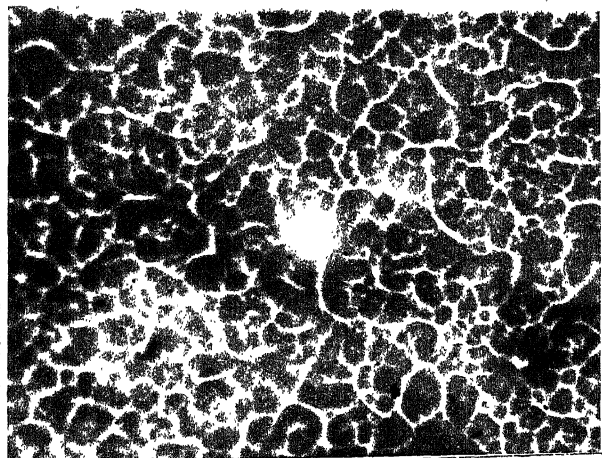
IV. 19: 10%/1100°C/ 10 min.



IV. 20: 10%/1100°C/ 1/2h.



IV. 21: 10%/1100°C/ 1h.



IV. 22: 10%/1100°C/ 2 h.

Figures 19-22: Microstructures of liquid phase sintered  $\text{BaTiO}_3$  samples with 10% glass addition sintered at 1100°C for different times.

(X150)

for this purpose were carried out on 150-250 grains in each case. These results are given in Table IV.6

Table IV.6 Variation of grain size and grain boundary Thickness with sintering temperature and time.

Sintering Time (h)	Sintering Temperature °C			
	1000		1100	
	Grain size / $\mu$	Boundary layer thickness / $\mu$	Grain Size / $\mu$	Boundary layer thickness / $\mu$
1/6	13	3	19	7
1/2	16	5	24	7
1	19	7	24	9
2	20	6	21	10

This table shows that the grain size is increasing with increasing sintering time from 1/6 to 2 h at a particular temperature and also for the corresponding times the grain size was more at 1100°C than at 1000°C. The grain boundary thickness is also increasing correspondingly with sintering time and temperature. The grain size range has also been found to be rather narrow. This is to be expected since in

the liquid phase sintering process during solution and reprecipitation stage smallest grains will get dissolve and reprecipitate on larger grains.

Through thermal analysis ( Section IV.2) and X-ray diffraction studies it is confirmed that the bismuth borate glass reacts with barium titanate at about 725°C forming  $\text{Ba Bi}_4 \text{Ti}_4 \text{O}_{15}$  and that the amount of  $\text{Ba Bi}_4 \text{Ti}_4 \text{O}_{15}$  reaches a maximum at 900°C and afterwards it is decomposing with increasing temperature from 900°C to 1000°C. The Kinetics of these reactions were discussed in detail in section IV.5 and sintering models in section IV.6. The sintering model presented clearly suggests that the grain size as well as the thickness of the glass layer increases as the temperature is raised from 1000 to 1100°C keeping sintering time constant, and also these parameters increase <sup>with</sup> ~~at~~ the sintering temperature. The observed microstructural changes therefore are in conformation with the proposed sintering models.

#### IV.5. X-ray diffraction studies:

The sequence of reactions taking place during liquid phase sintering of  $\text{Ba Ti O}_3$  mixed with bismuth borate glass was studied by X-ray diffraction techniques using (i) amount of glass added (ii) sintering temperature and (iii) sintering time as parameters. In general the X-ray diffraction patterns were taken on sintered pellets, except in special cases where the sintered pellet was crushed into powder before taking an X-ray diffraction pattern. Thus, unless otherwise mentioned, all the X-ray diffraction data presented here were obtained on sintered discs.

The X-ray diffraction patterns of sintered discs of  $\text{Ba Ti O}_3$  containing 0, 2, 10, 20, and 30 wt. pct bismuth borate glass is shown in Table IV.7. All the discs were sintered at  $1200^\circ\text{C}$  for 2 hrs. These patterns showed  $\text{Ba Ti O}_3$  is the predominant phase. With no noticeable shift in the lattice parameters. It indicates that no solid solutions were formed with  $\text{Ba Ti O}_3$  during liquid phase sintering. In addition there were some extra reflections observed whose intensity seem to increase with increasing glass constant. It may be mentioned that the glass tended to visibly ooze out to the lower side of the disc during sintering at a high temperature such as  $1200^\circ\text{C}$  particularly in the case of samples containing larger additions of glass. In order to study this more closely the two sides of a disc containing

TABLE IV.7

X-ray diffraction data of liquid phase  
sintered  $\text{BaTiO}_3$

wt.% of glass										$\text{BaTiO}_3$ (Ref. 9)	
0		2		10		20		30			
d	I/I <sub>0</sub>	d	I/I <sub>0</sub>	d	I/I <sub>0</sub>	d	I/I <sub>0</sub>	d	I/I <sub>0</sub>	d	I/I <sub>0</sub>
3.97	MS	4.01	MS	4.18	MS	4.04	MS	4.03	MS	4.058	20
										4.022	50
3.13*	VW	3.15*	VW	3.13*	VW	3.13	VW	-	-	-	-
				2.97	VW	2.99	MS	2.97	MS		
2.82	VVS	2.83	VVS	2.83	VVS	2.84	VVS	2.84	VVS	2.84	100
				2.74	VW	2.76	VW	2.76	MS		
2.31	S	2.32	S	2.32	S	2.32	S	2.32	S	2.315	60
2.01	MS	2.02	MS	2.00	VS	2.01	VS	2.00	VS	2.018	55
1.99	VS	2.02	VS							1.998	80
						1.94	VW				
1.82	W	1.79	W	1.79	W	1.80	W	1.79	W	1.804	15
								1.76	VW	1.791	15
1.63	VS	1.64	VS	1.63	VS	1.64	VS	1.64	VS	1.642	60
										1.634	80
										1.419	50

\* These values corresponds to  $\text{Ba}_2\text{TiO}_4$  phase.

30% glass sintered at 1200°C for 2 hrs. was subjected to X-ray diffraction and these results were included in Table IV.8. It may be noticed that there is a distinct difference in the location of some of the reflections on the two sides, but more importantly a substantial difference in intensity of certain lines was observed. The extra lines observed on the glassy side of the disc compare very well with those of  $\text{Bi}_4\text{Ti}_3\text{O}_{12}$ <sup>18</sup> though some serious enhancement of the intensity of some of the reflections was observed for certain reflections on the glassy side of the disc. Recalling that  $\text{Bi}_4\text{Ti}_3\text{O}_{12}$  has a layer type structure with a morphology like to that of mica it is not surprising to observe that some of the (ool) type lines exhibit anomalously large intensities characteristic of strong preferred orientation. In order to unambiguously identify the second phase in these materials and also to overcome the problems due to preferred orientation, the discs were ground to minus 325 mesh powder and an X-ray diffraction pattern was again obtained. These results are presented in Table IV.8. Here again  $\text{BaTiO}_3$  continues to be the predominant phase as can be expected. The coexisting second phase can now clearly be identified as  $\text{BaBi}_4\text{Ti}_4\text{O}_{15}$ <sup>19</sup>. The intensity of the  $\text{BaBi}_4\text{Ti}_4\text{O}_{15}$  lines appear to be increasing with increasing glass addition. It must be pointed out that the powdered sample of the disc with 30%

30% glass sample

[illegible]

glass also shows only a mixture of  $\text{Ba Ti O}_3$  and  $\text{Ba Bi}_4 \text{Ti}_4 \text{O}_{15}$  and does not show the presence of  $\text{Bi}_4 \text{Ti}_3 \text{O}_{12}$ . This apparent anomaly can be resolved if it is considered that only an exceedingly thin layer of  $\text{Bi}_4 \text{Ti}_3 \text{O}_{12}$  is formed on the glassy side of the disc and its amount in the overall volume of the disc is too small to be detected.

From what has been said above it is clear that the bismuth borate glass reacts with bariumtitanate forming barium bismuth titanate as a distinct phase. The thin layer of  $\text{Bi}_4 \text{Ti}_3 \text{O}_{12}$  that appears to form on the glassy side of the disc is so small in quantity that it may not be considered any further.

The kinetics of formation of  $\text{Ba Bi}_4 \text{Ti}_4 \text{O}_{15}$  as a function of time and temperature of sintering was studied in the case of samples with 10% glass. These samples were sintered at 1000, 1050, 1100, and 1150°C for 1/6, 1/2, 1 and 2 hrs. Varying amounts of  $\text{Ba Bi}_4 \text{Ti}_4 \text{O}_{15}$  was detected in nearly all the sintering experiments. In order to quantify the amount of  $\text{Ba Bi}_4 \text{Ti}_4 \text{O}_{15}$  formed under these conditions the ratio of the intensity of (109) reflection of  $\text{Ba Bi}_4 \text{Ti}_4 \text{O}_{15}$  (which is the strongest reflection for this material), to that of the (210) reflection of the  $\text{Ba Ti O}_3$  was computed for different sintering temperatures and times. These results are plotted in Fig. IV.23, as a function of sintering temperature



for fixed time as well as a function of sintering time for fixed temperature. The relative amount of  $\text{Ba Bi}_4 \text{Ti}_4 \text{O}_{15}$  present decreases gradually with increasing temperature for all sintering times or in other words the maximum  $\text{Ba Bi}_4 \text{Ti}_4 \text{O}_{15}$  was observed for the lowest sintering temperature employed namely  $1000^\circ\text{C}$ . The relative amount of  $\text{Ba Bi}_4 \text{Ti}_4 \text{O}_{15}$  present also decreases with increasing sintering time at a given temperature, though the decrease at and above  $1100^\circ\text{C}$  seems to be rather small. In order to provide further support for what has been said above and also to confirm the interpretation of thermal analysis of  $\text{Ba Ti O}_3$  with 20% glass (Section IV.2) two additional experiments were carried out. In the first experiment one sample of 74%  $\text{Bi}_2 \text{O}_3$  26%  $\text{B}_2 \text{O}_3$  glass employed in this study was heated by it self at  $525^\circ\text{C}$  for 8 h. A second sample was melted in a platinum crucible at approximately  $750^\circ\text{C}$  and taken out of the furnace and allowed to cool. X-ray patterns of these two samples given in Table IV.<sup>9</sup> were identical and consists of 2  $\text{Bi}_2 \text{O}_3 \cdot \text{B}_2 \text{O}_3$  and 12  $\text{Bi}_2 \text{O}_3 \cdot \text{B}_2 \text{O}_3$ <sup>(11)</sup> with the former in a larger concentration. From this it could be concluded that the crystallization of the bismuth borate glass employed here, takes place at temperatures as low as  $525^\circ\text{C}$  and the crystallized phases confirm to the ones expected from the phase diagram for 74%  $\text{Bi}_2 \text{O}_3$  26%  $\text{B}_2 \text{O}_3$  composition. In the second experiment a mixture of  $\text{Ba Ti O}_3$  powder with 20% glass powder was heated at 725, 800, 900,

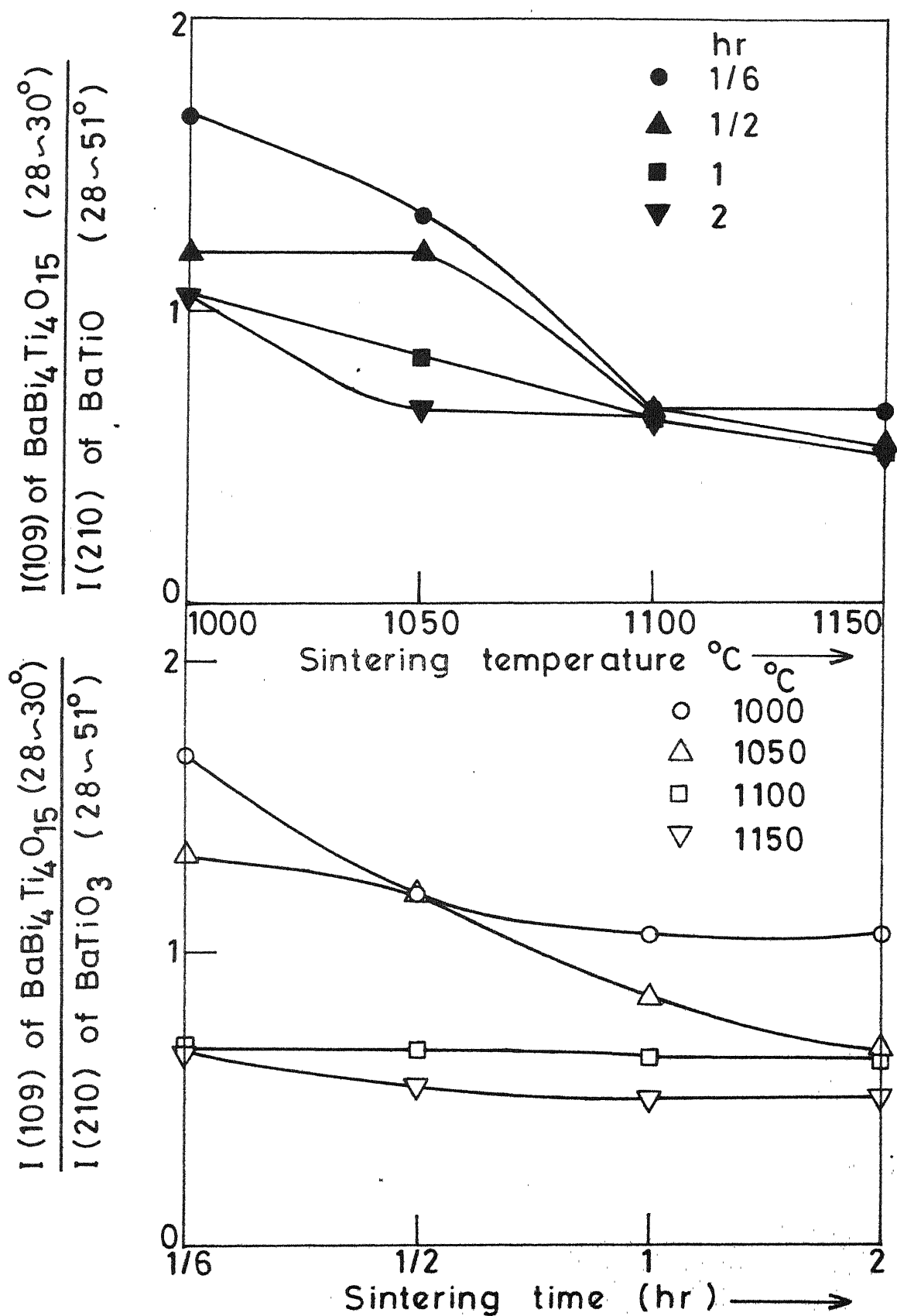


Fig. IV-23 Formation of  $\text{BaBi}_4\text{Ti}_4\text{O}_{15}$  at various sintering temperatures and times.

Table IV: 9 X-ray diffraction data of the 74%  $\text{Bi}_2\text{O}_3$ , 26%  $\text{B}_2\text{O}_3$  glass crystallized at 750°C and 525°C

Glass Crystallized at 750°C		525°C		$2 \text{ Bi}_2\text{O}_3 \cdot \text{B}_2\text{O}_3$		$12 \text{ Bi}_2\text{O}_3 \cdot \text{B}_2\text{O}_3$	
d	I/I <sub>0</sub>	d	I/I <sub>0</sub>	d	I/I <sub>0</sub>	d	I/I <sub>0</sub>
4.28	4	4.26	2	4.25	5		
3.97	16	3.96	10	3.98	12		
3.9	20	3.89	17	3.95	13		
				3.87	18		
3.6	25	3.58	34			3.574	30
3.41	7	3.40	10	3.39	8		
3.33	20			3.312	20		
				3.207	7		
3.21	100	3.21	100			3.198	100
				3.173	9		
3.11	70		80	3.111	63		
3.1	100	3.09	100	3.101	100		
				3.089	60		
2.94	60	2.94	65	3.075	45		
		2.93	30	3.045	24	2.918	28
2.85	9	2.86	10	2.842	11		
2.79	4	2.79	4	2.805	5		
				2.774	6		
2.72	79			2.748	5	2.702	75
2.52	6	2.53	6	2.52	22		
2.49	7	2.50	7	2.489	11		
2.17	9	2.16	18			2.157	17
2.06	9	2.07	10	1.976	9		
1.98	12	1.98	27	1.972	11		
1.93	20	1.93	14	1.929	14		
		1.87	14	1.87	11		
1.85	30	1.85	6	1.866	10		
		1.82	11	1.838	20		
1.74	39	1.74	45			1.735	34
1.69	20	1.69	20			1.686	16
1.65	30	1.65	25			1.641	24

1000 and 1100°C for 15 min. The same mixture was also heated at 725°C for 2 h.  $\ddot{A}$  powder X-ray pattern was obtained of all these materials. These results were given in table IV.10. It can be seen that the sample heated at 725°C for 15 min. shows  $\text{Ba Ti O}_3$  and a second phase, which was identified as  $12 \text{ Bi}_2 \text{ O}_3 \cdot \text{B}_2 \text{ O}_3$  which apparently crystallized from the bismuth borate glass added to  $\text{Ba Ti O}_3$ . However the sample heated at 725°C for a longer period namely 2h shows a mixture of  $\text{Ba Ti O}_3$ ,  $\text{Ba Bi}_4 \text{ Ti}_4 \text{ O}_{15}$  and  $12 \text{ Bi}_2 \text{ O}_3 \cdot \text{B}_2 \text{ O}_3$  phases. This means that given sufficient time the glass reacts with  $\text{Ba Ti O}_3$  to form  $\text{Ba Bi}_4 \text{ Ti}_4 \text{ O}_{15}$  at as low a temperature as 725°C. On the other hand the same sample heated to 800°C for 15 min. does not contain  $12 \text{ Bi}_2 \text{ O}_3 \cdot \text{B}_2 \text{ O}_3$  but shows  $\text{Ba Ti O}_3$  as the predominant phase with  $\text{Ba Bi}_4 \text{ Ti}_4 \text{ O}_{15}$  as a minor phase. The relative amount of  $\text{Ba Bi}_4 \text{ Ti}_4 \text{ O}_{15}$  formed appears to attain a maximum at 900°C and its amount appears to decrease at 1000°C and even more so at 1100°C.

The decreasing amount of  $\text{Ba Bi}_4 \text{ Ti}_4 \text{ O}_{15}$  as the sintering temperature is increased from 900 to 1000 to 1100°C is in line with the results discussed earlier on discs with 10% glass sintered between 1000 and 1100°C for periods varying from 10 min. to 2 h. The important results of the X-ray diffraction study of the liquid phase sintering process of  $\text{Ba Ti O}_3$  in the presence of  $\text{Bi}_2 \text{ O}_3 \cdot \text{B}_2 \text{ O}_3$

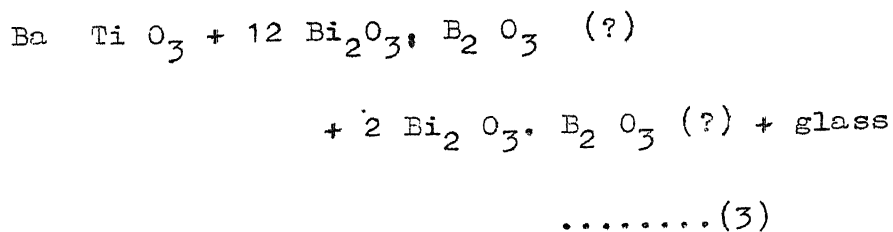
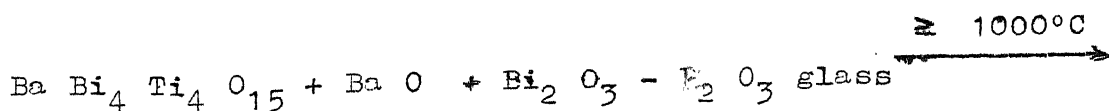
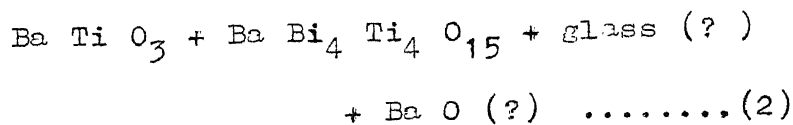
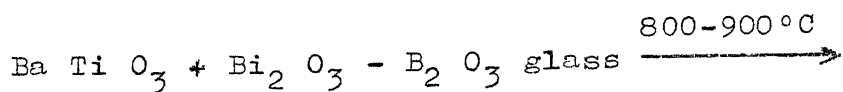
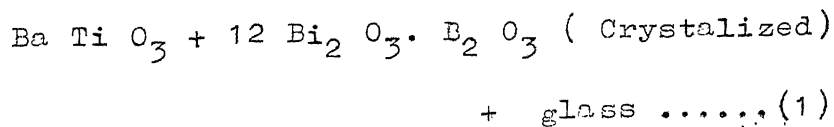
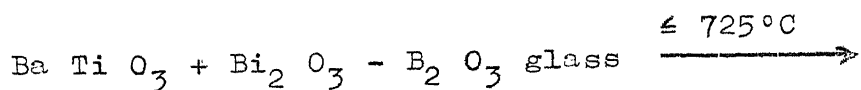
Table IV.10 X-ray Diffraction data of mixture of  $\text{BaTiO}_3$  and 20% glass mixture heated to different temperatures.

Temperature °C												BaTiO <sub>3</sub> ( )		BaBi <sub>4</sub> Ti <sub>4</sub> O <sub>15</sub> ( )		12Bi <sub>2</sub> O <sub>3</sub> ·B <sub>2</sub> O <sub>3</sub> ( )	
725		800		900		1000		1100									
15 min.		15 min		15 min		15 min		15 min									
d	I/I <sub>0</sub>	d	I/I <sub>0</sub>	d	I/I <sub>0</sub>	d	I/I <sub>0</sub>	d	I/I <sub>0</sub>	d	I/I <sub>0</sub>	d	I/I <sub>0</sub>	d	I/I <sub>0</sub>	d	I/I <sub>0</sub>
4.02	20	4.01	20	4.02	20	4.01	20	4.02	20	4.01	20	(4.058 20)					
												(4.022 50)					
3.6	3	3.22	5	2.97	10	2.98	10	2.98	11	2.98	5	2.97	2	3.87	70	3.574	30
3.22	13	2.97	10	2.98	10	2.98	100	2.84	100	2.84	100	2.84	100	2.98	100	3.198	100
2.93	4	2.84	100	2.84	100	2.84	100	2.84	100	2.84	100	2.84	100			2.918	28
2.84	100	2.73	5	2.74	5	2.74	40	2.32	40	2.32	40	2.32	40	2.74	70	2.702	75
2.72	9	2.73	5	2.74	5	2.74	40	2.32	40	2.32	40	2.32	40	2.33	60		
2.32	40	2.31	40	2.32	40	2.32	40	2.32	40	2.32	40	2.32	40	2.29	80		
														2.10	20		
														2.07	20		
2.00	30	2.00	30	2.00	30	2.00	30	2.00	30	2.00	30	2.018	55				
												1.998	80				
														1.934	70		
														1.910	30		
1.79	10	1.79	10	1.79	10	1.79	10	1.79	10	1.79	10	1.804	15				
												1.791	15				
1.74	5	1.74	2											1.773	70		
1.69	3															1.735	34
1.64	35	1.64	35	1.64	35	1.64	35	1.64	35	1.64	35	1.642	60			1.686	16
												1.634	80			1.641	24

glass may be summarised as follows. At temperatures as low as 725°C or even lower, bismuth borate glass tends to crystallize into  $12 \text{ Bi}_2 \text{O}_3 \cdot \text{B}_2 \text{O}_3$ . At about 800°C the bismuth borate glass reacts with  $\text{Ba Ti O}_3$  forming  $\text{Ba Bi}_4 \text{Ti}_4 \text{O}_{15}$ . At this stage the crystallized  $12 \text{ Bi}_2 \text{O}_3 \cdot \text{B}_2 \text{O}_3$  was no longer detected. It appears to have melted since the liquidus temperature corresponding to this composition was given as 743°C (11). The amount of  $\text{Ba Bi}_4 \text{Ti}_4 \text{O}_{15}$  formed increases up to 900°C and decreases at higher temperatures. This decrease in the relative amount of  $\text{Ba Bi}_4 \text{Ti}_4 \text{O}_{15}$  is interpreted as a decomposition of  $\text{Ba Bi}_4 \text{Ti}_4 \text{O}_{15}$  into  $\text{Ba Ti O}_3$  and some bismuth rich phase. The bismuth oxide released by the decomposition of  $\text{Ba Bi}_4 \text{Ti}_4 \text{O}_{15}$  may combine with  $\text{B}_2 \text{O}_3$  present to form additional glass, or alternately it may combine with  $\text{B}_2 \text{O}_3$  to form crystalline bismuth borate glasses. Some of the weak reflections observed at temperatures where a fair amount of decomposition of  $\text{Ba Bi}_4 \text{Ti}_4 \text{O}_{15}$  has proceeded may be accounted for by the strongest reflections of  $12 \text{ Bi}_2 \text{O}_3 \cdot \text{B}_2 \text{O}_3$  and  $2 \text{ Bi}_2 \text{O}_3 \cdot \text{B}_2 \text{O}_3$ . It may be recalled that the composition of the glass chosen for this study falls in between these two compounds in the phase diagrams (11).

The sequence of reactions taking place during the liquid phase sintering of  $\text{Ba Ti O}_3$  in the presence of bismuth borate glass ( 76 mole %  $\text{Bi}_2 \text{O}_3$ , 24 mole %  $\text{B}_2 \text{O}_3$  )

may tentatively be proposed as follows.



#### IV. 6 Densification Mechanisms:

In liquid phase sintering process there are three stages of densification corresponding to three mechanisms during sintering: 1) particle rearrangement (2) Solution precipitation (3) Coalescence. (20)

In the first stage liquid phase is formed, the pores are filled, and the solid particles are rearranged, resulting in close packing. In the second stage the fine particles go into solution, followed by reprecipitation on the large particles. In the third stage the substance is slowly consolidated as the result of the solid particles growing together in accordance with the rules of solid-phase sintering. The result is that a rigid skeleton is formed in the body undergoing sintering. The predominance of one mechanism or another depends on the nature of the phases and the amount of liquid present. Fig. IV 24 shows a hypothetical densification curve for these three stages of liquid phase sintering. An important condition for the occurrence of solution and precipitation as well as the regrouping process; is the penetration of the liquid between the grains. The extent to which the liquid enters the joints between the particles depends on the dihedral angle formed by the liquid phase at the boundary with two grains of the solid phase ( Fig. IV. 25).



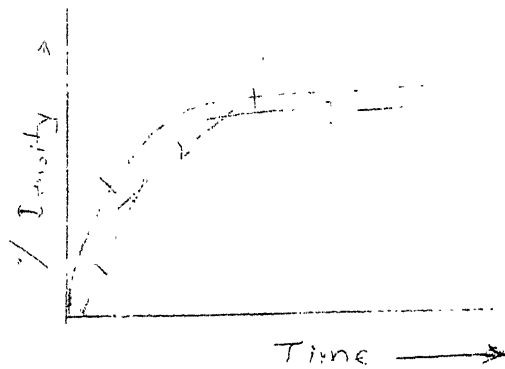


Fig. IV. 24 Hypothetical densification curve for liquid phase sintering.

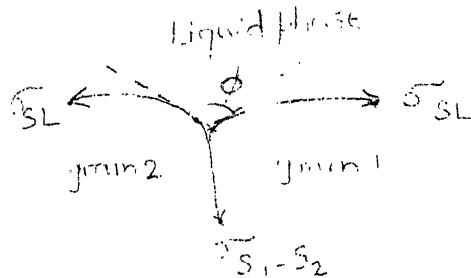


Fig. IV. 25 Dihedral angle formed by the liquid phase at the grain boundary.

$$\sigma_{S_1-S_2} = 2\sigma_{SL} \cos \phi/2$$

$$\text{or } \cos \phi/2 = \sigma_{S_1-S_2} / 2\sigma_{SL}$$

when  $\phi$  is zero or near zero penetration of the liquid phase between the grain faces occurs spreading the liquid over the surface of the grains.

**Particle rearrangement:** On initial formation of the liquid phase on melting, capillary pressure will tend to rearrange the solid particles in such a way as to give maximum packing and a minimum resultant pore surface. The process occurs very rapidly and is the principal reason for densification. With a sufficient quantity of liquid phase

the theoretical density can be attained as the result of the rearranging process alone. According to Kingery's calculations (21) , if the solid phase particles are spherical then the minimum quantity of liquid phase. required for complete densification is 35 Vol%. The degree of densification decreases at smaller quantities. In this case, other sintering processes are necessary for complete densification.

## 2. Solution and precipitation:

As mentioned earlier a limited solubility of solid in the liquid phase is necessary for this mechanism to occur. This stage leads to densification but at a slower rate than in the first stage.

According to Prince-Smithells-William (22) theory during solution-precipitation stage smaller particles will go into solution and precipitate on larger particles thereby leading to densification. The solubility of a substance increases with decreasing radius of curvature of the particles. For spherical surfaces

$$\ln \frac{C}{C_0} = \frac{2 \sigma_{S-L} V_0}{r R T} \quad 78,$$

where  $C/C_0$  is the ratio of the solubility of fine particles with a radius  $r$  and large particles with a radius  $r \rightarrow \infty$  (solubility of a substance with plane interfaces).

$\sigma_{S-L}$  is the specific free surface energy at the solid-liquid interface,  $V_0$  is the molar volume,  $R$  is the gas constant, and  $T$  is absolute temperature.

Thus, the fine particles are gradually reduced in size during sintering and dissolve in the liquid phase, while at the same time, due to the lower solubility of the large particles, an excess of the substance in solution is reprecipitated on the large particles, thereby still further increasing their size. The growth of the large particles continues until all the fine particles disappear and the structure becomes relatively uniform. In systems in which the solution and precipitation mechanisms is dominant the amount of liquid phase also affects the grain growth.

### 3. Coalescence process:

It is to be expected that during the sintering process a certain number of grains will be oriented such that the grain boundary energy is smaller than twice the solid-liquid interface energy (  $\sigma_{S_1-S_2} < 2 \sigma_{S-L}$  )

and consequently, liquid will not penetrate completely between the grains. In this case, along a line between grain centers the material will all be solid and in order for densification to take place, material must be transferred within the solid phase. Consequently, rapid densification corresponding to liquid phase processes are stopped, and densification rate should decrease to that observed for solid particles under similar conditions.

Liquid phase sintering results in the formation of characteristic structures consisting of evenly distributed grains of solid phase in a matrix of the crystallized liquid phase. Particles of different shape may be formed. If the surface tension at the interface between different crystallographic planes of the solid particles and the liquid phase is approximately identical then the particles have rounded shapes. If, however, the surface tension at the interface differs substantially for different crystallographic planes, then grains of prismatic shape are formed. In the systems forming spherical particles considerable grain growth occurs during sintering. While the grain growth is less in systems forming prismatic grains, a higher density is attained with comparatively small amounts of liquid phase.

In general it can be said that (1) an appreciable amount of liquid (2) a limited solubility of the solid (3) complete wetting are the necessary requirements for complete densification.

In the present work, the usability of the bismuth borate glass as an additive for the liquid phase sintering of  $\text{Ba Ti O}_3$  can be seen from the following observations:

(i) X-ray diffraction studies of the liquid phase sintered samples, showed that the glass reacts with  $\text{Ba Ti O}_3$  forming  $\text{Ba Bi}_4 \text{Ti}_4 \text{O}_{15}$  indicating a limited solubility of the solid in the liquid phase.

(ii) Microstructural observation of these samples shows complete wetting of  $\text{Ba Ti O}_3$  grains with glass.

In the present work sintering process was studied by volume shrinkage measurements during sintering, supplemented by weight loss measurements, Thermal analysis, density measurements, Microstructural observation and grain size measurements and X-ray diffraction studies.

Volume shrinkage measurements were made on 10% and 20% glass samples sintered at different temperatures and times. These results are plotted in Fig. IV. 26 and 27.

Fig. IV. 26 shows volume shrinkage for the samples with 10% glass addition sintered at different temperatures and times. From this figure it can be observed that at 1100 and 1150°C most of the densification is taking place within the first 10 min. and afterwards there is very little increase in density with increasing sintering time from 10 min. to 2h. At 1050°C, also it can be observed that most of the densification is taking place within first 10 min. but here there is gradual increase in density with sintering times from 10min. to 2h, whereas at 1000°C such a sharp rise in density was not observed. Here the density is increasing gradually with increasing sintering time.

As described previously there are three stages in liquid phase sintering (i) Particle rearrangement (ii) solution precipitation and (iii) coalescence. These three stages can be clearly observed in the densification curve at 1050°C. The large densification observed during the initial stages (first 10 min.) must be due to the particle rearrangement process by liquid flow. The increase in densification with increase in sintering time from 10 min. to 1h can be attributed to the solution and precipitation stage. After 1h the little increase in densification with increase in sintering time indicates that the third stage i.e. coalescence process is acting between 1 and 2h.

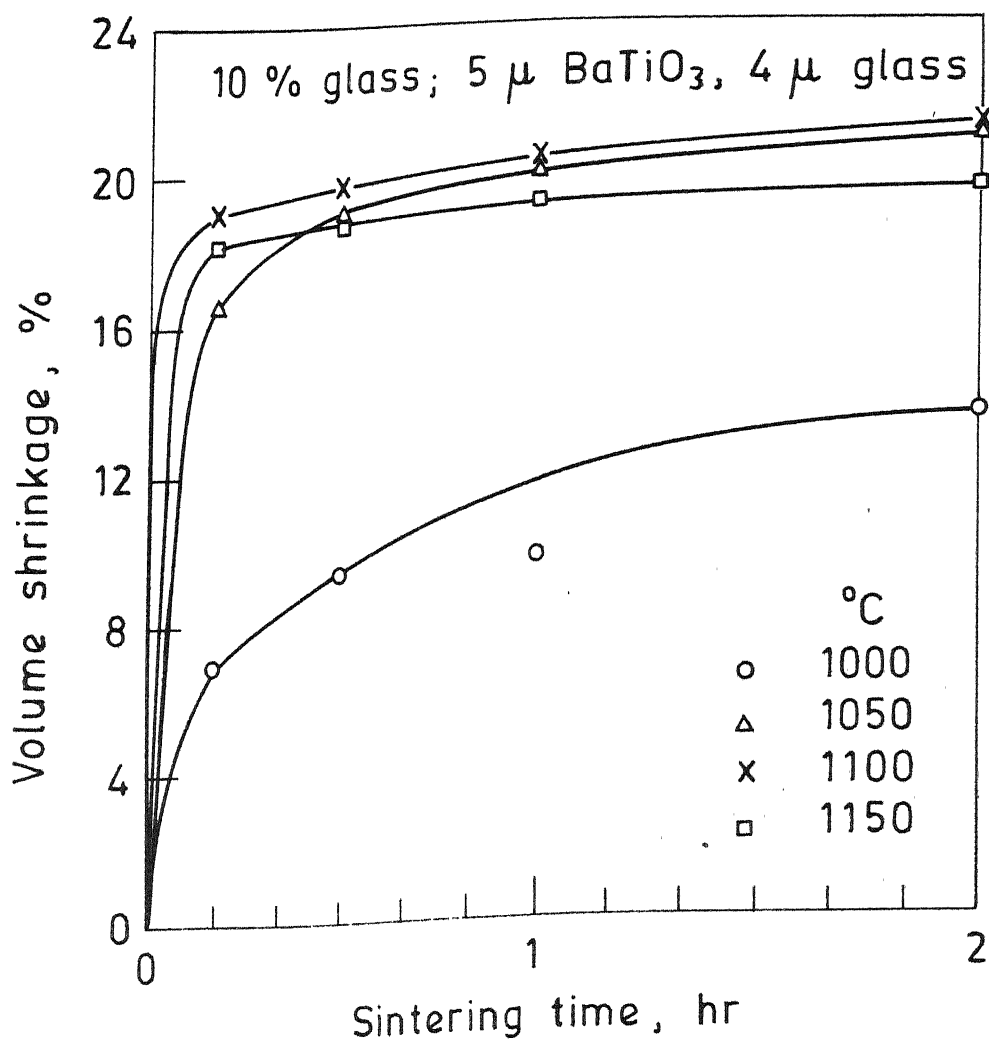


Fig. IV-26- Volume shrinkage vs sintering time for BaTiO<sub>3</sub> with 10 % glass addition at different sintering temperatures.

The absence of the sharp increase in densification in the initial stages at 1000°C indicates that the particle rearrangement stage is not prominent here. It may be due to the higher viscosity of the glass at this temperature. X-ray diffraction studies on  $\text{Ba Ti O}_3$  and glass mixture indicates that the glass is reacting with  $\text{Ba Ti O}_3$  forming  $\text{Ba Bi}_4 \text{ Ti}_4 \text{ O}_{15}$  at as low a temperature as 725°C. It indicates the solution of  $\text{Ba Ti O}_3$  in the liquid phase. So the gradual increase in densification observed at 1000°C may be due to the solution and precipitation process.

Again at 1100 and 1150°C the viscosity of the glass must be sufficiently low, facilitating particle rearrangement process as can be seen in the figure.

Because of this easy flow of the liquid at these temperatures most of the densification is taking place by particle rearrangement process and solution and precipitation stage is not so prominent, though this must also be present to some extent.

Volume shrinkage plots for 20% and 10% glass samples sintered at 1000 and 1100°C for 1/6, 1/2, 1 and 2h. are compared in Fig. IV.27. The volume shrinkage curves with 20% glass also shows similar trend as with 10% glass



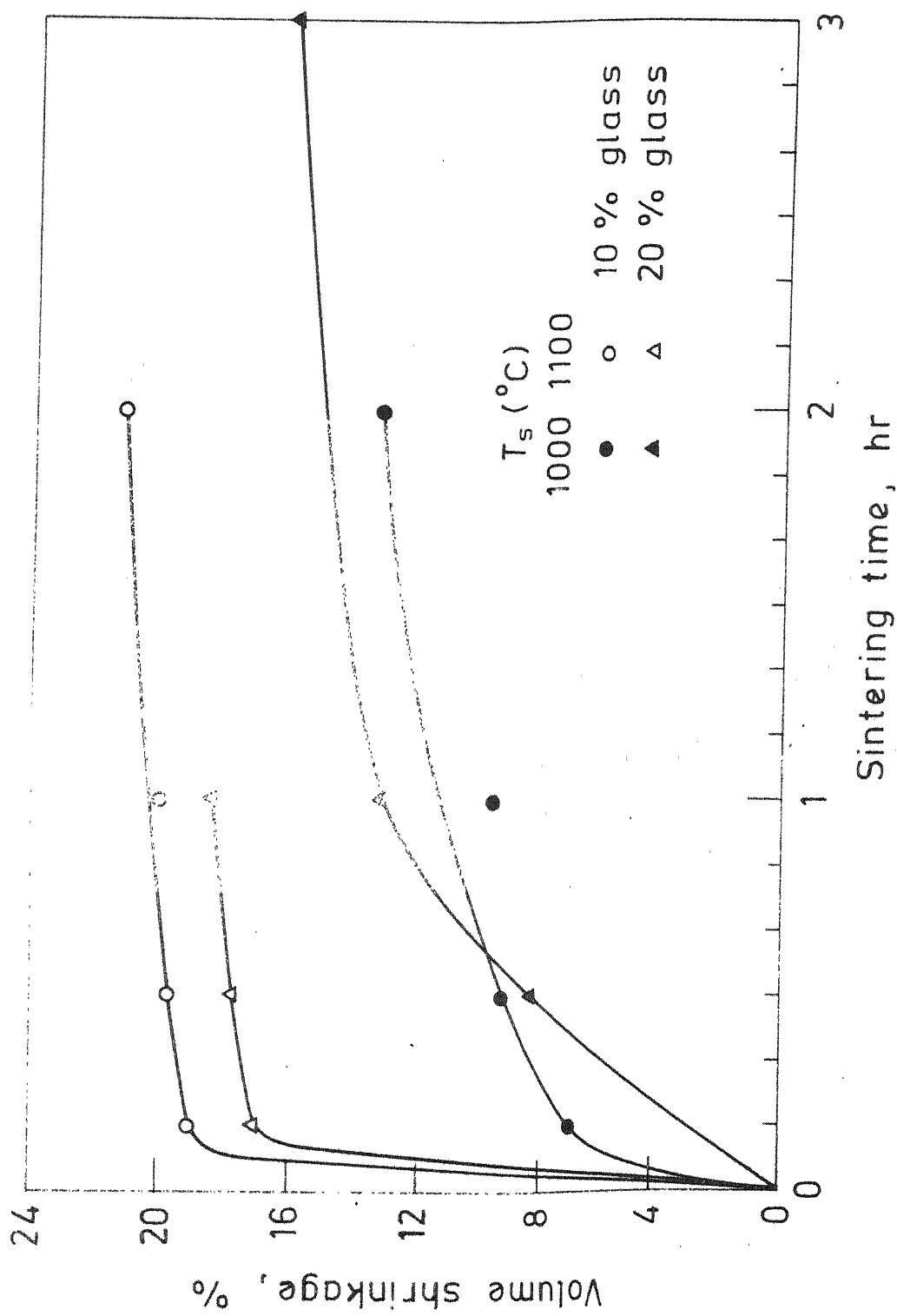


Fig. IV-27- Volume shrinkage vs sintering time for  $\text{BaTiO}_3$  with 10 % and 20 % glass addition at 1000 and 1100  $^\circ\text{C}$ .

indicating that the same mechanisms are applicable here also. It can be observed from this figure that at 1000°C the densification is slightly more with 20% glass addition than with 10% glass. It was mentioned earlier that at 1000°C the major mechanism causing densification is solution and precipitation process, rather than particle rearrangement process. So it can be expected that the densification will be more with higher glass addition as the solution of the solid will increase with increasing liquid phase. This figure also shows that at 1100°C the densification was more with 10% glass addition than with 20% glass addition. At this temperature most of the densification is taking by particle rearrangement process because of the easy flow of liquid. Actually the viscosity at this temperature must be too low as it is observed that some of the glass is oozing out from the pellet, particularly with higher glass additions like 20 and 30%. This may be reason for these 20% samples showing lower volume shrinkage than 10% samples at 1100°C.

Microstructural observation of the liquid phase sintered sample shows that the glass is distributing uniformly around the grains indicating complete wetting of the grains. Grain size measurements made on the 10% glass sample sintered at 1000 and 1100°C for 1/6, 1/2, 1 and 2h shows that at 1000°C there is a considerable grain

growth from 1/6 to 2h ( 13/ $\mu$ m to 20/ $\mu$ m ), where as at 1100°C the grain growth from 1/6 to 2h was less (19/ $\mu$ m to 21/ $\mu$ m). Considering the initial particle size of Ba Ti O<sub>3</sub> used ( 13/ $\mu$ m ), it can be observed that at 1100°C also there is a considerable grain growth taking place with in the first 10min. It indicates that at 1100°C even though particle rearrangement stage is predominant due to the easy flow of the liquid, solution precipitation stage is also acting at this temperature, where as at 1000°C it can clearly be observed that the major mechanism causing densification is solution and precipitation process.

IV.7 Dielectric Measurements:IV. 7.1 Temperature dependence of dielectric properties.

Dielectric properties ( dielectric constant and dissipation factor) were measured as a function of temperature for the liquid phase sintered Ba Ti O<sub>3</sub> samples to observe i) the effect of glass addition and ii) the effect of sintering temperature and time.

All the dielectric constant values reported were corrected for porosity using the relation given by ~~R~~ushman and Strivens ( 23 )

$$K = \bar{K} \frac{2 + V}{2(1-V)}$$

where V = Volume fraction of pores.

$\bar{K}$  = Dielectric constant measured with porosity.

K = Dielectric constant corrected for porosity.

1 i) Effect of glass addition:

Figs. IV28 and 29 show the effect of glass addition on dielectric properties. Fig. IV.28 shows the dielectric constant as a function of temperature for the samples with 0.4, 2, 10, 20 and 30 wt pct glass addition. All these samples were sintered at 1100°C for 1h. except the 30% sample which was sintered for 2h. It can be observed from this figure that the curie temperature was almost constant

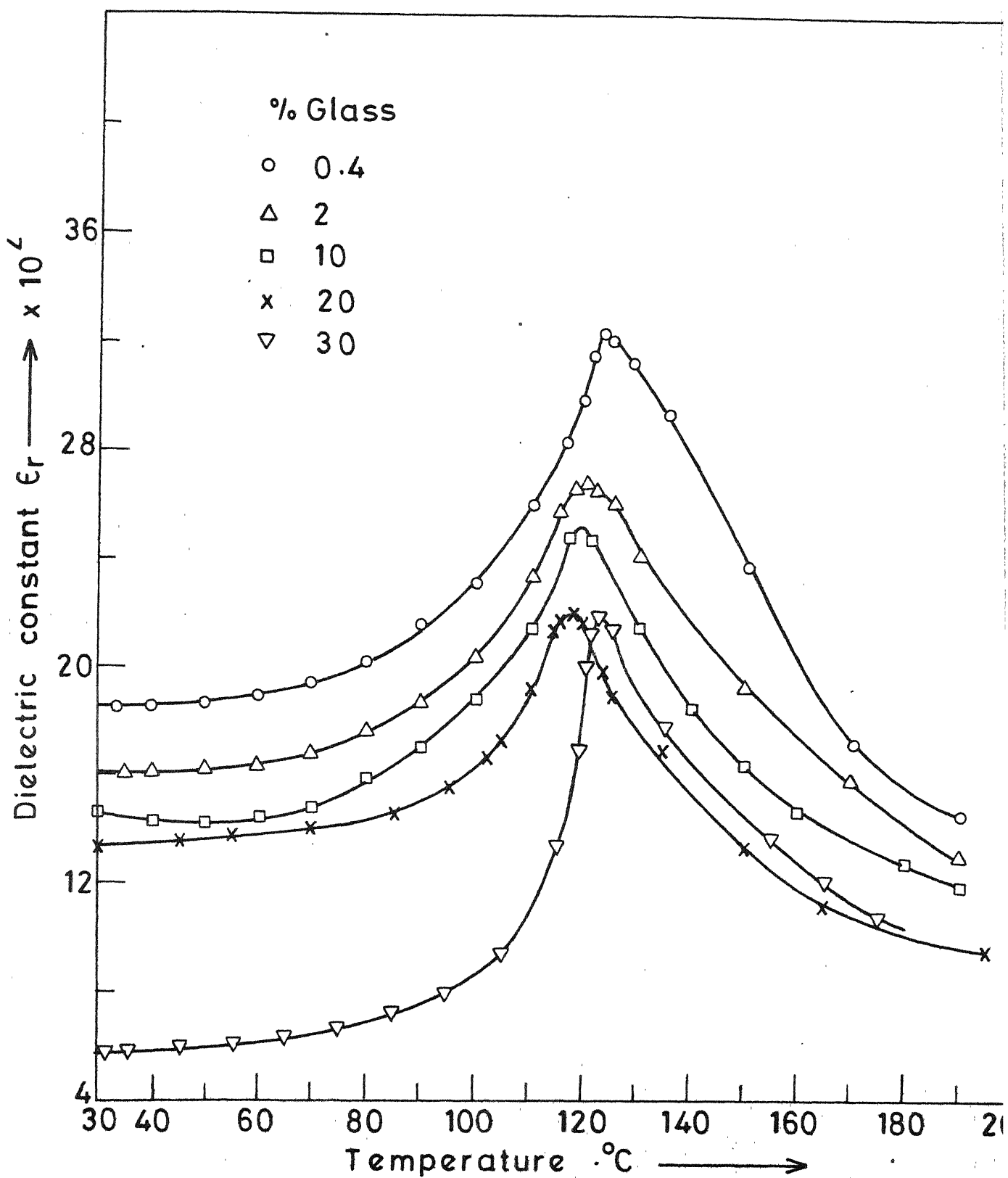


Fig. IV-28 Temperature dependence of dielectric constant for the samples with different glass additions

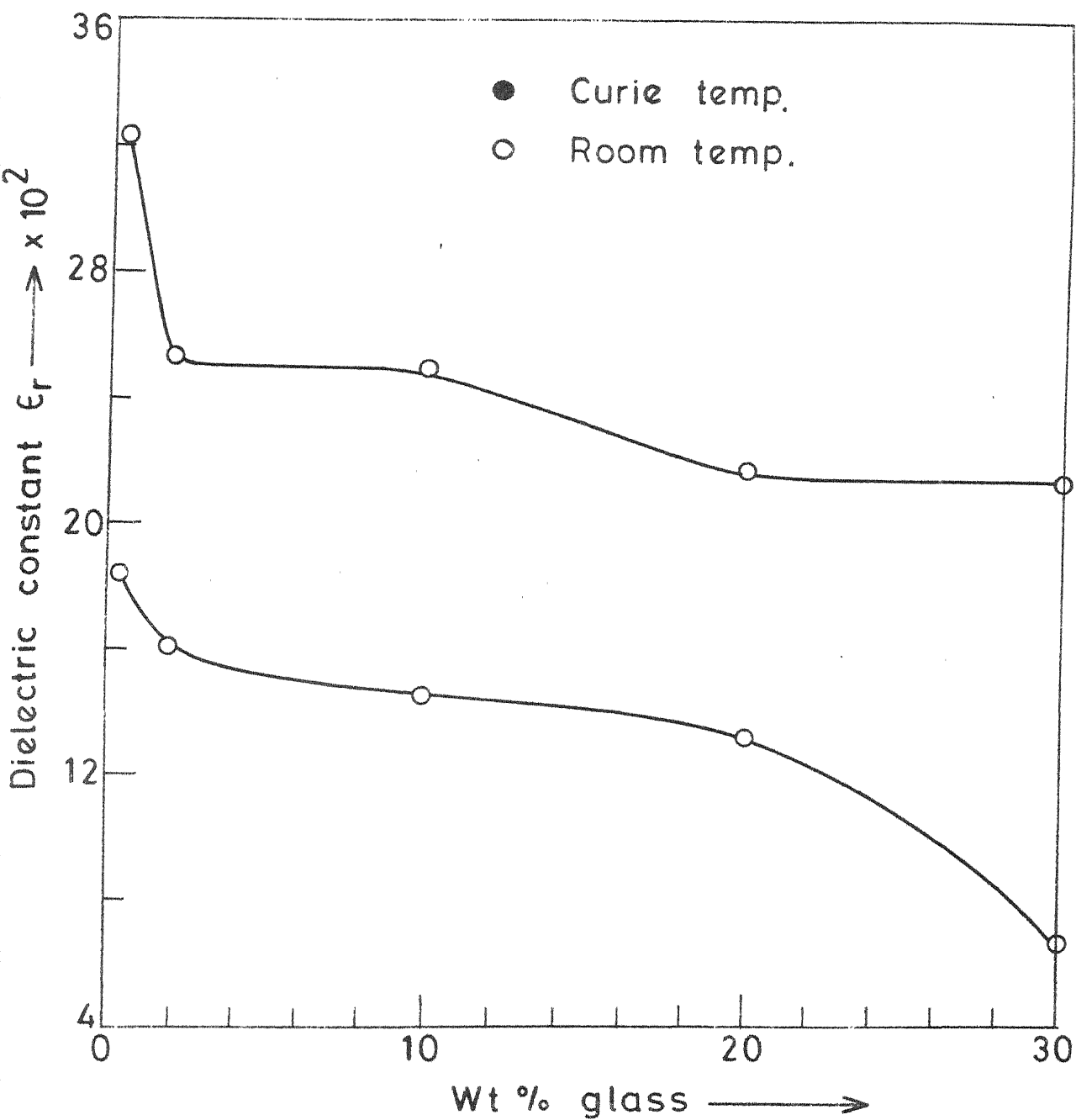


Fig. IV-29 Variation of dielectric constant with glass addition.

at 120°C for all these samples within the experimental error ( $\pm 2^\circ\text{C}$ ). This indicates that there is no change in the basic  $\text{Ba Ti O}_3$  structure due to liquid phase sintering with bismuth borate glass. This was also confirmed through X-ray diffraction studies, which show no shift of X-ray diffraction reflections. The dielectric constant at room temperature for 0.4, 2, 10 and 20% glass samples (1800-1300) are comparable with that of  $\text{Ba Ti O}_3$  (1500-2000) but the peak value is reduced from 6000-10000 for pure  $\text{Ba Ti O}_3$  to 2000 - 3000 for liquid phase sintered  $\text{Ba Ti O}_3$  samples. It can also be observed from this figure that the dielectric constant is decreasing with increasing glass content. These data are plotted separately in Fig. IV.29, which shows the variation of room temperature dielectric constant and maximum dielectric constant with glass content. This figure shows that the dielectric constant decreases with increasing glass content from 0.4 to 30%. This decrease is gradual from 0.4 to 10%, and there is very little decrease in dielectric constant with increase in glass content from 10-20% and afterwards it is decreasing very steeply between 20 and 30% glass ( to about 570).

Since the bismuth borate glass employed in liquid phase sintering has very low dielectric constant ( $\sim 50$ ) (as given in section III 1.3) compared to that of  $\text{Ba Ti O}_3$  it is expected that the dielectric constant should decrease considerably with increasing glass content. However a large

decrease in the room temperature dielectric constant was not observed till 20% glass. Through X-ray diffraction studies it is confirmed that the glass reacts with  $\text{Ba Ti O}_3$  at about  $725^\circ\text{C}$  forming  $\text{Ba Bi}_4 \text{Ti}_4 \text{O}_{15}$  which is also a ferroelectric material with a dielectric constant of ( $\epsilon_{25} - 150$  and  $\epsilon_{\text{max}} - 1650$ ) (24). It is also observed through X-ray diffraction studied that the formation of  $\text{Ba Bi}_4 \text{Ti}_4 \text{O}_{15}$  continues till  $900^\circ\text{C}$  and afterwards it is decomposing forming a glassy phase and  $12 \text{ Bi}_2\text{O}_3 \cdot \text{B}_2\text{O}_3$ . Microstructure observation of the liquid phase sintered samples with 0.4 - 30% glass showed that a glass is distributed uniformly around each grain as a coating over the grain and also the amount of glassy phase increases with increasing glass content. Grain growth was also observed with increasing glass content. So we can consider the whole sintered body as a composite consisting of  $\text{Ba Ti O}_3$  grains uniformly coated with layers of  $\text{Ba Bi}_4 \text{Ti}_4 \text{O}_{15}$  and  $\text{Bi}_2\text{O}_3 \cdot \text{B}_2\text{O}_3$  glass giving it a 3-0 connectivity (25). That is, the boundary layers are connected to each other in 3- dimensions and the  $\text{Ba Ti O}_3$  grains are separated from each other by these boundary layers. So the dielectric constant of this composite will depend on the volume fraction of the second phase(s) and also on its dielectric constant.



Three important results emerged from this study:

- i) With-in the experimental error the Curie temperature remains constant at 120°C irrespective of the amount of the glass added. varying from 0.4 to 30 wt pct. This clearly indicates that none of the constituents of the glass entered the Ba Ti O<sub>3</sub> lattice. This is in confirmity with the X-ray diffraction results.
- ii) The room temperature dielectric constant decreases with increasing amount of glass. In order to account for it one may consider the present materials as two phase mixtures of Ba Ti O<sub>3</sub> with a room temperature dielectric constant of 2000 and bismuth borate glass with a room temperature dielectric constant of about 50 . The dielectric constant of the composite could be computed assuming series and parallel arrangement of the two phase or by logarithmic mixing rule. The concepts have been recently reviewed by payne and cross (26) who give the following formulae for these three mixing rules:

a) parallel mixing:  $\bar{K} = V_1 K_1 + V_2 K_2$

b) series Mixing :  $\frac{1}{\bar{K}} = \frac{V_1}{K_1} + \frac{V_2}{K_2}$

c) Logarithmic mixing:  $\log \bar{K} = \sum V_i \log K_i$

where  $\bar{K}$  is the average dielectric constant,  $V_1$  and  $V_2$  are the two volume fractions such that  $V_1 + V_2 = 1$  and

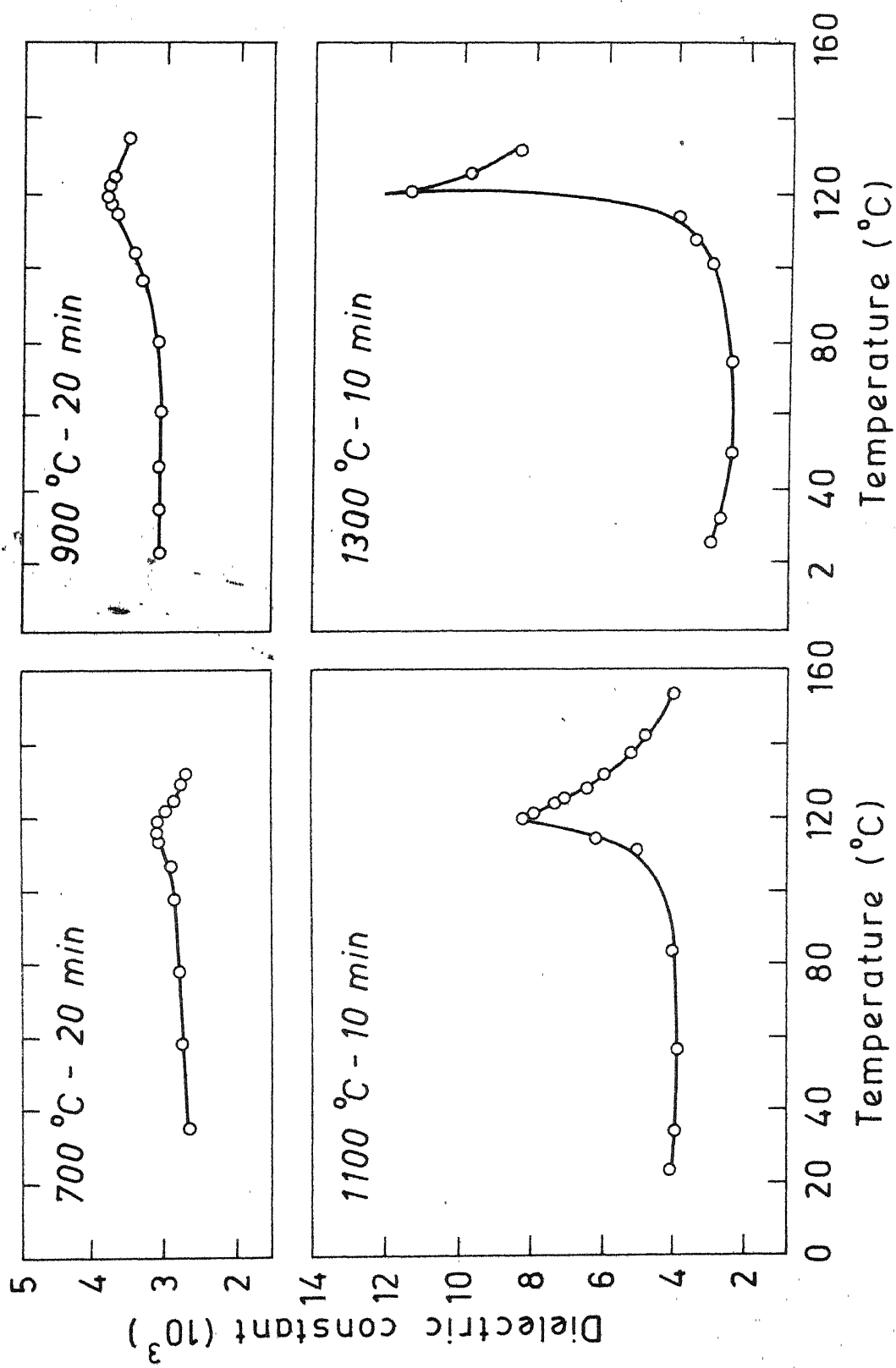


Fig. IV 30;

similar to the above data obtained on reheating of hot pressed Ba Ti O<sub>3</sub> ceramic. This may be due to the fact that the sintering temperatures employed in the present study are mostly 1000 to 1100°C. The reason for this behaviour may be the fact that the grain size does not increase from its initial value ( 13  $\mu$ m) even by a factor of 2 under the sintering conditions employed in the present study. On the other hand in conventional sintering of Ba Ti O<sub>3</sub> ceramics considerable grain growth takes place which leads to a prominent dielectric peak at the curie temperature. This line of reasoning is supported by the observation that a higher sintering temperature or a longer sintering time invariably lead to a higher dielectric constant at the curie temperature than the values corresponding to a lower temperature or shorter sintering time.

Table IV.11 Comparison of Observed dielectric constants and calculated values using mixed rules.

Wt% glass	Vol% Glass	Vol% BaTiO <sub>3</sub>	Dielectric Constant (K)			
			Experi- mental	Logari- thmic mixing	Parallel mixing.	Series Mixing.
0	0	0	2000	2000	2000	2000
0.4	0.3	99.7	1848	1925	1994	1800
2	1.5	98.5	1611	1850	1970	1286
10	7.67	92.33	1453	1475	1851	521
20	15.75	84.25	1325	1100	1693	293
30	24.27	75.73	571	820	1527	200

#### IV.7.1.2 Effect of sintering temperature and time:

Figs. IV. 31-25 show the effect of sintering temperature and time on dielectric properties. These results are briefly summarised in Table IV.12/ Fig. IV.31 shows the dielectric properties of the samples with 20% glass sintered at 1000°C for 1/2, 1 and 3 h. This figure shows that the dielectric constant values are slightly more for the samples sintered for 3 h, while they are very close for the samples sintered for 1/2 and 1h. The dielectric losses for all these samples are less than 3% till 120°C and afterwards they increase sharply upto 7% at 180°C. Fig. IV.32 shows

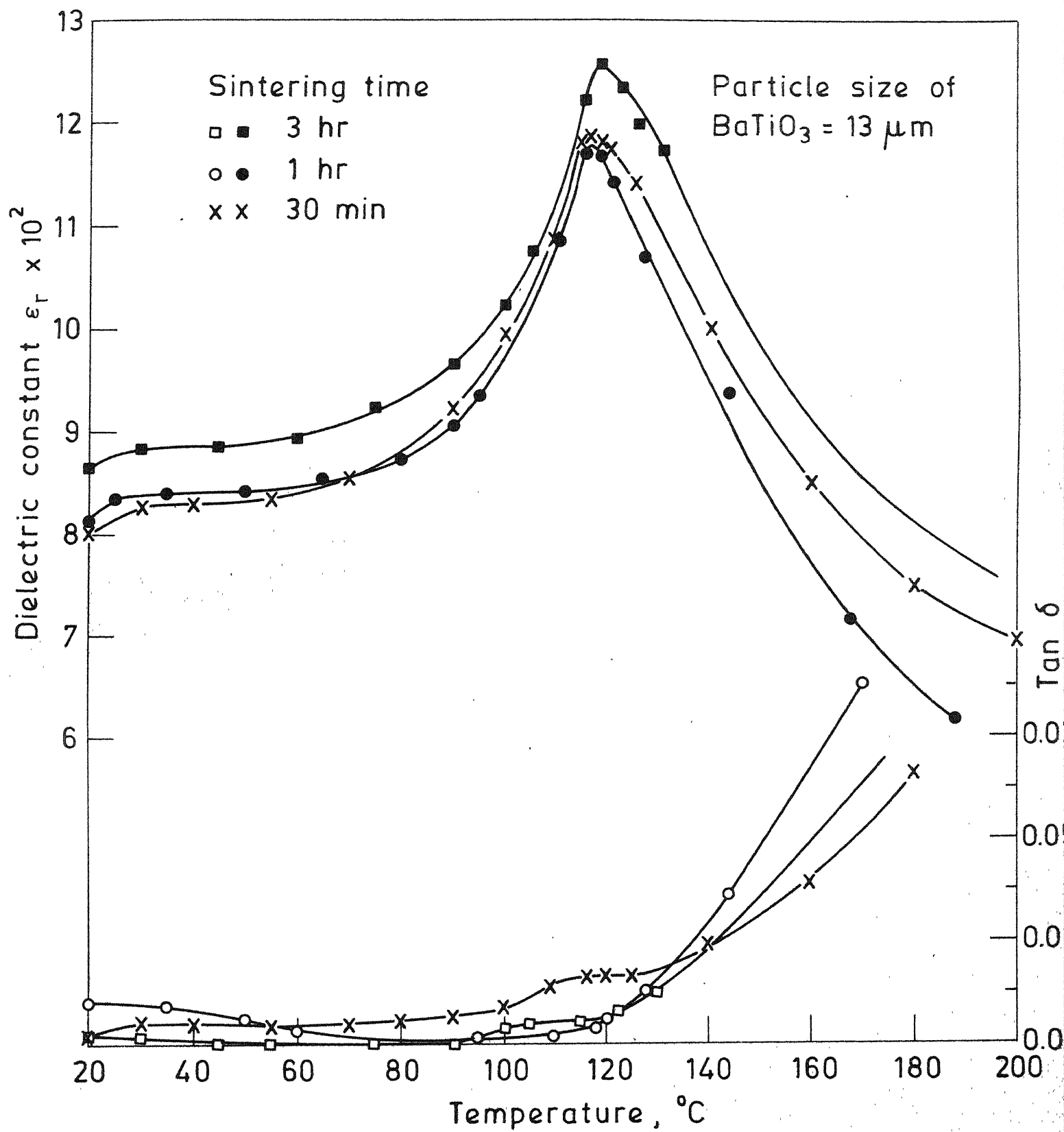


Fig. IV 31 - Relative dielectric constant vs temperature for the samples with 20 % glass addition sintered at  $1000^{\circ}\text{C}$  for different times.

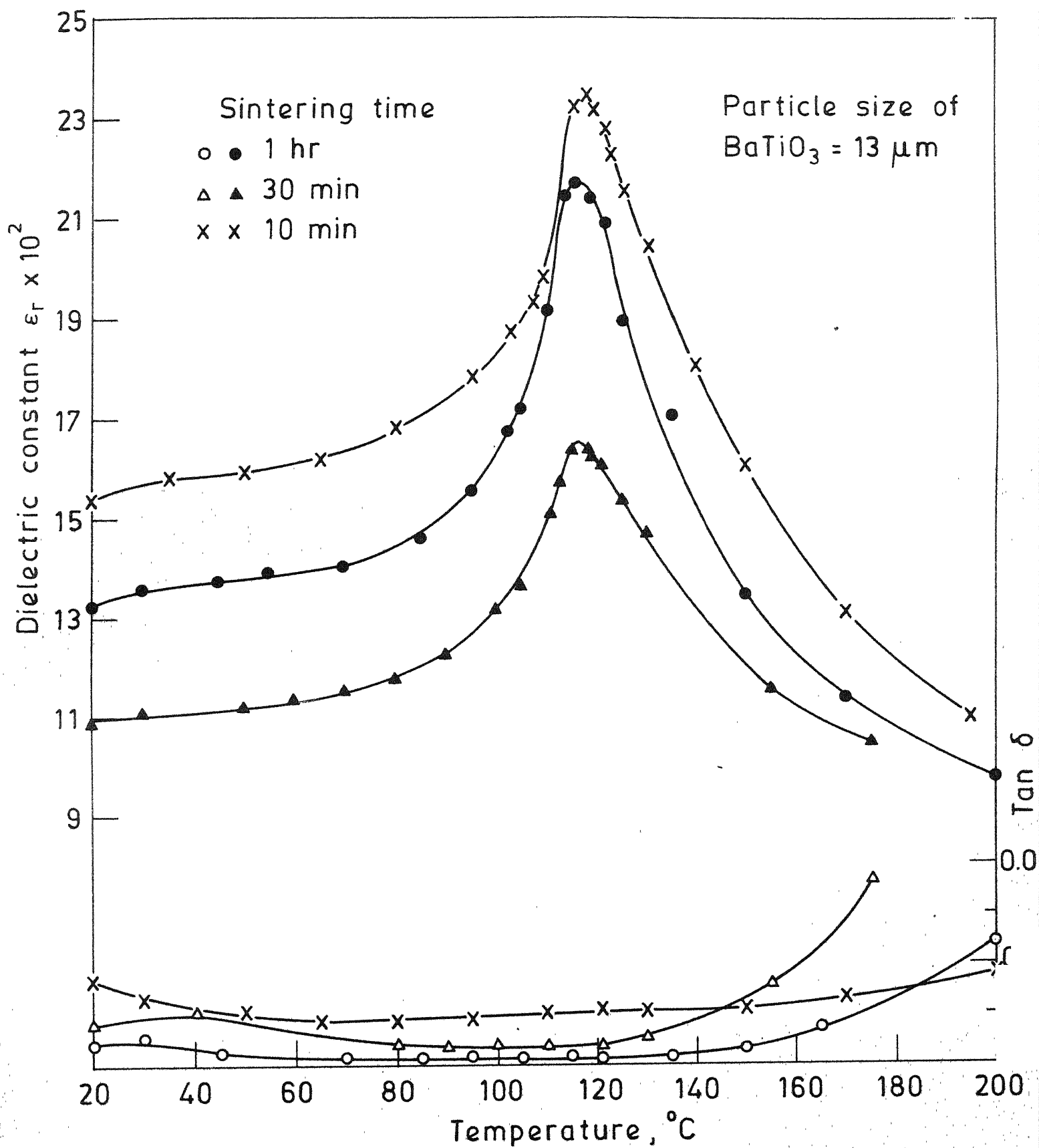


Fig. IV-32 - Relative dielectric constant vs temperature for the samples with 20 % glass addition sintered at 1100 for different times.

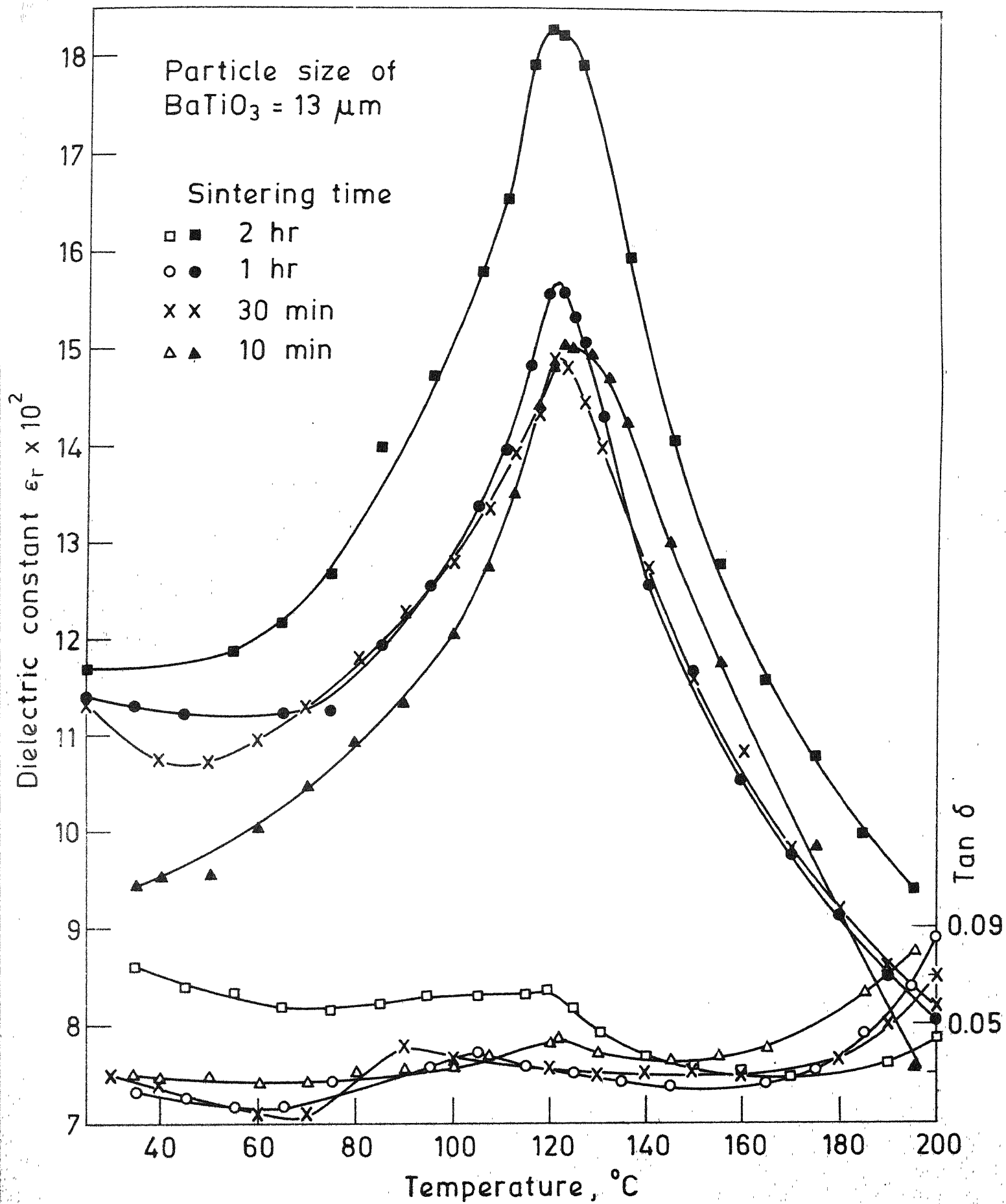


Fig. IV 33 - Relative dielectric constant vs temperature for the samples with 10 % glass addition sintered at  $1000^\circ\text{C}$  for different times.

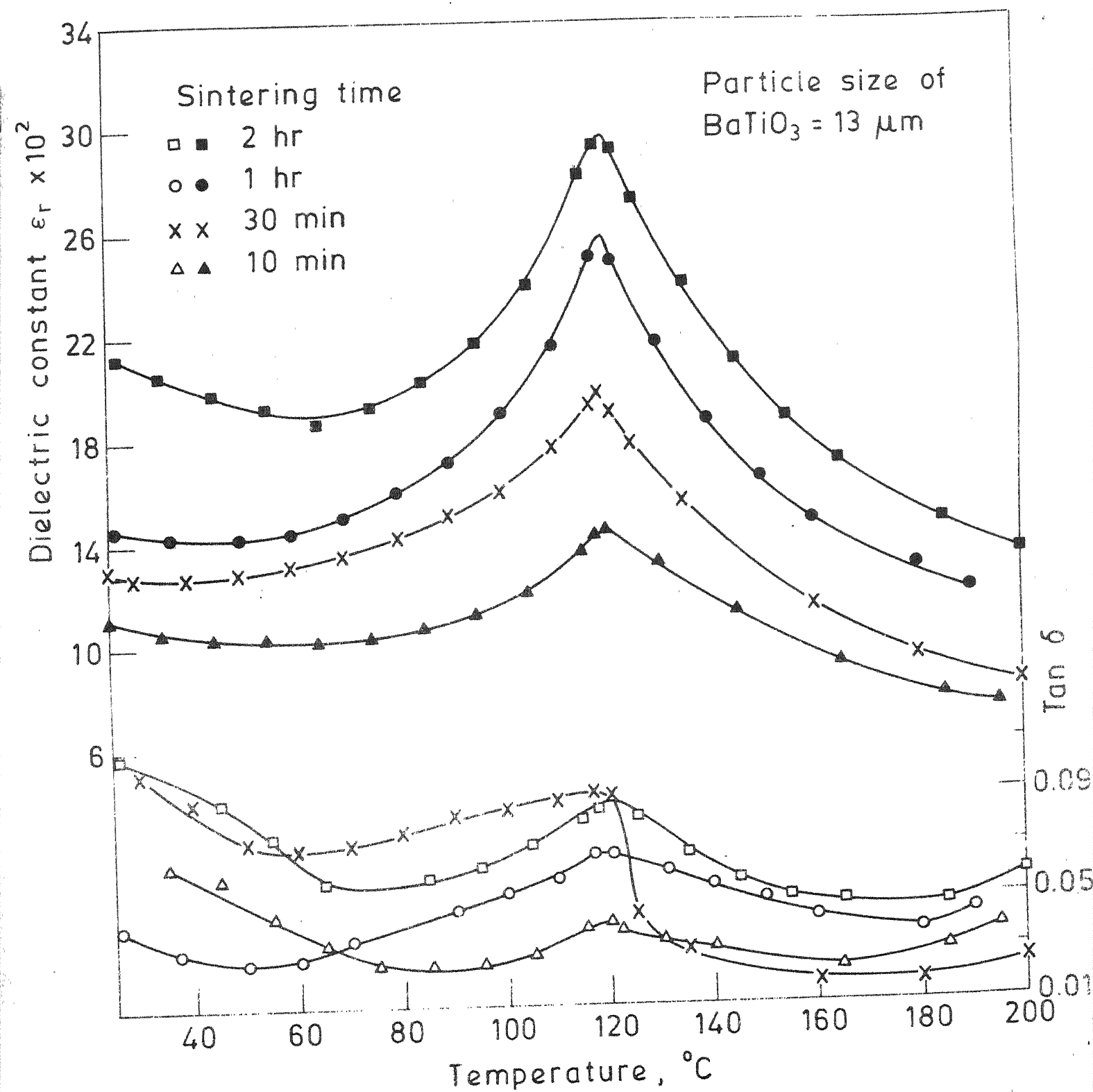


Fig. IV-34 - Relative dielectric constant vs temperature for the samples with 10 % glass addition sintered at  $1100^\circ\text{C}$  for different times.



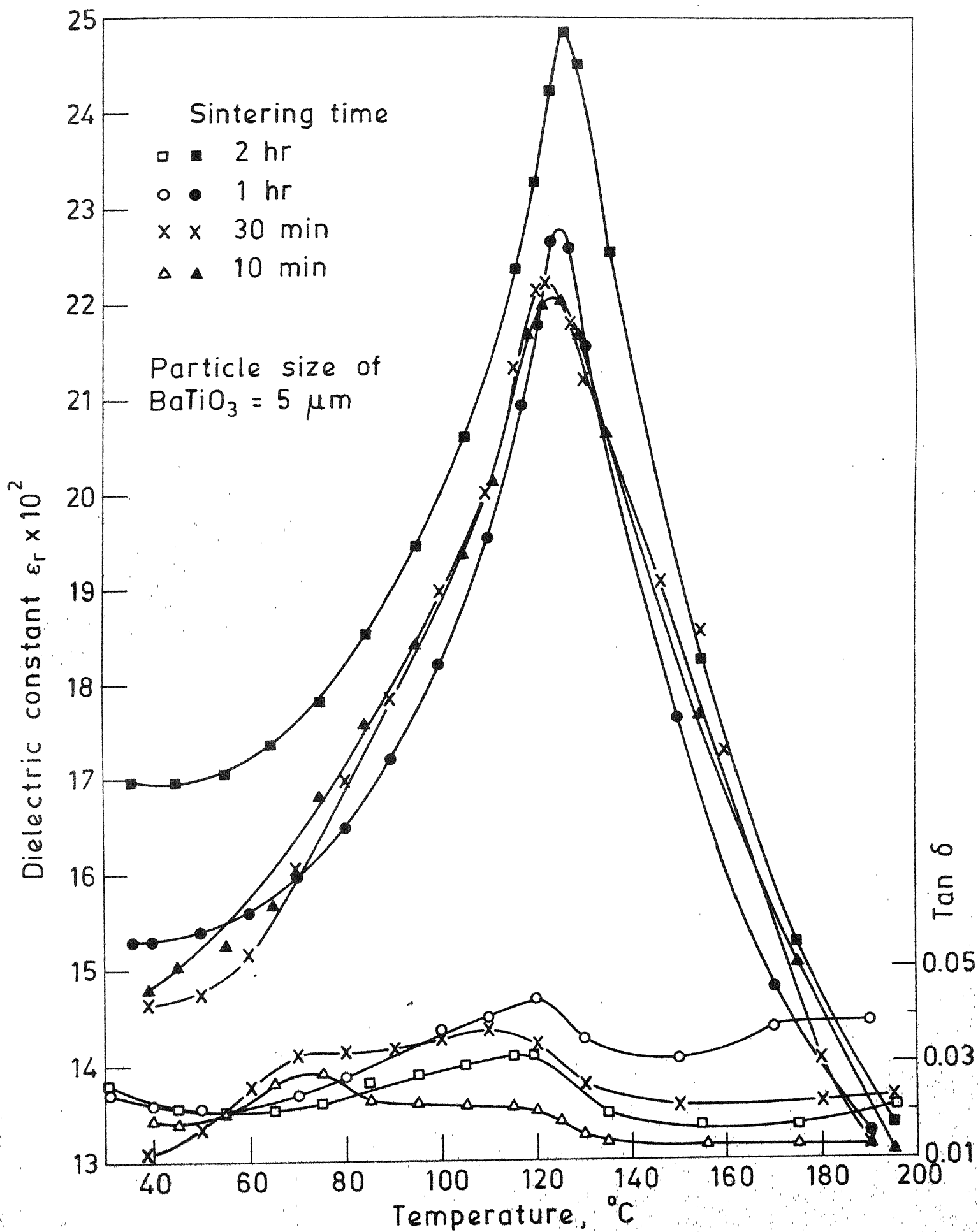


Fig. IV 35 - Relative dielectric constant vs temperature for the samples with 10 % glass addition sintered at 1050 °C for different times.

Table IV.12: Variation of dielectric constant with glass addition, sintering temperature and time.

Sample	Sinter- ing Temp. °C	Sinter- ing Time	Density g/cc	$\epsilon_r$ at RT	$\epsilon_r$ max
BaTiO <sub>3</sub> with 20% glass addition 13/ $\mu$ m BaTiO <sub>3</sub> 17/ $\mu$ m glass	1000	1/2 h	4.66 (77.4)	801	1192
		1 h	5.02 (83.4)	812	1168
		3 h	5.16 (85.7)	867	1253
	1100	10min.	5.10 (84.7)	1119	1634
		1/2 h	5.15 (85.5)	1539	2332
		1 h	5.18 (86.0)	1325	2165
	1000	10 min	4.78 (79.4)	942	1508
		1/2 h	4.87 (80.9)	1132	1462
		1 h	5.03 (83.6)	1136	1558
		2 h	5.26 (87.4)	1168	1827
	1100	10 min	5.06 (84.1)	1113	1414
		1/2 h	5.24 (87.0)	1300	1942
		1 h	5.25 (87.2)	1453	2495
		2 h	5.27 (87.5)	2119	2914
BaTiO <sub>3</sub> with 10% glass addition 5/ $\mu$ m BaTiO <sub>3</sub> 4/ $\mu$ m glass	1050	10 min	5.20 (86.4)	1479	2204
		1/2 h	5.32 (88.4)	1439	2219
		1 h	5.40 (89.7)	1529	2264
		2 h	5.37 (89.2)	1699	2459

the dielectric properties of the 20% samples sintered at 1100°C for 1/6, 1/2 and 1h. This figure shows that the dielectric constant values are more for the samples sintered for 10 min. and 1h. and least for the samples sintered for 1/2 h. Here also it can be observed that the dielectric losses for all the samples were less than 3% till 120°C and afterwards they are increasing sharply upto 9% and 7% for 1/2 and 1h. samples. The losses were minimum (4%) at 180°C for 10 min. sample.

Fig. IV.33&34 shows the dielectric properties of the samples with 10% glass sintered at 1000 and 1100°C for 1/6, 1/2, 1 and 2h. In both the cases it can be observed that the dielectric constant is increasing with increasing sintering time from 1/6 to 2h. at a particular sintering temperature. It can also be observed that the dielectric losses are more for the samples sintered at 2h than at 1/6. At both the temperatures the maximum losses till 200°C are less than 9%. For all the samples discussed above the initial particle size of Ba Ti O<sub>3</sub> and glass are nearly 13 and 17 μm respectively. Fig. IV<sup>35</sup> shows the dielectric properties of the samples with 10% glass sintered at 1050°C for 1/6, 1/2, 1 and 2h. Here the particle size of Ba Ti O<sub>3</sub> and glass are 5 μm and 4 μm respectively. These samples also show that the dielectric constant is increasing with increasing sintering time, though the values are very close for 10 min.

1/2h and 1h sintered samples. It can also be observed that the dielectric constant values for these samples are more compared to those values for the samples containing coarser Ba Ti O<sub>3</sub> sintered at 1000 and 1100°C ( Table IV.12 )

It was mentioned earlier that this liquid phase sintered body can be considered as a composite consisting of Ba Ti O<sub>3</sub> grains coated uniformly with Ba Bi<sub>4</sub> Ti<sub>4</sub> O<sub>15</sub> and a glassy phase giving it a 3-0 connectivity. Through the X-ray diffraction studies ( section IV.4 ) it is observed that the Ba Bi<sub>4</sub> Ti<sub>4</sub> O<sub>15</sub> is decomposing at higher temperatures there by reducing its amount as the temperature increases from 1000 - 1100°C, and also at a particular temperature the amount of Ba Bi<sub>4</sub> Ti<sub>4</sub> O<sub>15</sub> is decreasing with increasing sintering time Fig. IV.23. Microstructures of the 10% glass samples sintered at 1000 and 1100°C also showed, that the amount of glass portion around the grain boundaries is increasing with increasing sintering temperature and also at a particular sintering temperature it is increasing with sintering time. The grain size was also found to be increasing with sintering temperature and time . This may be due to the decomposition of Ba Bi<sub>4</sub> Ti<sub>4</sub> O<sub>15</sub> forming glass and Ba Ti O<sub>3</sub>, there by increasing the volume fraction of Ba Ti O<sub>3</sub>. So at a particular temperature with increasing sintering time the volume fraction of Ba Ti O<sub>3</sub> and the amount of glass around the grain is increasing. This

increase in the volume of  $\text{Ba Ti O}_3$  may be the reason for the samples showing more dielectric constant at higher sintering times. The same reasoning also can be applied for higher dielectric constants at  $1100^\circ\text{C}$  than at  $1000^\circ\text{C}$ . The trend observed in the dielectric losses, that is increasing losses with increasing sintering time may be due to the increase in the amount of glassy phase around the grains. As seen from Table II, the resistivity of the bismuth borate glass employed in liquid phase sintering decreases with increasing temperature from  $130$ - $230^\circ\text{C}$  by nearly three orders of magnitude. That is, the conductivity of these glasses is increasing at higher temperatures causing more dielectric losses. Hirayama and Subbarao (2) give the dissipation factor for this glass as  $0.01$  at  $130^\circ\text{C}$  increasing to  $0.14$  at  $230^\circ\text{C}$ . So the increase in dielectric losses at higher temperatures for the liquid phase sintered samples can be accounted for by the increase in dielectric loss of the glass with temperature.

So from these measurements of  $\epsilon_r$  and  $\tan \delta$  with sintering temperature and time, it can be said that the interaction between the glass and  $\text{Ba Ti O}_3$  at the temperatures ( $1000$  -  $1100^\circ\text{C}$ ) and the degree to which the reaction can proceed may be partially responsible for the attainment of various levels of electrical characteristics. To detect the presence of ferroelectric  $\text{Ba Bi}_4 \text{Ti}_4 \text{O}_{15}$  in

the liquid phase sintered samples, temperature dependence of dielectric properties were measured upto 420°C since  $\text{Ba Bi}_4 \text{Ti}_4 \text{O}_{15}$  has a curie point at 395°C (24). These measurements were done on two 20% samples sintered at 1000°C for 1h and 3 h. These results are shown in Fig. IV.36 It shows a little peak at about 395°C for these two samples. Since the dielectric losses are increasing very high (60-70%) at these temperatures, measurements become difficult and clear indication of  $\text{Ba Bi}_4 \text{Ti}_4 \text{O}_{15}$  peak could not be identified. But these measurements show the presence of  $\text{Ba Bi}_4 \text{Ti}_4 \text{O}_{15}$  which supports the X-ray diffraction results.

#### IV.2.2. Voltage dependence of dielectric properties:

Dielectric constant and  $\tan \delta$  were measured on a 10% glass sample sintered at 1050°C for 2h. with increasing and decreasing D.C. bias. Measurements were made upto 100V/mil (40 KV/cm) and no break-down was observed. These results are plotted in Fig. IV.37 and 38. Fig. IV 37 shows the percent change in permittivity with increasing and decreasing d.c. bias. This Figure shows 29% decrease in permittivity at 100V/mil.

In Fig. IV.38 change in permittivity with D.C. bias is compared for liquid phase sintered  $\text{Ba Ti O}_3$  of the present study with that of  $\text{Ba Ti O}_3$  (28) and glass bonded  $\text{Ba Ti O}_3$  (1). The figure show a similar behaviour for all these samples, but the decrease in permittivity at

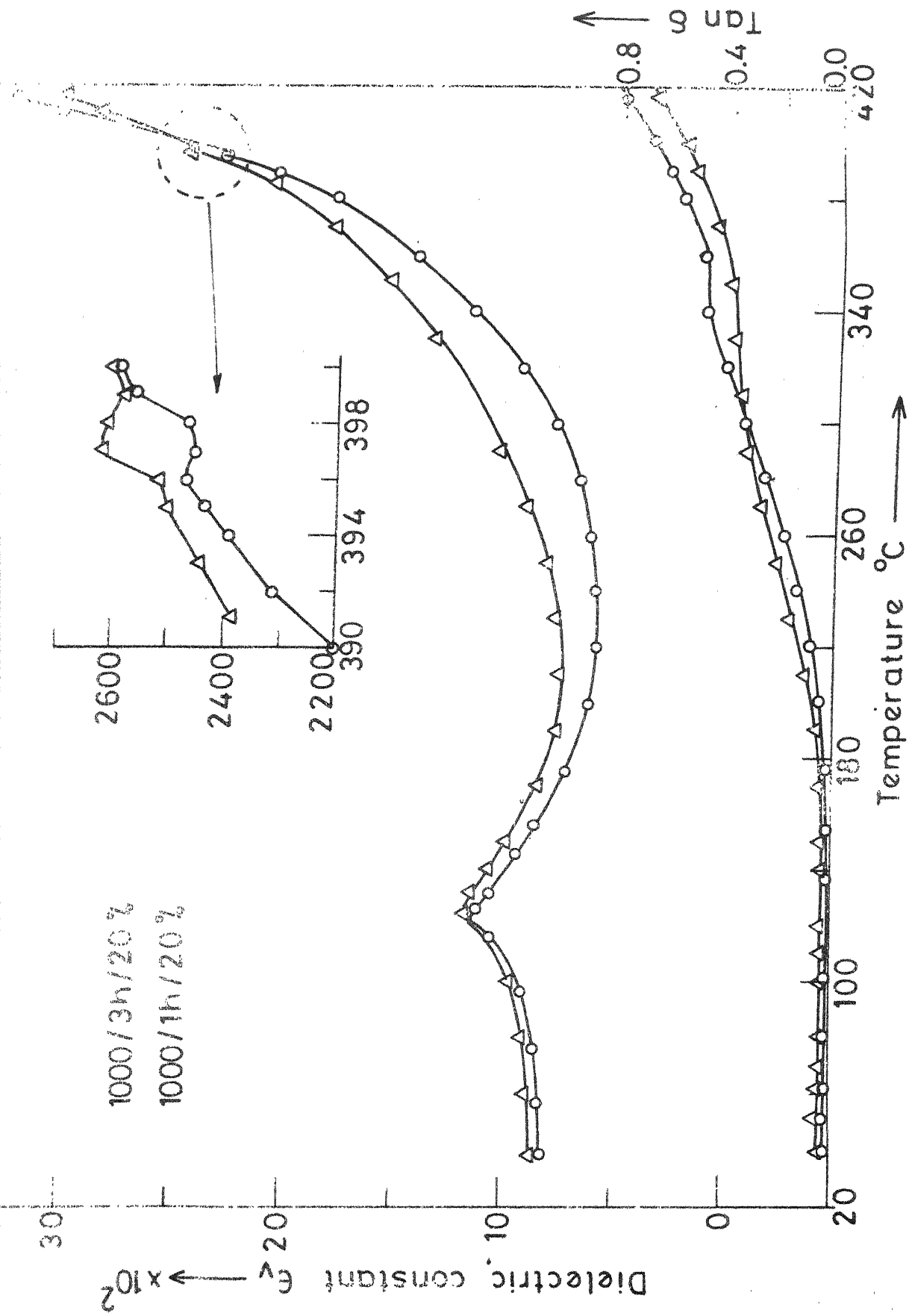


Fig. IV-36 Relative dielectric constant vs temperature for the samples with 20% glass addition sintered at  $1000^{\circ}\text{C}$  for different times.

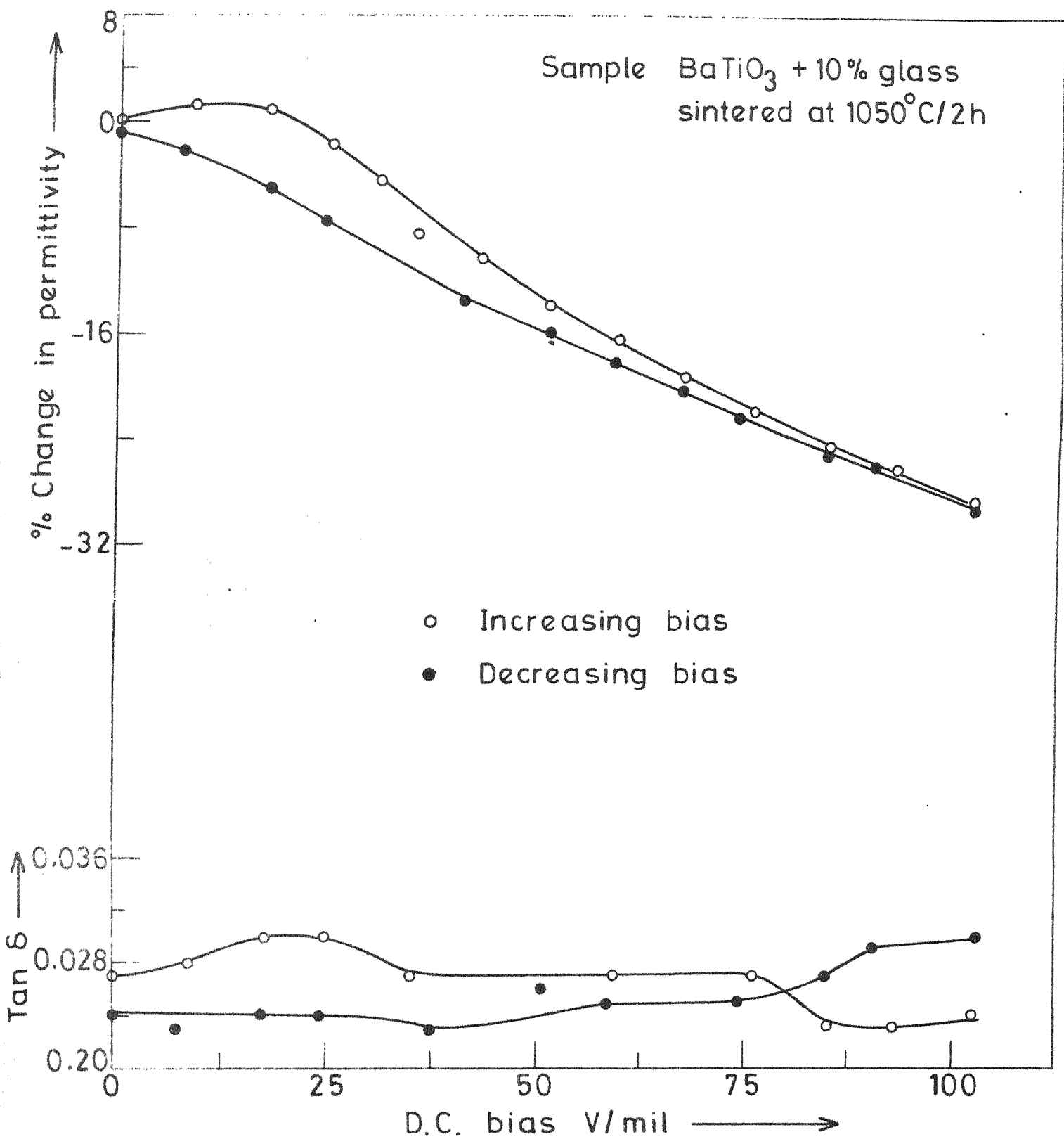


Fig. IV-37 Percent change in permittivity and dissipation factor with D.C. bias.



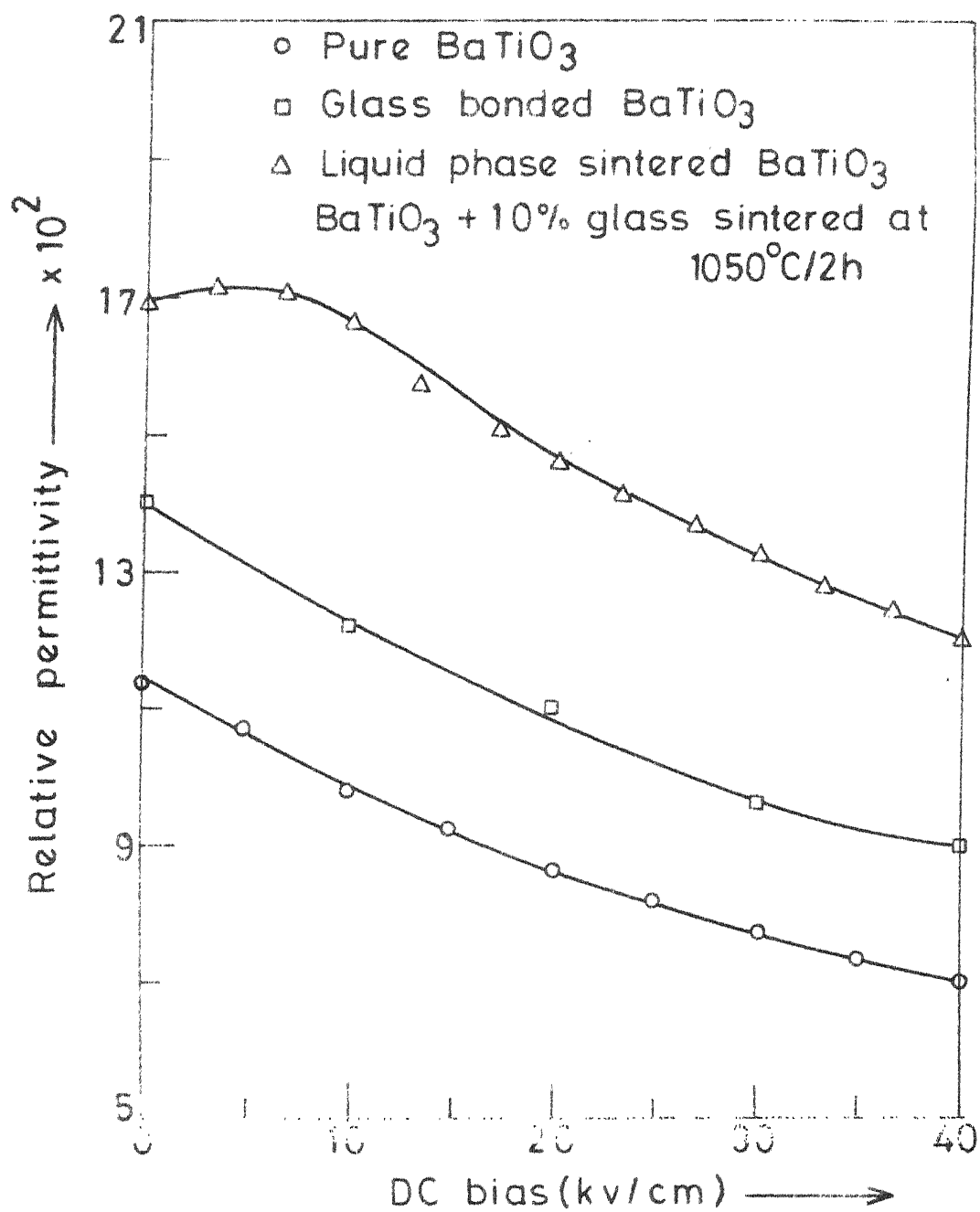


Fig. IV-38 Comparison of permittivity vs D.C. bias for different BaTiO<sub>3</sub> samples.

100 V/mil was 29% for liquid phase sintered Ba Ti O<sub>3</sub> and 36% for Ba Ti O<sub>3</sub>. The glass bonded Ba Ti O<sub>3</sub> is in between these two.

#### IV.7.3 Frequency dependence of dielectric properties:

Dielectric constant and  $\tan \delta$  were measured with respect to frequency on a 10% sample sintered at 1050°C/1h. These measurements were made at two temperatures namely room temperature (37°C) and 80°C and are shown in Fig. IV.39. This figure shows a dispersion at about 300 Hz at room temperature and this dispersion frequency was shifting to 1 KHz at 80°C. Very large change in the dissipation factor was observed with increasing frequency, for example it is changing from 0.3 at 100 Hz to 0.00038 at 100 KHz.

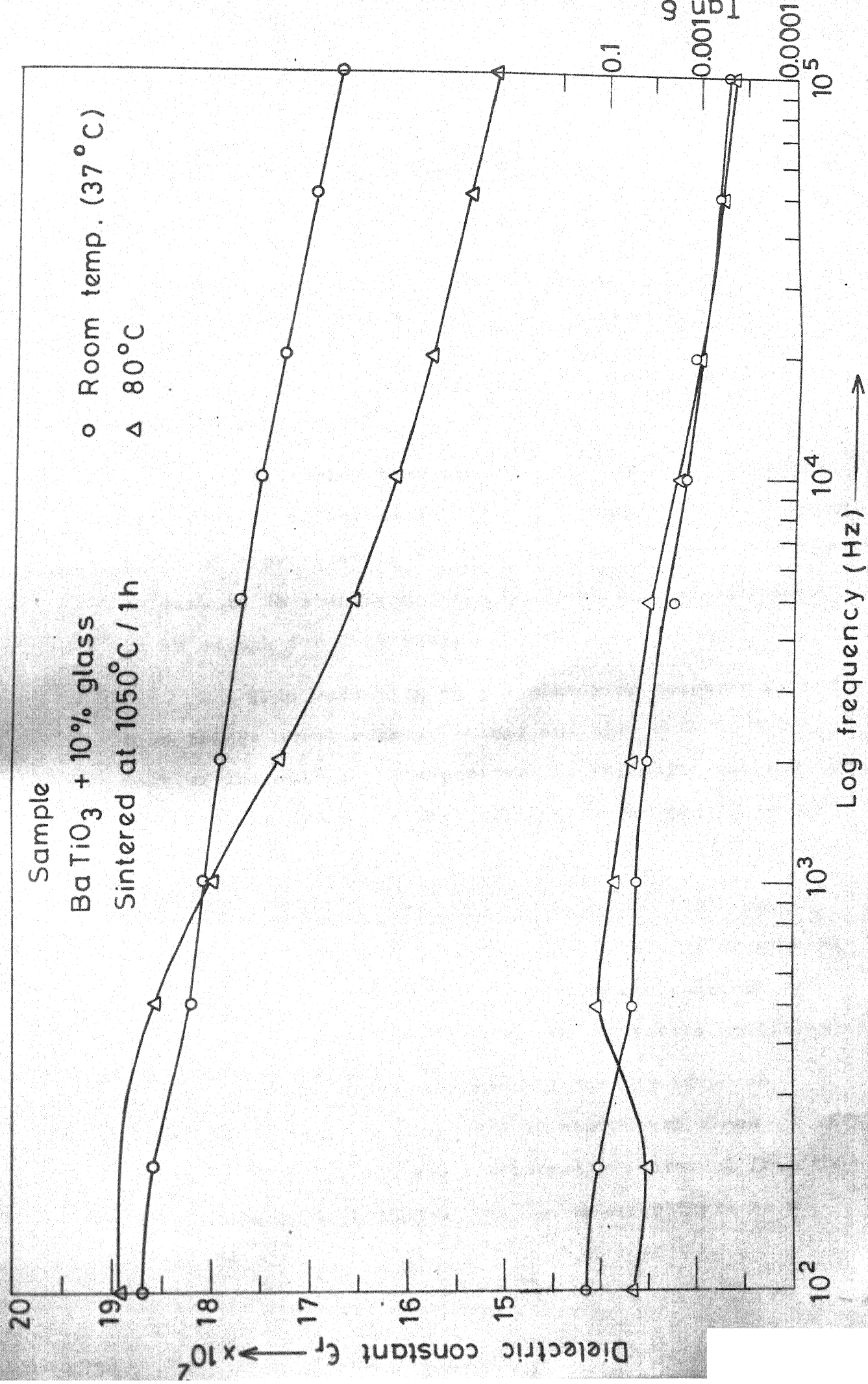


Fig. IV-39 Frequency dependence of dielectric constant for liquid phase sintered BaTiO<sub>3</sub>.

## V. CONCLUSIONS AND RECOMMENDATIONS

Sintering temperature of  $\text{Ba Ti O}_3$  has been reduced from the usual  $1350^\circ\text{C}$  to  $1050^\circ\text{C}$  by liquid phase sintering of  $\text{Ba Ti O}_3$  using a bismuth borate glass up to 10 to 20 wt percent.

Sintering time also has been reduced considerably without effecting the densification. A total heating cycle of approximately 6h consisting of 2h 30min. heating, 10 min. to 2h soaking and finally a 2h cooling are found to be enough for sintering.

This reduction in the sintering temperature and time brings about energy savings and also reduces the cost of the multilayer capacitors by replacing the costlier Pd and Pt electrodes with a relatively cheaper 70 Ag-30Pd alloy.

Both particle rearrangement and solution precipitation processes are found to be the major mechanisms causing densification, however the predominance of one over the other depends upon the sintering conditions.

Dielectric constants of the liquid phase sintered  $\text{Ba Ti O}_3$  samples with 10 and 20 wt% glass ( 1453 and 1325 ) are not considerably decreased from that of pure  $\text{Ba Ti O}_3$  ( 1500 - 2000 ). However there is a

marked decrease in peak value from 6000 - 10000 for pure Ba Ti O<sub>3</sub> to 2000 - 3000 for liquid phase sintered samples showing a less sensitivity with temperature. Response with d.c. bias of these samples seems to be slightly better than that of pure Ba Ti O<sub>3</sub> samples.

From the observations got during this study the following recommendations can be made which are worth considering.

- i) Effect of particle size has been studied in the present work but to a very limited extent. The particle size being an important parameter, the effect of that should be studied further particularly with lower particle sizes of Ba Ti O<sub>3</sub>.
- (ii) Detailed study on 20% samples should be done similar to that was done on 10% samples, because this glass range was found to be suitable for sintering at 1000 to 1100°C.
- (iii) Frequency response as a function of temperature should be studied thoroughly.

VI. APPENDIX - ACHEMICAL ANALYSIS

Chemical analysis of the glass used for liquid phase sintering, barium titanate and the liquid phase sintered barium titanate are undertaken. In the case of barium titanate, materials ground in an alumina jar with alumina balls to various particle sizes were also analysed to estimate the pick up of impurities during grinding. The procedure for the method for the preparations of the above substances was given in (1).

**VI.1** Analysis of Glass:

A weighed quantity of the powdered glass was heated with the minimum quantity of concentrated nitric acid. The solution was diluted, boiled, cooled and made up to a known volume.

**VI. 1.1** Determination of Bismuth:

Complexometric method was adopted for the determination of  $\text{Bi}^{2+}$ . Reagents used: Pyrocatechol violet. 0.1% solution in water, ammonia solution -0.5 M, EDTA - 0.01 M and pH indicator paper.

A known volume of the glass solution (20-40 mg of Bi) was pipetted out into a clean conical flask. The solution was diluted to about 100-150 ml and 3 to 4 drops of

the indicator solution were added. Dilute ammonia was added in drops until the violet colour changed to blue. The pH was checked with indicator paper to see that it was about 2. This was titrated against 0.01 M. EDTA until the colour changed to yellow.

If the amount of Bi is large an appreciable amount of hydrogen ions is released during the titration. Therefore the pH is checked during the titration either by indicator paper or by observing the colour of the bismuth-indicator complex.

Calculation: 1 ml of 0.01 M. EDTA corresponds to 2.09 mg of Bi. From the value obtained for Bi, the amount of  $\text{Bi}_2\text{O}_3$  was calculated.

#### IV. 1.2 Determination of Aluminium:

Aluminium also was analysed complexometrically. Titration procedure was the same as done by Bhargava<sup>(3)</sup>.

Reagents used: EDTA - 0.01 M, xylenol orange 0.1%, sodium hydroxide solution - 10% and 1%, zinc solution - 0.01 M, ammonium fluoride - 10% and acetate buffer - 136 g of sodium acetate trihydrate is dissolved in about 600ml water. 7 ml of glacial acetic acid is added and diluted to 1.1.

A known volume of the solution was pipetted out in a beaker and treated with excess of EDTA. For pH was

adjusted to 4 using a pH meter by dropwise addition of 10% sodium hydroxide solution till the pH reached 2.5 and then of 1% sodium hydroxide. The solution was diluted with water, covered, boiled and kept boiling for 10 minutes. The solution was cooled, added 7 drops of xylenol orange and 15 ml of acetate buffer. This mixture was titrated with zinc to pink colour. 10 ml of ammonium fluoride (10%) was added, boiled gently for 10 minutes, cooled and titrated against zinc.

Calculation: 1 ml of 0.01 M zinc corresponds to 0.27 mg of Al. From the value obtained for Al, the amount of  $\text{Al}_2\text{O}_3$  was calculated.

#### II. 1.3 Determination of Boron:

$\text{B}_2\text{O}_3$  was found out by difference. Results of analysis are given in Table 1.



REFERENCES

1. W.R. Buessem and T.I. Prokopowicz, *Ferroelectrics*  
10, 255 (1976)
2. *Metals Hand Book*, 8, 255
3. L. Burn and G.H. Maher. *J. Mat. Sci.*  
10, 645 (1963)
4. S.B. Desu, M. Tech. Thesis, I.I.T. Kanpur, 1979.
5. S.B. Desu and E.C. Subbarao, *J. Mat. Sci.*  
15, 2113 (1980)
6. S.B. Desu and E.C. Subbarao in *Advances in Ceramics*,  
Vol. 1, Am. Ceramic Soc. (1980) (in press)
7. E.C. Subbarao in *proc. Symp. on Sintering and*  
*Sintered products*, Bombay, 1979.
8. S.M. Park, Ph.D. Thesis, Univ. of Illinois.
9. J.L. Mukherjee and H.S. Ravishanker in *proc.*  
*Symp. on sintering and sintered products*, Bombay,  
1979, 281
10. D. Hennings, *Ber. Dtsch. Keram. Ges.*  
55, 359 (1978)
11. E.M. Levin and C.L. Mc Daniel, *J. Am. Ceram. Soc.*  
45, 355, (1962)
12. C. Hirayama and E.C. Subbarao, *Phys. Chem. Glasses*,  
3, 111 (1962)

13. S. Nanamatsu, H. Sugiyama, K. Doi and Y. Kondo  
J. Phys. Soc. Japan 31 , 616 (1971 )
14. J.F. Murray, Am. Ceram. Soc. Bull. .  
37, 476 (1958)
15. D.E. Rase and Rustam Roy, J. Am. Ceram. Soc.  
38, 102 (1955)
16. F. Kulcsar, J. Amer. Ceram. Soc.  
39 , 13 ( 1956 )
17. J.V. Biggers and W.A. Schulze, Am. Ceram. Soc.  
Bull., 51 , 620 (1972)
18. A.S.T.M. X-ray diffraction data Card No. 12-213
19. A.S.T.M. X-ray diffraction data Card No. 8-261.
20. V.N. Eremenko, Yu. V. Naidich and I.A. Lawrineko,  
"Liquid Phase Sintering". A special research report  
translated from Russian Consultants bureau.
21. W.D. Kingery, J. Appl. Phy.  
30, 301 (1959)
22. T. Prince, C. Smithells and S. Williams,  
J. Inst. Met. 62 , 239 (1938)
23. D.F. Rushman and M.A. Strivens, Trans. Faraday Soc.  
42A, 231 (1946).

24. E.C. Subbarao, Int. J. Phys and Chem. of Solids.  
23, 665 (1962 )
25. R.E. Newnham, D.P. Skinner and L.E. Cross,  
Mat. Res. Bull. 13, 525 (1978)
26. D.A. Payne and L.E. Cross " Ceramic Microstructures  
1976" Ed. R.M. Fulruth and J. A. Park. Proc. of the  
Sixth International Materials Symposium. Univ. of  
California, Berkeley, Aug. 1976.
27. H.C. Graham, N.M. Tallam and K.S. Mazdiasni.  
J. Am. Ceram. Soc. 52, 548 (1967)
28. S. Roberts, Phys. Rev. 71, 890 (1947)
-

ME-1981-M-CHO-LIQ